Volume 67
September 2024
ISSN 2217-8139 (Print)
ISSN 2335-0229 (Online)
UDK: 06.055.2:62-03+620.1+624.001.5(497.1)=861

GRAĐEVINSKI MATERIJALI I KONSTRUKCIJE

BUILDING MATERIALS AND STRUCTURES

3

Society for Materials and Structures Testing of Serbia
University of Belgrade Faculty of Civil Engineering
Association of Structural Engineers of Serbia




GRAĐEVINSKI MATERIJALI I KONSTRUKCIJE

BUILDING MATERIALS AND STRUCTURES

ISSN 2217-8139 (PRINT)
ISSN 2335-0229 (Online)

VOLUME 67(3)
September 2024

CONTENTS

GRAĐEVINSKI MATERIJALI I KONSTRUKCIJE

BUILDING MATERIALS AND STRUCTURES

ISSN 2217-8139 (PRINT)
ISSN 2335-0229 (Online)

VOLUME 67(3)
September 2024

Aims and scope

Building Materials and Structures aims at providing an international forum for communication and dissemination of innovative research and application in the field of building materials and structures. Journal publishes papers on the characterization of building materials properties, their technologies and modeling. In the area of structural engineering Journal publishes papers dealing with new developments in application of structural mechanics principles and digital technologies for the analysis and design of structures, as well as on the application and skillful use of novel building materials and technologies.

The scope of Building Materials and Structures encompasses, but is not restricted to, the following areas: conventional and non-conventional building materials, recycled materials, smart materials such as nanomaterials and bio-inspired materials, infrastructure engineering, earthquake engineering, wind engineering, fire engineering, blast engineering, structural reliability and integrity, life cycle assessment, structural optimization, structural health monitoring, digital design methods, data-driven analysis methods, experimental methods, performance-based design, innovative construction technologies, and value engineering.

Publishers Society for Materials and Structures Testing of Serbia**,** Belgrade, Serbia, veb sajt: www.dimk.rs
University of Belgrade Faculty of Civil Engineering, Belgrade, Serbia, www.grf.bg.ac.rs
Association of Structural Engineers of Serbia, Belgrade, Serbia, dgks.grf.bg.ac.rs

Print Razvojno istraživački centar grafičkog inženjerstva, Belgrade, Serbia

Edition quarterly

Peer reviewed journal

Journal homepage www.dimk.rs

Cover Experimental testing of 3D printed segmental beam from *Experimental investigation of bearing capacity of 3D printed concrete segmental girder* by Stefan Ž. Mitrović and Ivan Ignjatović

Financial support Ministry of Education, Science and Technological Development of Republic of Serbia
University of Belgrade Faculty of Civil Engineering
Institute for testing of materials-IMS Institute, Belgrade
Faculty of Technical Sciences, University of Novi Sad, Department of Civil Engineering
Serbian Chamber of Engineers

CIP - Каталогизација у публикацији
Народна библиотека Србије, Београд

620.1

GRAĐEVINSKI materijali i konstrukcije = Building materials and structures / editor-in-chief Snežana Marinković
. - God. 54, br. 3 (2011)- . - Belgrade : Society for Materials and Structures Testing of Serbia : University of Belgrade, Faculty of Civil Engineering : Association of Structural Engineers of Serbia, 2011- (Belgrade : Razvojno istraživački centar grafičkog inženjerstva). - 30 cm

Tromesečno. - Je nastavak: Materijali i konstrukcije
= ISSN 0543-0798. - Drugo izdanje na drugom medijumu:
Građevinski materijali i konstrukcije (Online) = ISSN 2335-0229
ISSN 2217-8139 = Građevinski materijali i konstrukcije
COBISS.SR-ID 188695820

Građevinski materijali i konstrukcije
Building Materials and Structures
journal homepage: www.dimk.rs

https://doi.org./10.5937/GRMK2400007R UDK: 666.972.1:620.1
691.327:620.17

Original scientific paper

Influence of curing period on some mechanical and durability-related properties of limestone powder concrete

Andrija Radović*[1], Vedran Carević[2], Aleksandar Radević[3], Branislav Stupar[4], Darko Veličkov[4]

[1] *University of Priština in Kosovska Mitrovica, Faculty of Technical Sciences, Knjaza Miloša 7, 38220, Kosovska Mitrovica, Serbia. ORCID 0000-0002-7879-0458*
[2] *University of Belgrade, Faculty of Civil Engineering, Bulevar kralja Aleksandra 73, 11000, Belgrade, Serbia. ORCID 0000-0002-8887-6722*
[3] *University of Belgrade, Faculty of Civil Engineering, Bulevar kralja Aleksandra 73, 11000, Belgrade, Serbia. ORCID 0000-0002-3224-8145*
[4] *University of Belgrade, Faculty of Civil Engineering, Bulevar kralja Aleksandra 73, 11000, Belgrade, Serbia*

Article history
Received: 17 August 2024
Received in revised form: 27 August 2024
Accepted: 27 August 2024
Available online: 10 September 2024

Keywords
Limestone powder concrete,
curing period,
mechanical properties,
durability

ABSTRACT
This study investigates the influence of curing periods on the mechanical and durability-related properties of limestone powder concrete, focusing on the potential of limestone as a sustainable alternative to traditional materials, primarily cement. The research explores the effects of varying cement replacement percentages (30-55%) and curing durations (1, 3, 7, 14, and 28 days) on concrete properties such as compressive strength, flexural strength, water permeability, and resistance to chloride ingress. The limestone fineness was also tested using two powders from the same chemical composition, but different particles size. Results indicate that longer curing periods generally enhance concrete performance, but not in all cases. The greatest benefits of extending the curing period was observed in the case of water penetration depth, so the average difference between 1 and 28 days curing was about 50%. Flexural strength also saw a substantial increase of up to 24% over the same curing period. However, increasing the curing period from 7 to 28 days resulted in an unexpected average reduction in concrete compressive strength of 13%. Despite previous results, a positive impact of a higher limestone powder content was observed in all cases, except for resistance to chloride penetration. Concretes that contained limestone powder had a significantly lower (as much as 186%) resistance to chloride penetration, compared to the reference (with the highest dispersion of results). The study found no significant influence of limestone particle size on concrete properties.

1 Introduction

The construction industry, particularly the concrete sector, significantly impacts the environment due to its extensive use of raw materials, high energy consumption, and substantial waste production. With an annual production nearing 35 billion tons [1], [2], the concrete industry is a major contributor to environmental degradation, primarily through the use of natural stone aggregates and the large carbon dioxide (CO_2) emissions from cement production [3]. Moreover, cement production alone accounts for approximately 7-10% of all anthropogenic CO_2 emissions [4], making it one of the most carbon-intensive industries globally. Efforts to address these environmental impacts have led to a growing emphasis on finding sustainable alternatives to traditional processes and materials within the concrete industry. This transition is crucial for achieving a carbon-neutral future and addressing the urgent need to combat climate change. To improve the sustainability of concrete production, there has been a focus on reducing the clinker content in cement by using supplementary cementitious materials (SCMs) such as fly ash and ground granulated blast furnace slag (GGBS), [5]. These materials can partially replace ordinary Portland cement (OPC), thus reducing CO_2 emissions. However, the availability of SCMs is limited, and their supply is expected to decrease as coal-fired power plants are phased out and the steel industry's slag production declines [6], [7]. This scarcity necessitates the investigation of alternative, eco-friendly materials, such as finely ground limestone (LS), despite their lower reactivity, even inertness [8], and potentially negative impact on the mechanical and durability properties of concrete [9]. Therefore, the key challenge remains to balance environmental and economic benefits with the technical performance requirements of concrete [10].

Replacing OPC with LS powder can significantly influence the workability of concrete. While high replacement

* Corresponding author:
E-mail address: andrija.radovic@pr.ac.rs

percentages of OPC with LS powder (30-55%) can decrease workability [11], [12], applying suitable water-reducing admixtures and adjustments in the mix design can mitigate these effects [13]–[16]. The fine particles of limestone fill voids between cement grains, reducing the water demand and improving the fluidity of the mix [17]. Some studies [18]–[20] suggest that the incorporation of LS powder, especially in combination with the appropriate powder paste (OPC + LS + water) volume and a dose of superplasticizer, can maintain or even enhance concrete workability, making it easier to cast and place.

The role of LS powder on the compressive strength of concrete is multifaceted. At lower replacement levels (up to 10-20%), limestone powder can improve compressive strength by enhancing particle packing and providing nucleation sites for cement hydration, resulting in a denser and stronger microstructure [8], [21]. Some other studies have shown that even replacing OPC with a high LS powder content (40-60%), while reducing water and increasing superplasticizer content, can achieve comparable or even higher compressive strength [11], [12], [17], [20], [22]. Additionally, the particle size distribution of LS powder plays a significant role; finer particles enhance higher strength due to better packing density and acceleration of initial hydration [9], [12], [21], [23]. It is essential to carefully manage the amount of LS powder, the quantity of paste, and the water-to-cement ratio to ensure comparable strength. Other mechanical properties are usually closely related to the compressive strength [24]–[28].

LS powder affects various durability-related properties through different mechanisms [29]. The water permeability of concrete depends on the degree of cement hydration, the porosity and pores structure of the cement matrix, the quality of the transit zone between the cement matrix and aggregates, but also on the intensity of water pressure [30]. LS powder primarily influences this property by its filler effect, increasing the density and reducing porosity of the concrete matrix [17]. By filling voids and minimizing capillary pores, LS powder has mainly positive effects and decreases the water permeability of concrete [24]. This improvement is better if finer particles are used. However, an excessive replacement ratio can also increase the porosity if not properly balanced with other mix components, potentially compromising the resistance to water penetration [31].

Unlike water penetration, incorporating LS powder as a substitute for OPC has a predominantly negative influence on the resistance of concrete to chloride ingress [16], [24], [31]–[34]. The difference is more pronounced with higher replacement percentages. In this case, the dilution effect becomes prominent [8]. Moreover, the inert nature of limestone powder reduces the overall content of cementitious material, which reduces the aluminate phase and consequently, the concrete resistance. The chemical reaction between LS powder and available aluminates further diminishes the already insufficient aluminate phase, making this effect more expressed [9]. In this type of concrete, the transport of chloride ions by diffusion is also higher [35]. However, Li and Kwan [24] have demonstrated that is possible to make concrete with a high LS contribution (as much as 60%) that possesses better resistance against chloride penetration compared to the reference OPC concrete. This has been accomplished through meticulous mix design and the optimization of powder paste volume.

1.1 Influence of curing on concrete properties

Regardless of the importance of the amount of cement replaced by LS powder, curing of concrete under specific thermo-hygrometric conditions during a certain period after compacting could be pivotal in ensuring the desired concrete performance. Proper curing enhances the hydration process, significantly improving all mechanical and durability-related properties of concrete. Despite its importance, the influence of curing on LS powder concrete properties has been insufficiently investigated. More precisely, a review of the available literature has identified only four studies [16], [36]–[38].

Dhir et al. [16] analyzed the effect of curing on the compressive strength of concrete. Five concrete mixtures with different percentages of cement replacements (0%, 15%, 25%, 35%, and 45% by mass) were prepared and tested. The reference concrete (0% of cement replacement) contained 310 kg/m^3 of cement with a water-to-cement ratio (w/c = 0.6). LS powder concretes maintained the same total amount of powder components (OPC + LS = 310 kg/m^3) and the same water-powder ratio (w/p = 0.6). The samples were cured in water for 1 day, 3 days, 7 days, and 28 days (including initial storage in steel molds covered with plastic film for the first 24 hours). After water curing, the samples were stored under constant laboratory conditions at 20°C and 55% relative humidity (RH). Testing was conducted at 1, 3, 7, and 28 days. The authors emphasized that the samples tested at 3, 7, and 28 days were removed from water 12, 24, and 48 hours before testing, respectively. This was done to achieve the same moisture conditions for all specimens.

The 28-day water-cured OPC mixture had the highest compressive strength (41.0 MPa). Due to the adopted approach (w/p = const), an increase in LS powder content was accompanied by a decrease in compressive strength. Mixtures with 15%, 25%, 35%, and 45% replaced cement had 11%, 28%, 43%, and 59% lower compressive strength, respectively, compared to the reference.

The ratio of compressive strength for the samples cured for "i" days (f_{cm}^{i}) to the corresponding samples cured for "28" days (f_{cm}^{28}), for concretes with different LS powder content, is shown in Figure 1.

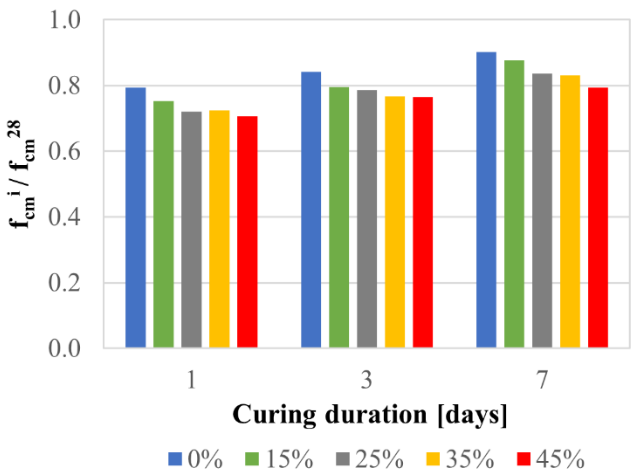

Figure 1. The effect of curing duration on the compressive strength of concrete with different LS powder content, data from [16]

Increasing the curing period positively affects the compressive strength of all tested mixtures. However, this effect is more pronounced in mixtures containing LS powder. OPC mixtures were less sensitive, with strength reductions ranging between 10–20%, while mixtures with 45% LS powder experienced declines of around 20–30%. These conclusions align well with the observations of Sun and Chen [38], but contradict the findings of Bonavetti et al. [39]. Namely, Bonavetti et al. [39] showed that the samples wet-cured for 7 days had higher compressive strength (10–17%) compared to those wet-cured for 28 days. Larger differences correspond to a higher LS powder content. The same study also found that samples air-cured in laboratory conditions throughout had the lowest strength (15–32%), with losses being greater in OPC mixtures than in LS powder concretes. Contradictory findings indicate the need for additional experimental research to clarify these effects.

The same trend as for compressive strength under different curing conditions was observed for tensile strength, [39]. Moreover, these values are almost linearly correlated.

From the aspect of durability, the lack of results is evident. Unfortunately, no paper was found addressing the effects of initial curing on the water permeability of LS powder concrete. The situation was not much better in the case of concrete resistance to chloride penetration.

Sun and Chen [38] investigated the influence of three different curing periods on the resistance of LS powder concrete to chloride ingress. In addition to OPC concrete (400 kg/m^3 cement) three more mixtures containing 8%, 16%, and 24% of LS powder were designed. All concretes were divided into two groups. In the first group, the same w/p ratio (0.45) was adopted. The second group aimed to achieve a similar compressive strength of about 53 MPa, so different w/p ratios were used. Three curing periods were chosen for all concretes: 1) Standard curing period of 28 days under 20°C and 95% RH; 2) 7 days of curing at 20°C and 95% RH, followed by 21 days under laboratory conditions at 20°C and 40–50% RH; 3) 3 days of curing at 20°C and 95% RH, then 25 days under laboratory conditions at 20°C and 40–50% RH.

When considering the standard curing period of 28 days for the first group of samples, the results suggest that LS powder can improve concrete resistance, but only at a low replacement percentage. The mixture with 8% LS had the lowest charge passed, about 6% lower than OPC. This can be explained by the fact that very fine LS powder can affect the interconnections between the pores [39], [40]. However, further increasing the LS content to 16% and 24% reduced the concrete's resistance by approximately 10% and 30%, compared to OPC. According to the authors [38] the high volume of LS powder significantly decreases the hydration products, increasing porosity and pore connectivity.

For the second group, which contained the same strength concretes, the results were different. In this case, OPC showed the worst performance. Increasing the LS content improved the concrete's resistance to chloride ingress. Mixtures with 8%, 16%, and 24% LS powder showed a 17%, 23%, and 29% reduction in charge passed, respectively. It was attributed to the better microstructure provided by a lower w/p ratio that overcomes the negative effects of binder dilutions. Similar observations were obtained for the other curing conditions.

Comparing the results for the same concretes under different curing conditions, the advantages of a longer curing period are undeniable. Deviating from the standard curing conditions and reducing the curing period from 28 to 7 days compromised concrete permeability, increasing the charge passed by an average of 10%. Further shortening the curing period to only 3 days additionally jeopardizes concrete performance. The total charge passed through the specimens increased by about 18% overall.

The further prolongation of the curing period to 90 or 180 days resulted in a significant increase in concrete resistance by 10–20% and 40–60% respectively [31], [38]. However, these long curing periods are not suitable for practical application.

2 Objectives

Although some aspects of the impact of LS powder on concrete properties, such as workability and compressive strength, have been relatively well-analyzed, investigations into durability properties are significantly lacking. Moreover, many studies are limited to low-to-medium LS powder content. The literature review also highlighted a substantial gap in understanding the effect of the curing period on all concrete properties. Therefore, the main objective of this research is to investigate how different curing periods influence the properties of concrete containing a high volume of LS powder (30-55% of the cement content). The potential impact of LS powder fineness was also examined. To achieve this aim, an experimental study was designed to provide a better understanding of the interplay between curing duration and the effectiveness of LS powder in enhancing concrete performance.

3 Experimental procedures

3.1 Materials and methods

Ordinary Portland cement CEM I 42.5R (max 5% additional constituents) according to EN 197-1 [41], with a mean particle size of $d_{50} \approx 11$ µm was used. Two types of commercially available LS powder with the same chemical compositions (98% $CaCO_3$ content) in line with EN 197-1 [41] were applied. The designation of LS powder was adopted according to mean particle size (d_{50}). L_3 corresponds to $d_{50} \approx$ 3 µm, which is much finer than cement, while L_{12} had a similar particle size distribution ($d_{50} \approx 12$ µm) to OPC. Natural aggregate was divided into three fractions I (0–4 mm), II (4–8 mm), and III (8–16 mm) which originate from the Danube River. All mixtures contained the same total amount of aggregate (1850 kg/m^3) with the following contribution of individual fractions I (52%), II (21%), and III (27%).

The final composition of the mixtures was determined by the absolute volume method. The mixtures were designed to fulfill the high workability requirements prescribed for consistency class S4 or S5 with a target slump ≥ 200 mm [42]. The workability was controlled by an appropriate dose of second-generation superplasticizer (1-2% powder component).

Since the idea was to compare the properties of different types of concrete with similar strengths, the target mean compressive strength (f_{cm}) 48±4 MPa (measured on a 100 mm cube), was chosen, corresponding to commonly used concrete classes C25/30 and C30/37 [43].

Reference OPC concrete was designed with 334 kg/m^3 cement and w/c = 0.51. Besides that, two groups of LS powder concrete (L_3 and L_{12}) with three different percentages of cement replacement (30%, 45%, and 55%) were made. The higher LS powder content than the replaced cement amount is the result of the volumetric replacement of cement paste. This enabled a parallel reduction of water, and achieving the target workability and strength, despite the significantly reduced amount of cement. The proportioning of the tested concrete mixtures is shown in Table 1.

3.2 Casting, curing, and testing of specimens

After mixing, the workability of each concrete mix was verified by a standard slump test [44]. All concretes were cast into plastic and steel moulds and compacted using a vibrating table. The samples are covered with a plastic sheet and protected from moisture loss. After 24 hours, the specimens were demoulded and stored under different curing conditions for the first 28 days. Depending on the desired test, five different curing conditions were adopted. Curing modes are marked with numbers representing days (1, 3, 7, 14, and 28 days) under standard curing conditions [45]. These are listed and explained in detail in Table 2.

Mechanical properties were determined on samples cured in all five conditions. Compressive strength tests were performed on 100 mm cubic samples at different ages, according to EN 12390-3 [46]. For flexural strength, 28-day-old prismatic specimens (100 x 100 x 300 mm) were tested using a three-point bending test [47].

Durability-related properties were determined on samples cured under three different conditions (1, 7, and 28 days). Water penetration depths were tested on 150 mm cubic samples at 28 days old, after exposure to a water pressure of 0.5±0.05 MPa for 72±2 h [48]. Chloride penetration depths were determined using non-steady-state chloride migration tests [49]. For this purpose, a 50 ± 2 mm thick slice was cut from the central portion of the cylinder (∅100/H200 mm). After preconditioning, the specimens were placed between catholyte (10% NaCl solution) and anolyte (0.3N NaOH solution) reservoirs and subjected to the appropriate external electrical potential axially. Using the measured chloride penetration depths, non-steady-state chloride migration coefficients (D_{nssm}) were determined.

All tests conducted in this research, considering curing conditions and the age of the concrete at the time of testing, are listed in Table 3 for transparency. All reported results represent the mean values of three measurements.

Table 1. Mix proportions of tested concrete

Concrete mix	m_c [kg/m^3]	m_{LS} [kg/m^3]	m_w [kg/m^3]	w/c [–]	SP [%]
OPC	334	0	171	0.51	1.0
L_3-30	230	200	143	0.62	1.5
L_{12}-30	230	200	143	0.62	1.5
L_3-45	182	252	127	0.70	2.0
L_{12}-45	182	252	127	0.70	2.0
L_3-55	153	285	114	0.75	2.0
L_{12}-55	153	285	114	0.75	2.0

Table 2. Curing conditions of concrete samples

Curing period	Curing (1)	Curing (3)	Curing (7)	Curing (14)	Curing (28)
1 day	M	M	M	M	M
1-3 days	A	W	W	W	W
3-7 days	A	A	W	W	W
7-14 days	A	A	A	W	W
14-28 days	A	A	A	A	W

M – in the mold; **A** – in the air 20°C, 65% RH; **W** – in the water 20°C

Table 3. Conducted tests considering curing conditions and the age of concrete

Age at the time of testing	Curing (1)	Curing (3)	Curing (7)	Curing (14)	Curing (28)
1 day	CS	CS	CS	CS	CS
7 days	CS	/	CS	/	CS
28 days	CS, FS, WP, CP	CS, FS	CS, FS, WP, CP	CS, FS	CS, FS, WP, CP

CS – Compressive strength; **FS** – Flexural strength; **WP** – Water penetration; **CP** – Chloride penetration

4 Results and discussions

4.1 Workability

A well-designed mixtures with an appropriate powder component, customized w/c ratio, and sufficient superplasticizer content ensured excellent workability. The consistency class S5 [42] with a slump value over 220 mm was obtained across all concrete mixtures. However, mixtures with higher percentages of cement replacement demanded more superplasticizer to maintain the same level of workability. This is primarily due to the reduced water content in these mixtures, even though their w/c ratios were higher than those of OPC, owing to the lower cement content. If lower workability is acceptable, the superplasticizer dosage can be reduced. Alternatively, the same effect can be achieved by increasing the water content, though this would result in a decrease in strength.

4.2 Mechanical properties

4.2.1 Compressive strength

In Figure 2, the average compressive strengths at 28 days of age for concrete mixes cured under different conditions are shown. For samples cured in water for 28 days, the measured compressive strengths ranged from 44 MPa to 51.8 MPa, which corresponds to the initial hypothesis of producing concrete mixes with uniform strength.

The curing period of concrete in water up to 7 days had a positive effect on the achieved compressive strength values. The longer the concrete was cured in water, the higher the compressive strength. In contrast, concrete mixes cured in water for 28 days showed lower compressive strength values compared to all other curing regimes. The reason for these unexpected results may be the greater amount of water that the concrete was able to absorb and which remained in the concrete at the time of testing under compressive force. Specifically, the retained water in the concrete, when external load is applied, leads to the development of internal stresses and water vapor pressure, resulting in reduced fracture toughness. Similar conclusions, albeit with different types of concrete, were reached in the studies by [50]–[52]. It is assumed that complete drying of samples cured in water for 28 days would lead to higher compressive strength compared to other curing regimes.

A similar effect is observed in concrete cured in water for 14 days. Except for the L_3-55 mix, all other mixes showed measured values approximately equal to the compressive strengths of concrete cured for 7 days in water.

Figure 3 shows the relationship between the compressive strength of concrete cured under different conditions (f_{cm}^{i}) and the compressive strength of the same type of concrete cured in water for 28 days (f_{cm}^{28}). Both strengths (f_{cm}^{i}) and (f_{cm}^{28}) refer to samples tested at 28 days of age.

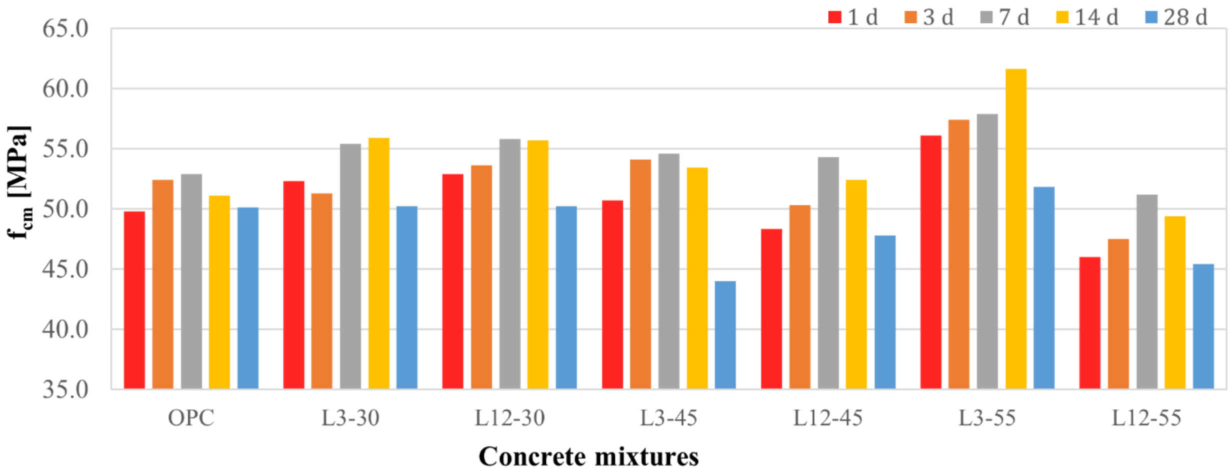

Figure 2. The compressive strength of concrete mixtures with different curing duration at the age of 28 days

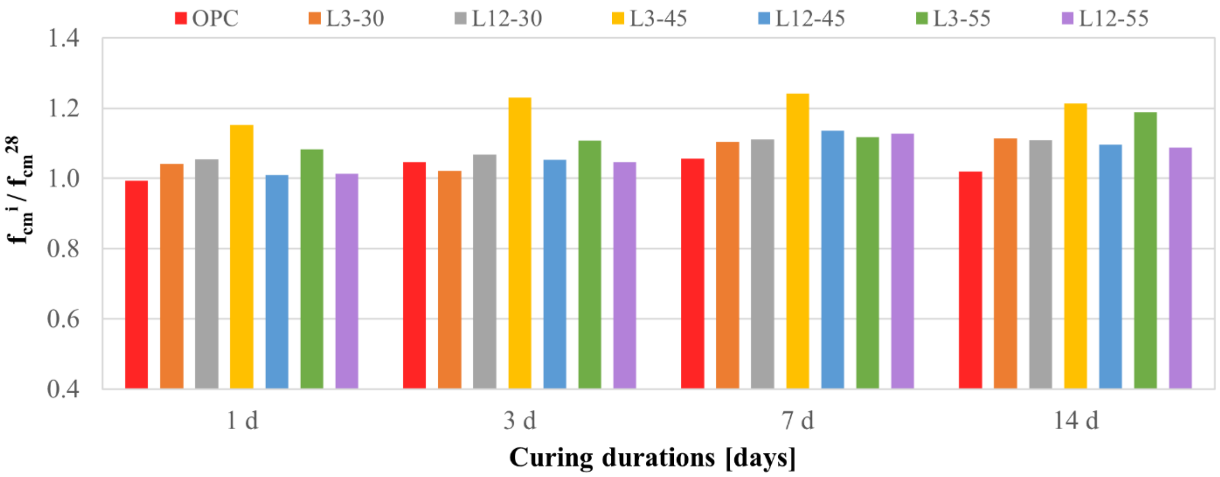

Figure 3. The effect of curing duration on the compressive strength of different concrete mix

As can be seen, the effect of curing had a greater impact on the development of compressive strength in LS concretes compared to OPC concrete. For instance, compared to concrete cured for 28 days in water, the compressive strengths of concrete cured under other conditions range from -0.6% to 5.6% for OPC concrete, from 2.2% to 24.1% for L3 concretes, and from 1.0% to 13.6% for L12 concretes. When comparing only LS concretes, it can be concluded that with an increase in the fineness of the limestone powder used, the sensitivity of the concrete mix to the curing regime also increases. This behavior of the concrete may be due to the relatively small amounts of water used in mixes with a high content of LS powder. Specifically, this water is used not only for cement hydration but also for moistening the LS grains. In mixes with finer LS grains, a larger amount of water is needed because the specific surface area of the grains is greater.

The diagrams of strength gain rates for concretes cured in water for 7 and 28 days are shown in Figure 4. The diagrams clearly show that only the L_{12}-55 mixture exhibits a noticeably slower strength gain in the first three days. In the period from 7 to 28 days, the strength gain rate for LS concretes under pressure is consistent (the lines on the diagram are parallel) and is slightly higher compared to OPC concretes. It can be concluded that different curing regimes did not have a significant impact on the strength gain rate of the tested concretes.

4.2.2 Flexural strength

In contrast to the results of compressive strength tests, the results of flexural strength (see Figure 5) clearly indicate that, with increased curing duration of concrete in water, the measured flexural strengths also increase for most concrete mixtures. These results are consistent with the explanations provided in section 4.2.1, as during flexural tests, a linear force acts on the center of the span of prismatic samples, which does not induce pore pressures in water-saturated samples, unlike in compressive strength tests where such pore pressures have influenced the decrease in these values. The only exceptions are the results obtained from the L_{12}-30 and L_{12}-55 mixtures for samples cured in water for 28 days, as it was found during testing that the rate of load application did not meet the conditions of the EN 12390-5 [47] standard.

If, due to the pronounced effect of pore pressure, compressive strengths of concrete from samples cured in water for 7 days are considered as the reference, a clear correlation can be drawn between the results shown in Figure 5 and the compressive strength results for different concrete mixtures. Specifically, concrete mixtures that had higher compressive strengths logically also had proportionally higher flexural strengths. Additionally, there is no significant impact of the coarseness of the used limestone powder on the obtained bending strength values, which is consistent with the research by Kim et al. [26].

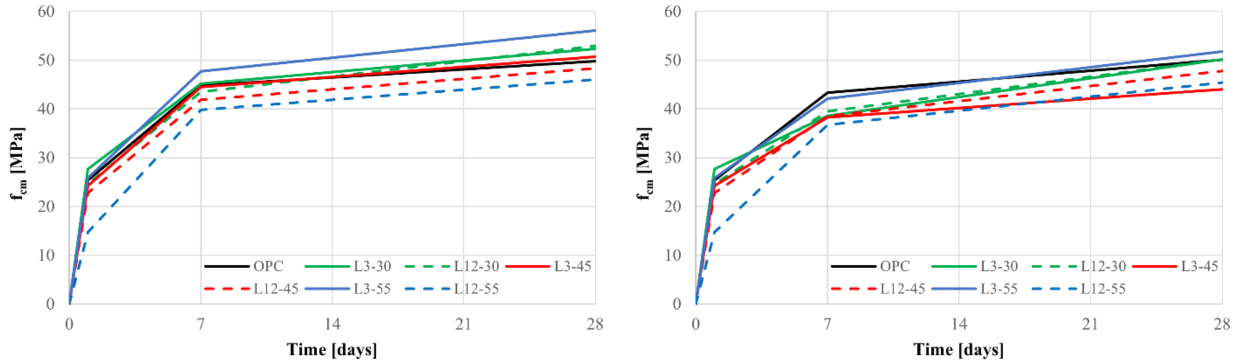

Figure 4. The effect of curing duration on the development of concrete compressive strength: 7 days in water (left); 28 days in water (right)

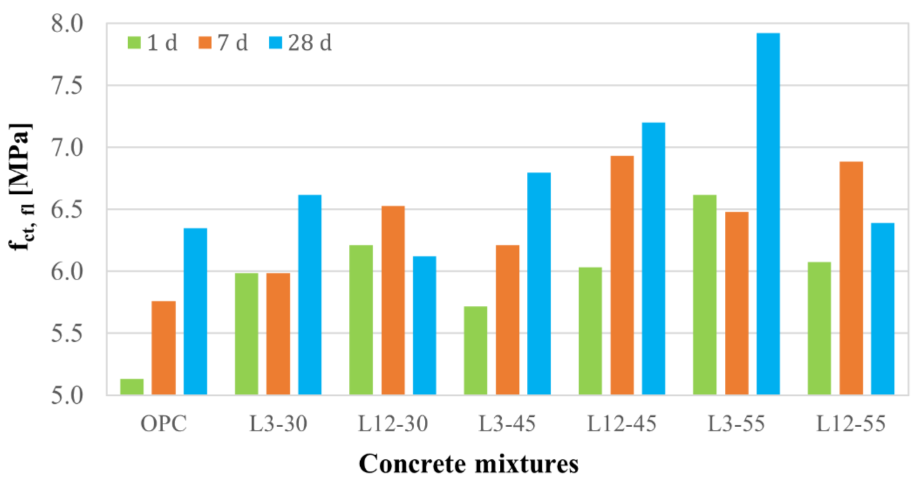

Figure 5. The effect of curing duration on the development of flexural strength maesured at 28 days

4.3 Durability

4.3.1 Water penetration

The measured water penetration values are shown in Figure 6. Compared to OPC concrete, concretes with partial cement replacement by limestone powder exhibited lower water penetration depths. This is attributed to the better "packing" of LS particles, which resulted in concrete with higher density. Other studies also confirm these results [17], [24].

The impact of curing duration on the measured water penetration values is even more pronounced (see Figure 7). For example, OPC concretes cured for 1 and 7 days in water show water penetrations that are 78% and 87% higher, respectively, compared to the same concrete cured for 28 days in water. For LS concretes, these differences range from 38% to 183% for L_3 concretes and from 34% to 114% for L_{12} concretes. However, unlike OPC concrete, LS concretes show a significant difference in measured water penetrations between samples cured for 1 day and those cured for 7 days in water. Additional curing between 1 and 7 days allowed for a reduction in water penetration of up to 50% in LS concretes. These results indicate that, in the case of using limestone powder, proper curing can significantly improve the waterproofness of concrete compared to OPC concretes.

Generally, considering the test results for all mixtures cured in water for 28 days, which aligns with the EN 12390-8 standard [48], all concretes meet the requirement for the waterproof concrete (according to the Serbian national annex of the EN 206 standard [53]). On the other hand, except for the L_3-55 mixture, no other mixture cured in water for 1 day meets the criteria for waterproof concrete. This highlights the importance of proper curing for concrete used in structural elements that are required by the design to be waterproof.

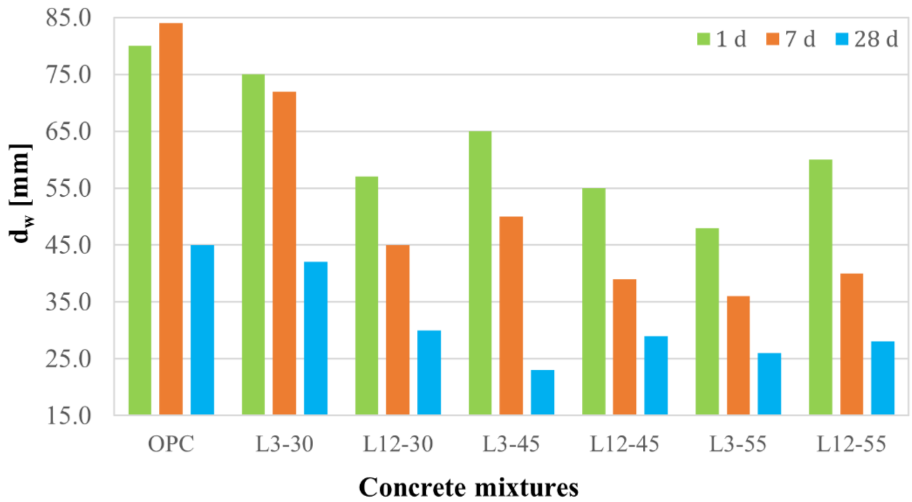

Figure 6. Water penetration depth of concrete mixtures with different curing duration measured at 28 days

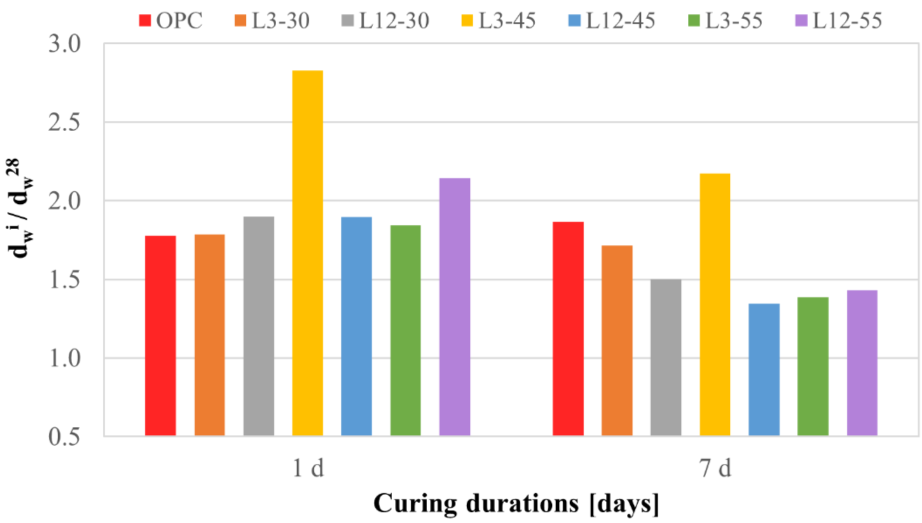

Figure 7. The effect of curing duration on the water penetration depth of different concrete mix

4.3.2 Chloride penetration

The calculated values of chloride migration coefficients (D_{nssm}) are shown in Figure 8. The values were calculated using measured chloride penetration depths, according to EN 12390-18 [49]. With the increase in the curing period, there was a decrease in the chloride penetration depth, and therefore decrease in the migration coefficient. For concrete L_3-30 and L_3-45, 7 days curing period showed slightly better results compared to 28 days curing. However, with OPC concrete, the best results were shown for 1 day curing period, which cannot be explained by physico-chemical processes inside the concrete. Therefore, it is necessary to repeat these and perform additional tests with these concretes in the future.

The results showed that with an increase in the LS replacement percentage, there is no decrease in resistance. Also, there was no significant difference between the types of LS powder. The only difference was observed at 30% replacement of cement with LS. However, LS concretes showed significantly worse chloride penetration resistance compared to OPC concretes. The far worse chloride penetration resistance of LS concretes can be attributed to the reduced content of the aluminate phase [9], [35] and to the dilution effect of the cement paste and increased porosity [8], [54].

The impact of water curing duration on the chloride migration resistance is shown on Figure 9. Curing between 1 and 7 days allowed for a chloride migration coefficient up to 20% in LS concretes. These results indicate that, in the case of using LS powder, proper curing can improve the chloride resistance. However, it is still necessary to look for a way to improve the chloride resistance of these concretes, so that their performances can be closer to OPC concretes.

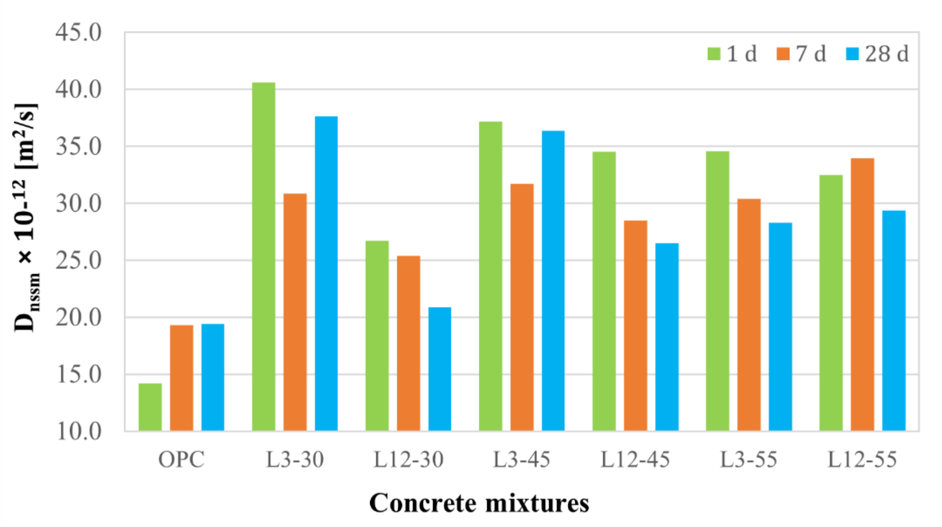

Figure 8. The chloride migration coefficient of concrete mixtures with different curing periods

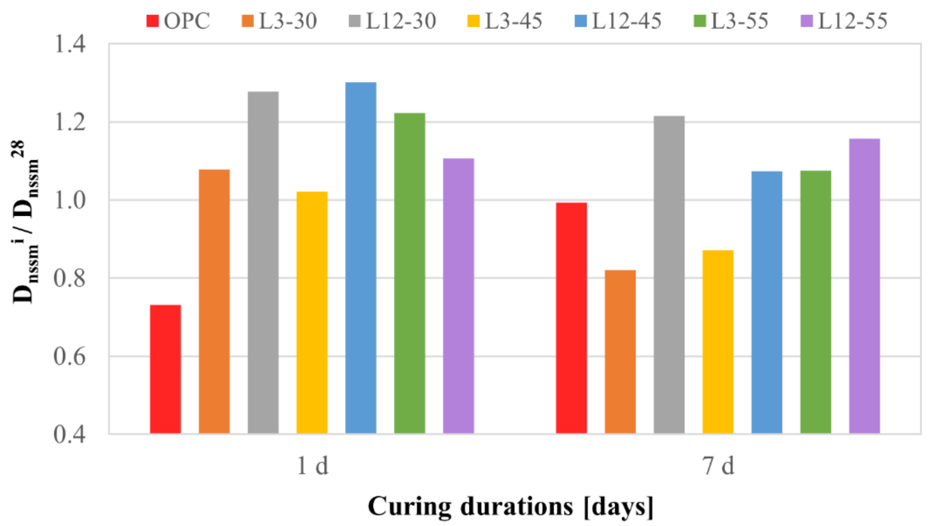

Figure 9. The effect of curing duration on the chloride migration coefficient for different concrete mixtures

5 Conclusions

The main objective of this study was to analyse the impact of different curing periods on the properties of concrete containing a high volume of LS powder (30-55% of replaced cement). The potential impact of LS powder fineness was also examined. An experimental study with five different curing periods (1, 3, 7, 14 and 28 days) and two different LS was designed to examine the interplay between curing duration and the effectiveness of LS powder in enhancing concrete performance. Based on the own experimental results, the following conclusions can be made:

- The curing period of concrete in water up to 7 days had a positive effect on the achieved compressive strength values. The longer the concrete was cured in water, the higher the compressive strength. Contrary to expectations, 28 days of curing did not result in the best concrete performance. Concretes cured for 7 days had an average compressive strength of about 13% higher than concrete cured for 28 days, regardles the LS powder content.
- The effect of curing had a greater impact on the development of compressive strength in LS concretes compared to OPC concrete. When comparing only LS concretes, it can be concluded that with an increase in the fineness of the LS powder used, the sensitivity of the concrete mix to the curing regime also increases.
- The results of flexural strength indicate that with increase in curing period flexural strengths also increase (up to 24%). Additionally, there is no significant impact of the coarseness of the used LS powder on the obtained flexural strength values.
- The positive effect of water curing duration on the measured water penetration was even more pronounced. On average, a 50% less water penetration depth was observed for mixtures cured for 28 days compared to mixtures cured for only 1 day. The obtained results also indicate that, in the case of using LS powder, proper curing can significantly improve the waterproofness of concrete compared to OPC concretes.
- With the increase in the curing period, there was a decrease in the chloride penetration depth, and therefore decrease in the migration coefficient. The results showed that with an increase in the LS replacement percentage, there is no decrease in resistance. Also, there was no significant difference between the types of LS powder. However, LS concretes showed significantly worse penetration resistance chloride (up to 186% with a significant scatter) compared to OPC concretes, which needs to be research in more detail in the future.

CRediT authorship contribution statement:

Andrija Radović: Conceptualization, Formal analysis, Investigation, Methodology, Visualization, Writing - original draft, Writing - review & editing. **Vedran Carević:** Conceptualization, Methodology, Supervision, Writing - original draft. **Aleksandar Radević:** Conceptualization, Funding acquisition, Visualization, Writing - original draft. **Branislav Stupar:** Investigation. **Darko Veličkov:** Investigation.

Declaration of Competing Interests:

The authors declare that they have no known competing financial interests or personal relationships that could have appeared to influence the work reported in this paper.

Acknowledgement:

This work was supported by the Ministry for Education, Science and Technology, Republic of Serbia [grant number 200092].

References

[1] GCCA, “CONCRETE FUTURE: The GCCA 2050 Cement and Concrete Industry Roadmap for Net Zero Concrete,” Glob. Cem. Concr. Assoc., p. London, 2021, [Online]. Available: https://gccassociation.org/concretefuture/wp-content/uploads/2021/10/GCCA-Concrete-Future-Roadmap.pdf

[2] ISO/TC 071, “Strategic Business Plan ISO/TC 071 (ISO Technical Committee for concrete, reinforced concrete and prestressed concrete),” 2016, [Online]. Available: https://www.iso.org/

[3] S. Marinković, V. Radonjanin, M. Malešev, and I. Ignjatović, “Comparative environmental assessment of natural and recycled aggregate concrete,” Waste Manag., vol. 30, no. 11, pp. 2255–2264, 2010, doi: 10.1016/j.wasman.2010.04.012.

[4] S. A. Miller, A. Horvath, and P. J. M. Monteiro, “Readily implementable techniques can cut annual CO2 emissions from the production of concrete by over 20%,” Environ. Res. Lett., vol. 11, no. 7, 2016, doi: 10.1088/1748-9326/11/7/074029.

[5] CEMBUREAU, “Cementing the European Green Deal - Reaching climate neutrality along the cement and concrete value chain by 2050,” Eur. Cem. Assoc. Brussels, pp. 1–38, 2020, [Online]. Available: https://cembureau.eu/media/kuxd32gi/cembureau-2050-roadmap_final-version_web.pdf

[6] K. L. Scrivener, V. M. John, and E. M. Gartner, “Eco-efficient cements: Potential economically viable solutions for a low-CO2 cement-based materials industry,” Cem. Concr. Res., vol. 114, no. February, pp. 2–26, 2018, doi: 10.1016/j.cemconres.2018.03.015.

[7] Working group UNEP-SBCI, “Eco-efficient cements: Potential economically viable solutions for a low-CO2 cement-based materials industry,” United Nations Environ. Progr. - Sustain. Build. Clim. Initiat., pp. 1–64, 2015, [Online]. Available: https://wedocs.unep.org/bitstream/handle/20.500.11822/25281/eco_efficient_cements.pdf

[8] V. M. John, B. L. Damineli, M. Quattrone, and R. G. Pileggi, “Fillers in cementitious materials — Experience, recent advances and future potential,” Cem. Concr. Res., vol. 114, pp. 65–78, 2018, doi: 10.1016/j.cemconres.2017.09.013.

[9] D. Wang, C. Shi, N. Farzadnia, Z. Shi, and H. Jia, “A review on effects of limestone powder on the properties of concrete,” Constr. Build. Mater., vol. 192, pp. 153–166, 2018, doi: 10.1016/j.conbuildmat.2018.10.119.

[10] A. Radović, H. Hafez, N. Tošić, S. Marinković, and A. de la Fuente, “ECO2 framework assessment of limestone powder concrete slabs and columns,” J. Build. Eng., vol. 57, no. October, p. 104928, 2022, doi: 10.1016/j.jobe.2022.104928.

[11] K. Tešić, S. Marinković, and A. Savić, “Influence of cement replacement with limestone filler on the properties of concrete,” Build. Mater. Struct., vol. 64, no. 3, pp. 165–170, 2021, doi: 10.5937/grmk2103165t.

[12] A. Radović, S. Marinković, and A. Savić, “Compressive strength of green concrete with low cement and high filler content”, Build. Mater. Struct., vol. 64, no. 2, pp. 93–108, 2021, doi: 10.5937/grmk2102093r.

[13] M. Rezvani, T. Proske, S. Hainer, and C. Graubner, “Rheology of eco-friendly self-compacting concretes with limestone-rich cements,” in Proceedings of International Symposium on Eco-Crete, Reykjavik, Island, 2014, p. 8.

[14] T. Proske, S. Hainer, M. Rezvani, and C.-A. A. Graubner, “Eco-friendly concretes with reduced water and cement content – Mix design principles and application in practice,” Constr. Build. Mater., vol. 67, pp. 413–421, Sep. 2014, doi: 10.1016/j.conbuildmat.2013.12.066.

[15] M. S. Meddah, M. C. Lmbachiya, and R. K. Dhir, “Potential use of binary and composite limestone cements in concrete production,” Constr. Build. Mater., vol. 58, pp. 193–205, 2014, doi: 10.1016/j.conbuildmat.2013.12.012.

[16] R. K. Dhir, M. C. Limbachiya, M. J. McCarthy, and A. Chaipanich, “Evaluation of Portland limestone cements for use in concrete construction,” Mater. Struct., vol. 40, pp. 459–473, 2007, doi: 10.1617/s11527-006-9143-7.

[17] J. J. Chen, A. K. H. Kwan, and Y. Jiang, “Adding limestone fines as cement paste replacement to reduce water permeability and sorptivity of concrete,” Constr. Build. Mater., vol. 56, pp. 87–93, 2014, doi: 10.1016/j.conbuildmat.2014.01.066.

[18] A. Radović, V. Carević, S. Marinković, J. Plavšić, and K. Tešić, “Prediction model for calculation of the limestone powder concrete carbonation depth,” J. Build. Eng., vol. 86, no. June, p. 108776, 2024, doi: 10.1016/j.jobe.2024.108776.

[19] M. Rezvani and T. Proske, “Influence of chemical-mineralogical properties of limestone on the shrinkage behaviour of cement paste and concrete made of limestone-rich cements,” Constr. Build. Mater., vol. 157, pp. 818–828, 2017, doi: 10.1016/j.conbuildmat.2017.09.101.

[20] A. K. H. Kwan, J. J. Chen, and Y. Jiang, “Adding limestone fines as cement paste replacement to reduce shrinkage of concrete,” Mag. Concr. Res., vol. 65, no. 15, pp. 942–950, 2015, doi: 10.1680/macr.13.00028.

[21] T. Proske, S. Hainer, M. Rezvani, and C. A. Graubner, “Eco-friendly concretes with reduced water and cement contents - Mix design principles and laboratory tests,” Cem. Concr. Res., vol. 51, pp. 38–46, 2013, doi: 10.1016/j.cemconres.2013.04.011.

[22] T. Proske, S. Hainer, M. Rezvani, and C. A. Graubner, “Eco-Friendly Concretes With Reduced Water and Cement Content: Mix Design Principles and Experimental Tests,” Handb. Low Carbon Concr., pp. 63–87, 2017, doi: 10.1016/B978-0-12-804524-4.00004-X.

[23] M. Lundgren, “Limestone Filler as Addition in Cement Mortars: Influence on the Early-Age Strength Development at Low Temperature,” Nord. Concr. Res., no. 31, pp. 50–63, 2004.

[24] L. G. Li and A. K. H. Kwan, “Adding limestone fines as cementitious paste replacement to improve tensile strength, stiffness and durability of concrete,” Cem. Concr. Compos., vol. 60, pp. 17–24, 2015, doi: 10.1016/j.cemconcomp.2015.02.006.

[25] A. M. Diab, I. A. Mohamed, and A. A. Aliabdo, “Impact of organic carbon on hardened properties and durability of limestone cement concrete,” Constr. Build. Mater., vol. 102, pp. 688–698, 2016, doi: 10.1016/j.conbuildmat.2015.10.182.

[26] Y. J. Kim, R. van Leeuwen, B. Y. Cho, V. Sriraman, and A. Torres, “Evaluation of the efficiency of limestone powder in concrete and the effects on the environment,” Sustain., vol. 10, no. 2, pp. 1–24, 2018, doi: 10.3390/su10020550.

[27] K. Robalo, E. Soldado, H. Costa, L. Carvalho, R. do Carmo, and E. Júlio, “Durability and time-dependent properties of low-cement concrete,” Mater., vol. 13, no. 3583, pp. 1–29, 2020, doi: 10.3390/MA13163583.

[28] P. D. Tennis, “Portland-Limestone Cements : History , Performance , and Specifications T,” Portland-Limestone Cem., vol. 2, no. 1, pp. 1–45, 2011.

[29] M. Marinković, A. Radović, and V. Carević, “Carbonation of limestone powder concrete: “State-of-the-art overview”, Build. Mater. Struct., vol. 66, no. 00, pp. 127–139, 2023, doi: 10.5937/grmk2300005m.

[30] M. Muravljov, D. Zakić, and A. Radević, “ Concrete technology: theory and practice,” University of Belgrade Faculty of Civil Engineering, 2022. (In Serbian)

[31] A. A. Ramezanianpour, E. Ghiasvand, I. Nickseresht, M. Mahdikhani, and F. Moodi, “Influence of various amounts of limestone powder on performance of Portland limestone cement concretes,” Cem. Concr. Compos., vol. 31, no. 10, pp. 715–720, 2009, doi: 10.1016/j.cemconcomp.2009.08.003.

[32] P. Faustino, C. Chastre, Â. Nunes, and A. Brás, “Lifetime modelling of chloride-induced corrosion in concrete structures with Portland and blended cements,” Struct. Infrastruct. Eng., vol. 12, no. 9, pp. 1013–1023, 2016, doi: 10.1080/15732479.2015.1076487.

[33] L. Bertolini, F. Lollini, and E. Redaelli, “The Effect of Ground Limestone Addition on Carbonation and Chloride Resistance of Concrete,” XII DBMC Int. Conf. Durab. Build. Mater. Components, pp. 1–8, 2011.

[34] L. Bertolini, F. Lollini, E. Redaelli, M. Dipartimento, and I. Chimica, “Influence of concrete composition on parameters related to the durability of reinforced concrete structures,” Int. RILEM Work. Integr. Serv. Life Model. Concr. Struct., no. November, pp. 71–78, 2013.

[35] E. Gruyaert, “Effect of blast-furnace slag as cement replacement on hydration, microstructure, strength and durability of concrete,” Ghent Univ. Fac. Eng. Archit., pp. 345, Doctoral dissertation, 2011.

[36] V. Bonavetti, H. Donza, V. Rahhal, and E. Irassar, “Influence of initial curing on the properties of concrete containing limestone blended cement,” Cem. Concr. Res., vol. 30, pp. 703–708, 2000.

[37] W. Jin, L. Jiang, L. Han, L. Chen, X. Yan, and C. Chen, “Influence of curing temperature on the mechanical properties and microstructure of limestone powder mass concrete,” Struct. Concr., vol. 22, no. S1, pp. E745–E755, 2021, doi: 10.1002/suco.201900549.

[38] J. Sun and Z. Chen, “Influences of limestone powder on the resistance of concretes to the chloride ion penetration and sulfate attack,” Powder Technol., vol. 338, pp. 725–733, 2018, doi: 10.1016/j.powtec.2018.07.041.

[39] V. Bonavetti, H. Donza, G. Menéndez, O. Cabrera, and E. F. Irassar, “Limestone filler cement in low w/c concrete: A rational use of energy,” Cem. Concr. Res., vol. 33, no. 6, pp. 865–871, 2003, doi: 10.1016/S0008-8846(02)01087-6.

[40] H. Hornain, J. Marchand, V. Duhot, and M. Moranville-Regourd, “Diffusion of chloride ions in limestone filler blended cement pastes and mortars,” Cem. Concr. Res., vol. 25, no. 8, pp. 1667–1678, 1995, doi: 10.1016/0008-8846(95)00163-8.

[41] EN 197-1, “Cement - Part 1: Composition, specifications and conformity criteria for common cements,” Eur. Comm. Stand. Brussels, 2013.

[42] EN 206, “Concrete - Specification, performance, production and conformity,” Eur. Comm. Stand. Brussels, 2021.

[43] EN 1992-1-1, “Eurocode 2: Design of concrete structures - Part 1-1, General rules and rules for buildings,” Eur. Comm. Stand. Brussels, 2015.

[44] EN 12350-2, “Testing fresh concrete – Part 2: Slump test,” Eur. Comm. Stand. Brussels, 2019.

[45] EN 12390-2, “Testing hardened concrete - Part 2: Making and curing specimens for strength tests,” Eur. Comm. Stand. Brussels, 2019.

[46] EN 12390-3, “Testing hardened concrete - Part 3: Compressive strength of test specimens,” Eur. Comm. Stand. Brussels, 2019.

[47] EN 12390-5, “Testing hardened concrete - Part 5: Flexural strength of test specimens,” Eur. Comm. Stand. Brussels, 2019.

[48] EN 12390-8, “Testing hardened concrete - Part 8: Depth of penetration of water under pressure,” Eur. Comm. Stand. Brussels, 2019.

[49] EN 12390-18, “Testing hardened concrete - Part 18: Determination of the chloride migration coefficient,” Eur. Comm. Stand. Brussels, 2018.

[50] V. Carević, “ Influence of cracks on the deterioration mechanisms and durability of reinforced concrete structures,” University of Belgrade Faculty of Civil Engineering, pp. 233, Doctoral dissertation, 2020. (In Serbian)

[51] J. Dragaš, “Ultimate capacity of high volume fly ash reinforced concrete beams,” University of Belgrade Faculty of Civil Engineering, pp. 501, Doctoral dissertation, 2018.

[52] N. Tošić, “Behaviour of reinforced concrete beams made with recycled and waste materials under long-term loading,” University of Belgrade Faculty of Civil Engineering, pp. 641, Doctoral dissertation, 2017.

[53] SRPS U.M1.206, “Guidance and rules for national technical requirements for production of concrete applied in concrete, reinforced concrete and prestressed concrete structures,” Inst. Stand. Serbia, 2023.

[54] Q. Wang, J. Yang, and H. Chen, “Long-term properties of concrete containing limestone powder,” Mater. Struct., vol. 50, no. 3, 2017, doi: 10.1617/s11527-017-1040-8.

Građevinski materijali i konstrukcije
Building Materials and Structures
journal homepage: www.dimk.rs

https://doi.org/10.5937/GRMK2400005B UDK: 666.972.1:620.1
691.322:620.17

Original scientific paper

Impact of manufactured sand and sintered fly ash aggregate on the mechanical and durability characteristics of normal-strength concrete

Ranjith Babu Baskaran*[1)], Nagarajan Divyah[2)]

[1)] *Department of Civil Engineering, PSNA College of Engineering and Technology, Dindigul. ORCID 0000-0002-4690-7834*
[2)] *Department of Civil Engineering, PSG Institute of Technology and Applied Research, Coimbatore.ORCID 0000-0001-5381-8226*

Article history
Received: 26 April 2024
Received in revised form: 29 June 2024
Accepted: 03 July 2024
Available online: 30 August 2024

Keywords
sintered flyash aggregates,
mechanical properties,
impact strength,
M-sand,
durability studies

ABSTRACT

This study examined the impact of substituting Natural Coarse Aggregate (NCA) with varying quantities of sintered fly ash aggregate (SFA) in concrete. To ensure sustainability, manufactured sand (M-Sand) was consistently substituted for river sand in all mixtures. Slump values increased as the SFA content increased, which positively impacted workability. The results suggest that a complete replacement of the coarse aggregates can achieve substantial weight reduction potential. Even though compressive strength, split tensile strength, flexural strength, and Young's modulus decreased as the SFA content increased, all compositions (SFA0, SFA50, and SFA100) surpassed the minimum field requirement of 20 MPa compressive strength. Impact testing adversely affected the impact strength of the SFA50 mix, while SFA0 and SFA100 demonstrated comparable failure modes. It is important to note that replacing 50% NCA with SFA resulted in an increase in concrete durability, as demonstrated by a lower average sorptivity value. The results of this study indicate that SFA is a potential partial replacement for NCA. It provides advantages in terms of workability, weight reduction, and potential enhanced durability, while still maintaining adequate strength for field applications.

1 Introduction

Concrete construction has demonstrated the numerous advantages of using lightweight materials like sintered flyash aggregates, crushed clay bricks, and coconut shells. The advantages include possible cost savings, a decrease in autogenous shrinkage, and a reduction in concrete density when compared to ordinary concrete [1, 2 and 3]. Low bulk density, strong thermal insulation, and fire resistance are just a few of the benefits that make lightweight concrete a viable choice for both structural and non-structural building applications. The use of lightweight aggregates in concrete significantly reduces pouring costs.

The Sintered Flyash Aggregates (SFA) are produced with the help of flyash from thermal power plants mixed with 90 % water to convert in the form of pelletization and further, it is heated to produce lightweight aggregate. These sintered aggregates have an advantage in the construction industry in making structural lightweight concrete, arrestor beds, filter media, roof tiles, and land drainages [4]. Manufactured Sand (M-Sand) is made by crushing the hard granite stones into small, angular-shape particles that are washed and finely graded to be used as an alternative to river sand. The M-sand has almost an equal character as compared to river sand, which is less expensive and free from silt and clay particles [5].

The compressive strength of lightweight aggregates is never entirely dependent on porosity [6-7]. Several associated variables, such as changes in the mineralogical composition [8], the melting temperature of binders [9], the margin of densification during sintering [10], aggregate bloating [11], and internal flaws caused by thermal pressures [12], further influence the compressive strength. The recommended methods for designing concrete mixes for the development of Lightweight Aggregate Concrete (LWAC) differ greatly from standard approaches for designing aggregate concrete mixes [13]. The majority of mix design approaches, regardless of the aggregate properties and necessary strength, focus on fixing the paste volume of concrete or aggregate content [14]. This approach highlights the durability and strength of the material. Because lightweight aggregate is porous [15], it has a lower compressive strength capability and less free water in the paste matrix. Therefore, a substantial amount of cement paste is required to achieve optimal workability and strength. This might have an impact on the durability requirements of structural concrete.

The addition of sintered flyash aggregate strengthens the bond between the aggregate surfaces and cement paste [16, 17]. Extensive research is being carried out on the sustainable production of lightweight concrete using sintered flyash aggregates [18]. The researchers observed an

* Corresponding author:
E-mail address: ranjithbabucivil@psnacet.edu.in

increase in water absorption and voids as the proportion of sintered aggregates increased. Replacing 40% (by mass) of sintered flyash aggregate with 100% natural aggregates can increase the strength of the concrete [19]. Furthermore, reports indicate that using manufactured sand in ultra-high-strength concrete produces hydration products that are denser than those made with natural sand [20, 21].

The spherical shape of sintered flyash aggregate positively impacts the LWAC's workability. When comparing sintered flyash aggregates to regular angular aggregates, it is seen that a comparatively smaller amount of superplasticizer is needed to produce the required slump. Increased water-to-cement ratios or the use of plasticizer are suggested as ways to improve the workability of concrete made completely of manufactured sand [22]. Previous research revealed better compressive strength outcomes when compared to conventional aggregate concretes. It was also observed that the Interfacial Transition Zone (ITZ) has a major role in regulating the strength of the LWAC and that the strength of the aggregate alone does not influence the compressive strength of the concrete that is formed. When compared to regular concrete, variables such as test specimen size, loading rate, multi-axial stress, etc. have negligible effects in LWAC. Furthermore, it is noted that the correlations between cylinder and cube strength in standard concrete and LWAC differ.

Concrete's high permeability and capillary permeability primarily contribute to its durability. One such simple laboratory-based measurement, sorptivity, determines the durability index by measuring the amount of water that penetrates the concrete, and it holds practical significance. The lower the sorptivity value, the concrete will have a higher paste and a densified microstructure [16].

By analyzing the combined effects of Manufactured Sand (M-Sand) and Sintered Flyash Aggregate (SFA), this initiative pushes the limits of sustainable concrete production. The research successfully develops structurally lightweight concrete while simultaneously promoting resource conservation through the partial and complete replacement of natural river sand with SFA. This represents a substantial contribution due to the potential cost savings and weight reduction benefits of lightweight concrete. The compressive strength, split tensile strength, flexural strength, Young's modulus, impact resistance against drop weight, and sorptivity of these samples are then experimentally examined. Overall, this study illuminates the potential of SFA and M-Sand as viable materials for sustainable construction applications, demonstrating encouraging outcomes in terms of strength, workability, and durability.

2 Experimental programme

2.1 Materials

The components utilized in creating the concrete mix were the following.

2.1.1 Cement

In this study, Ordinary Portland Cement (OPC) of 53 grade, produced by KPC Limited in India and meeting the IS:12269 standards [23], served as the binding agent. The laboratory assessed several properties of the cement, including specific gravity, fineness, setting time, and consistency, through various standard experiments as per the BIS code (IS 4031 Part 2, 4, 5, 11) [24-27]. Table 1 details the outcomes of these experiments.

2.1.2 Manufactured sand (M-sand)

The M-sand utilized in the concrete blend was procured from local suppliers in the vicinity. A grading analysis for the manufactured sand is in accordance with [28]. The sieve analysis graph in Figure 1 shows that the manufactured sand fits into Zone III of IS:383, and the particle size distribution is within the range of values given in IS:383. Additionally, the properties of manufactured sand are determined in accordance with BIS specifications [28, 29], which is enumerated in Table 2.

Table 1. Physical Properties of Cement Under Examination

Properties	Test results	Test method
Specific gravity	3.15	IS: 4031 (Part- 11) [27]
Fineness (m^2/kg)	320	IS: 4031 (Part- 2) [24]
Consistency (%)	33	IS: 4031 (Part- 4) [25]
Setting times (min)		IS: 4031 (Part- 5) [26]
(a) Initial setting time	52	
(b) Final setting time	300	

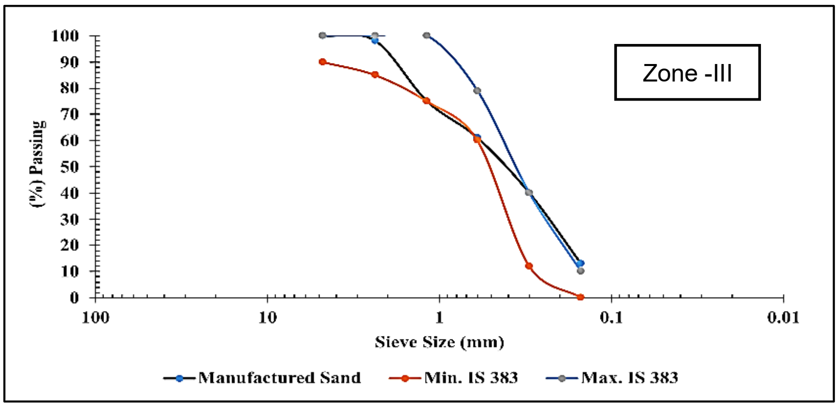

Figure 1. Gradation Curve for Manufactured Sand

Table 2. Physical Properties of Manufactured Sand

Properties	M-sand	Test method
Bulk density (Loose)	1632 kg/m^3	IS: 2386 (part -3) [29]
Bulk density (Compacted)	1797 kg/m^3	IS: 2386 (part -3) [29]
Specific gravity	2.5	IS: 2386 (part -3) [29]
Water absorption	0.4 %	IS: 2386 (part -3) [29]
Fineness modulus	2.14	IS: 2386 (part -1) [28]

2.1.3 Natural coarse aggregates (NCA)

The NCA used in the concrete mix was sourced from locally convenient suppliers. Grading analysis for coarse natural aggregates was carried out [28]. Figure 2 presents the sieve analysis graph. Table 3 also displays the properties of natural coarse aggregates determined according to BIS specifications [28, 29].

2.1.4 Sintered fly ash aggregates (SFA)

The SFA has been purchased from Ahmedabad, Gujarat, India, for use in the concrete mix. The SFA is spherical and brownish-grey, as seen in Figure 3. The various properties of SFA acquired in accordance with IS codal regulations are listed in Table 4. Table 4 shows that SFA was more capable of absorbing water than NCA. This increased water absorption influenced the porous nature of SFA. Figure 4 shows the sieve analysis graph and the grading analysis for sintered fly ash aggregate [28].

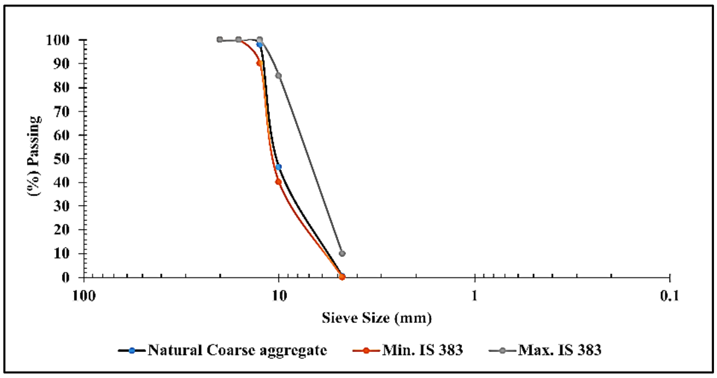

Figure 2. Gradation Curve for Natural Coarse Aggregates

Table 3. Tested Physical Properties of Natural Coarse Aggregates

Properties	NCA	Test method
Bulk density (Loose)	1467 kg/m^3	IS: 2386 (part -3) [29]
Bulk density (Compacted)	1640 kg/m^3	IS: 2386 (part -3) [29]
Specific gravity	2.4	IS: 2386 (part -3) [29]
Water absorption	1 %	IS: 2386 (part -3) [29]
Fineness modulus	2.6	IS: 2386 (part -1) [28]

Figure 3. Typical View of Sintered Fly ash Aggregates

Table 4. Physical Properties of Sintered Fly ash Aggregates

Properties	SFA	Test method
Bulk density - Loose	778 kg/m^3	IS: 2386 (part -3) [29]
Bulk density - Compacted	862 kg/m^3	IS: 2386 (part -3) [29]
Specific gravity	1.6	IS: 2386 (part -3) [29]
Water absorption	16.8 %	IS: 2386 (part -3) [29]
Fineness modulus	2.87	IS: 2386 (part -1) [28]
Impact value	27.78 %	IS: 2386 (part -4) [30]
Crushing value	15.63 %	IS: 2386 (part -4) [30]

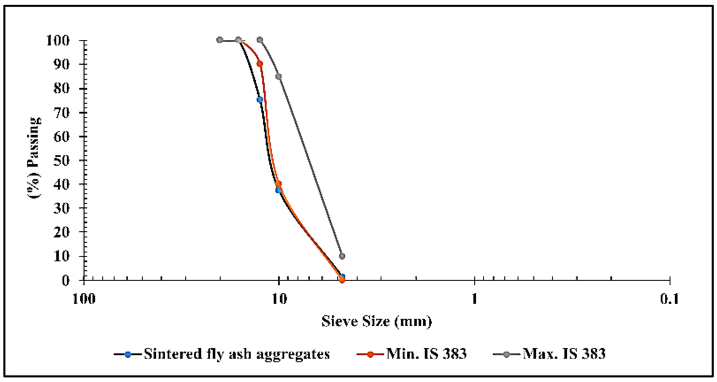

Figure 4. Gradation Curve for Sintered Fly ash Aggregates

2.1.5 Water

Portable water from the laboratory supply [31] was utilized in the production of this concrete mix.

2.1.6 Superplasticizer (SP)

Conplast SP430, a chloride-free additive based on sulphonated naphthalene polymers, was incorporated to enhance the workability of the concrete mix and serves as a water-reducing agent. All concrete mixes with a brown hue and a specific gravity of 1.22 received a dosage of 2% SP relative to the cement content.

2.2 Concrete Mix

The design of M30-grade concrete [32] used a control mix with a slump of 95 +/- 5 mm. Following the guidelines, coarse aggregates were utilized in Saturated Surface Dry (SSD) conditions for all mixes. Unlike SFA and NCA, where SFA exhibited a higher water absorption percentage, we maintained the water-to-cement ratio constant across all mixes. To achieve SSD conditions, additional water was introduced to the aggregate surfaces before mixing. SFA was substituted in the concrete mix by 50% and 100% of NCA, respectively, with the specific weight of the SFA serving as the primary parameter for coarse aggregate replacement. Table 5 provides detailed mix specifications.

2.2.1 Casting and curing of specimens

The initial step in preparing the concrete mix involved dry-mixing the ingredients - cement, M-sand, NCA, and SFA - in the concrete mixer machine for three minutes. Subsequently, the dry mix was blended with water for five minutes to ensure uniformity in the concrete mixture. The concrete was poured into designated moulds, such as cubes, cylinders, prisms, and discs, after conducting a slump test to determine its consistency, and allowed it to set for 24 hours. Afterwards, the concrete samples were removed from the moulds and immersed in a concrete water curing tank until they reached the required curing age of 28 days. To facilitate various tests, specimens for each concrete mix were cast as follows.

- 3 nos. of 100 mm cubes both fresh and dry, were used to measure the compressive strength after 28 days.
- 3 nos. of 100 x 200 mm cylinders were tested for split tensile strength after 28 days.
- 3 nos. of 150 x 300 mm cylinders were used for Young's modulus test after 28 days;
- 3 nos. of 100 x 100 x 500 mm prisms were used for the determination of flexural strength after 28 days;
- 3 nos. of 150 x 64 mm discs were used for the determination of drop weight impact test after 28 days;
- 2 nos. of 100 x 50 mm discs were used for the determination of water sorptivity test after 28 days.

Table 5. Mix details for concrete

Mix Designation	Replacement of NCA with SFA (%)	Cement (kg/m^3)	M - Sand (kg/m^3)	NCA (kg/m^3)	SFA (kg/m^3)	Water (kg/m^3)	SP(%)
SFA0	0	435	771	904	0	152.4	2
SFA50	50	435	771	301	301	152.4	2
SFA100	100	435	771	0	603	152.4	2

2.3 Testing Procedures

BIS and ASTM standards [33-37] were referenced to find various properties of the concrete specimens, including density (both fresh and dry), compressive strength, split tensile strength, flexural strength, Young's modulus, drop weight impact tests, and sorptivity tests.

3 Test results and discussion

3.1 Workability Measures

Figure 5 shows the change in slump values for different levels of SFA in concrete. Using M-sand in concrete instead of river sand reduces the slump value. The concrete mix without SFA has a lower slump value than the concrete mix containing 50% and 100% SFA. When SFA is replaced, the slump value increased by 55% and 73% compared to the concrete mix that does not contain SFA.

3.2 Wet and dry density

Figure 6 provides the change in the wet and dry density of the concrete mix. The concrete mix containing 0% SFA has a wet density of 2650 kg/m^3. The addition of 50% and 100% SFA in the concrete mix reduced the wet density by 13% and 20%, respectively. A similar trend in the dry mix was observed. The dry density of the concrete mix, which contains 0% SFA, is 2570 kg/m^3. Further additions of 50% and 100% SFA in the concrete mix reduce the dry density to 14% and 19%, respectively. M-sand is used in all concrete mixes to increase wet and dry density. Concrete with a combination of light and normal weight aggregate [37] has a specific density greater than 2480 kg/m^3 and can be defined as structural concrete.

3.3 Compressive Strength Test

Figure 7 displays the average test results of concrete cube samples after 28 days of normal water-curing. The 50% replacement of SFA in concrete reduces the compressive strength of the concrete by 17.14% and the 100% replacement of SFA reduces the compressive strength by 31.4%. The 100% SFA replacement signifies its structural lightweight nature, as its compressive strength is more than 21 MPa [37].

3.4 Split Tensile Strength

Figure 8 displays the 28-day split tensile strength values based on [34]. The increased SFA content in the concrete decreases the split tensile strength. 50% SFA in concrete decreases the split tensile strength by 27.2%, and 100% SFA in concrete decreases the split tensile strength by 20.3%.

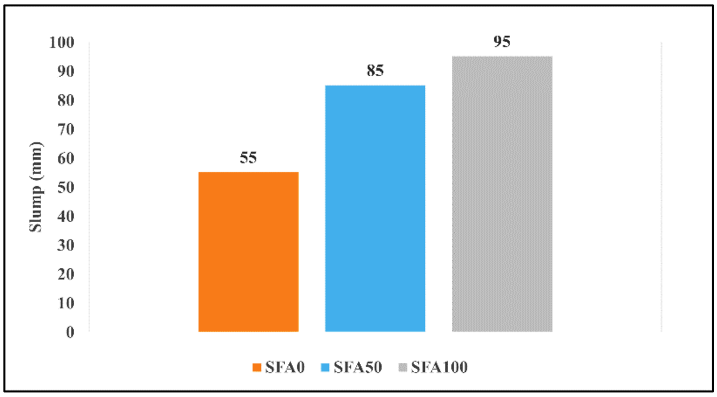

Figure 5. Variation of Slump Value for Different Levels of SFA In Concrete Mix

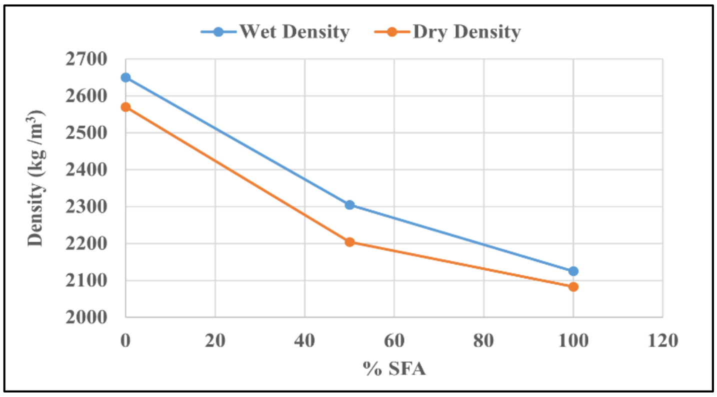

Figure 6. Wet And Dry Density of Concrete Mix Contains Varying SFA

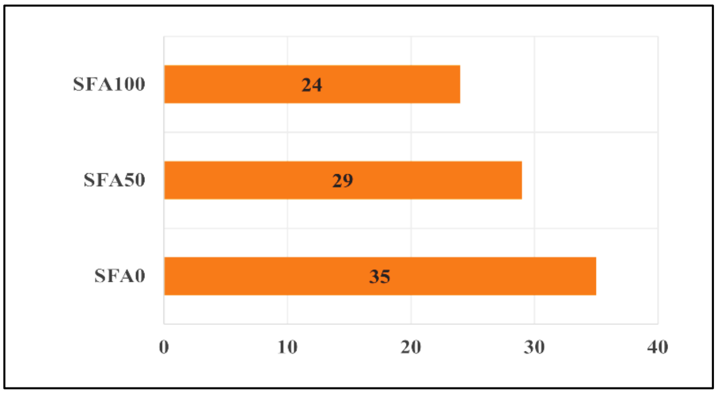

Figure 7. The Compressive Strength of Concrete Mix Contains Varying SFA

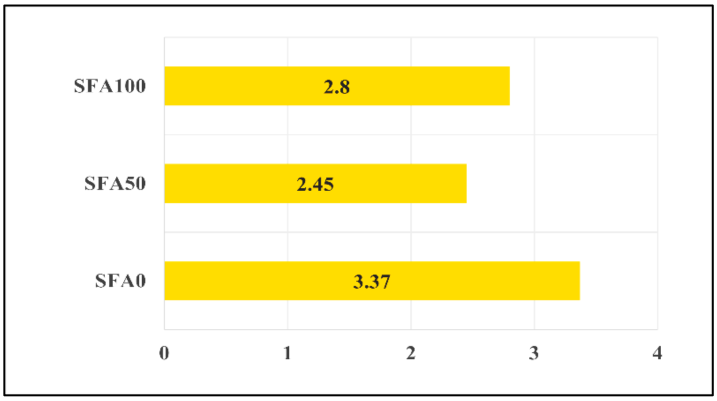

Figure 8. Split Tensile Strength of Concrete Mix Contains Varying SFA

Figure 9 illustrates the failure mode of tested split tensile cylindrical specimens. Various international codes were used [38–42] to compare the experimental values of split tensile strength. Table 5 provides the empirical formulas used for the prediction. The required cylinder compressive strength for the prediction of split tensile strength is calculated by multiplying 0.8 with cube compressive strength [43]. Figure 10 displays the predicted split tensile strength at 28 days using empirical formulas.

According to the ACI code regulation, replacing 50% of the coarse aggregate (SFA) in a concrete mix results in a split tensile strength that is higher than the strength of the tested samples. The observed values were greater than the projected values in the remaining codes. The drop in strength causes the SFA to rupture and pop out at 50% and 100% in the concrete mix [18]. The use of M-sand in concrete demonstrates its equivalence with river sand.

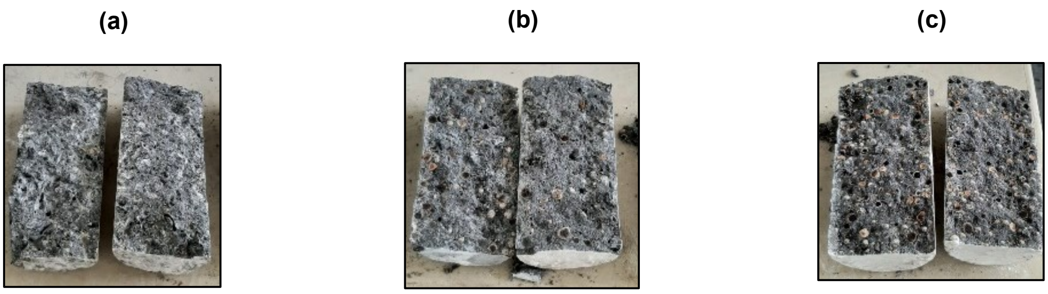

Figure 9. 28-Day Split Tensile Failure of Concrete Cylinders Contains SFA (a) 0% (b) 50% (c) 100%

Table 5. Formulas to Predict Split Tensile Strength (fsp), Flexural Strength (fcr), and Modulus of Elasticity (E) from Compressive Strength (fc or f'c)

Split tensile strength (fsp)	Flexural strength (fcr)	Modulus of elasticity (E)
$f_{sp} = 0.56\sqrt{f_c'}$[38]	$f_{cr} = 0.62\sqrt{f_c'}$[38]	$E = 4700\sqrt{(0.8f_c)}$[38]
$f_{sp} = 1.56\left[\frac{f'_c-8}{10}\right]^{\frac{2}{3}}$[39]	$f_{cr} = 0.70\sqrt{f_c}$[45]	$E = 5000\sqrt{f_c}$[45]
$f_{sp} = 0.21(f_c')^{\frac{2}{3}}$[40]	$f_{cr} = 0.81\sqrt{f_c}$[39]	$E = \left(\frac{100000}{2.8+\frac{40.1}{f_c}}\right)$ [44]
$f_{sp} = 0.19(f_c')^{0.75}$[41]	$f_{cr} = 0.75\sqrt{f_c}$[44]	
$f_{sp} = 0.19(f_c')^{\frac{2}{3}}$[42]		
Note: f_c and f'_c are 28-day cube and cylinder compressive strength, respectively.		

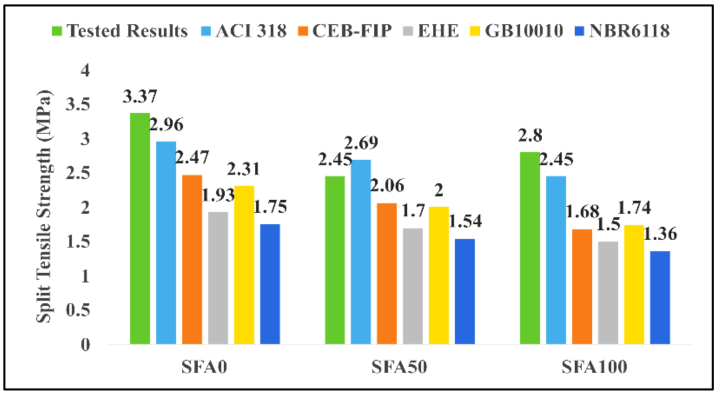

Figure 10. Comparison Between Predicted and Experimental Split Tensile Strength for The Concrete Mixture Containing Varying Percentages of SFA

3.5 Flexural Strength Test

The flexural strength was determined in the concrete cast [33]. Figure 11 depicts the variation in flexural strength at 28 days for concrete prisms made with an SFA-containing concrete mix. The flexural strength values exhibit a similar pattern to that observed in the split tensile and compressive strength data. For concrete mixes containing 50% and 100% SFA, respectively, the flexural strengths dropped by 25% and 14.8%. This decrease is caused by the addition of SFA to the concrete mix. The complete substitution results in a decrease in flexural strength of 14.8% when compared to a 50% SFA mixture. This suggests that a 100% SFA mixture exhibits the characteristics of lightweight concrete. Figure 12 depicts the failures of the evaluated flexural strength prism specimens.

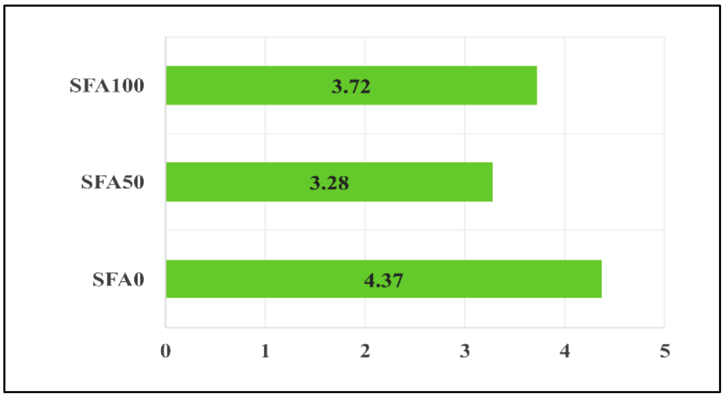

Figure 11. Flexural Strength of Concrete Mix Contains Varying SFA

The experimental flexural strength values were compared with various international codes available [38, 45, 39, 44]. Table 5 provides the empirical formulas used for predicting flexural strength. The formula suggests multiplying the cylinder's compressive strength by a factor of 0.8 by its corresponding cube compressive strength [43]. Figure 13 displays the predicted flexural strength results for the mix after 28 days. In comparison to the other codes, CEB-FIP predicts flexural strength with the highest accuracy. The flexural strength values for the concrete mix with 0% and 100% SFA predicted by the code DG/TJ demonstrate good agreement with experimental values. As the SFA content increased, the flexural strength values decreased. All concrete mixes contain M-sand, which had the similar properties as river sand.

3.6 Modulus of Elasticity

Figure 14 shows the variation of the 28-day tested secant modulus of elasticity (working stress) values, which are based on the cylindrical compressive stress-strain values. As the percentage replacement of SFA increased, the concrete mix's modulus of elasticity decreased. The split tensile and flexural strength values also follow the same trend.

The percentage decrease in secant modulus is 24.2% for SFA 50% and 46% for SFA 100. These reductions in elastic values are only due to the presence of SFA in the concrete mix. The modulus of elasticity determined experimentally is compared with various international codal provisions [38, 45, 44]. Table 5 lists the empirical values. Figure 15 displays the predicted values. The anticipated outcomes indicate that the

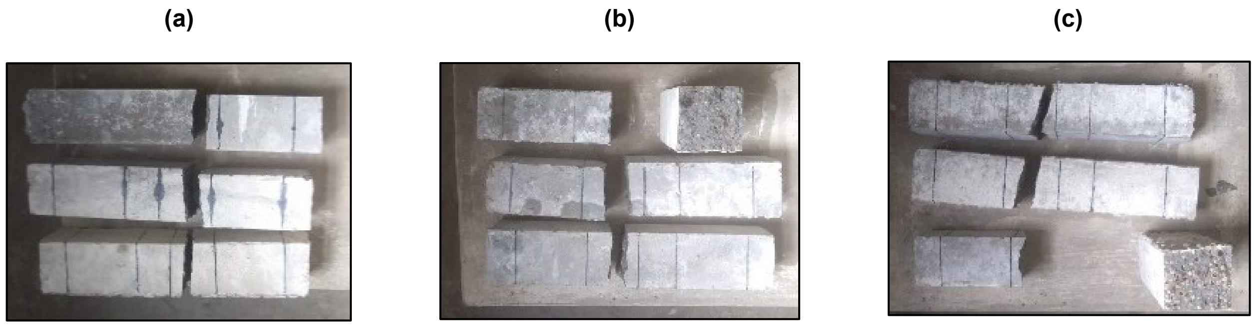

Figure 12. Flexural Failure of Concrete Prisms Contains. SFA (a) 0 % (b) 50 % (c) 100 %

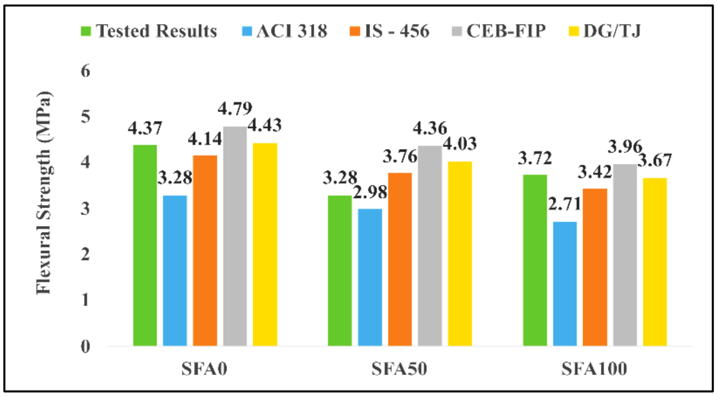

Figure 13. Comparison Between Predicted and Experimental Flexural Strength for The Concrete Mixture Containing Varying Percentages of SFA

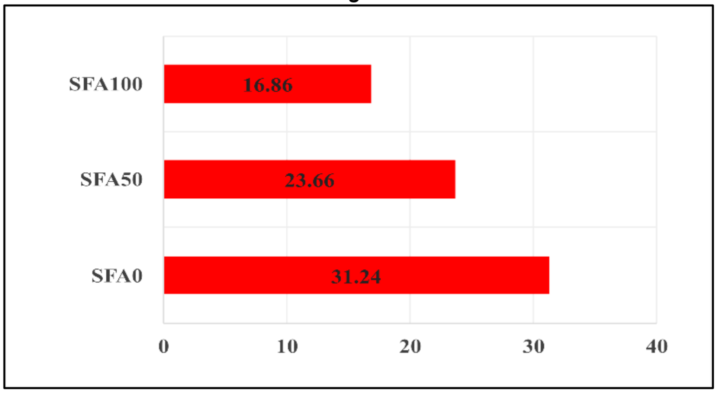

Figure 14. Modulus of elasticity of concrete mixture contains varying SFA

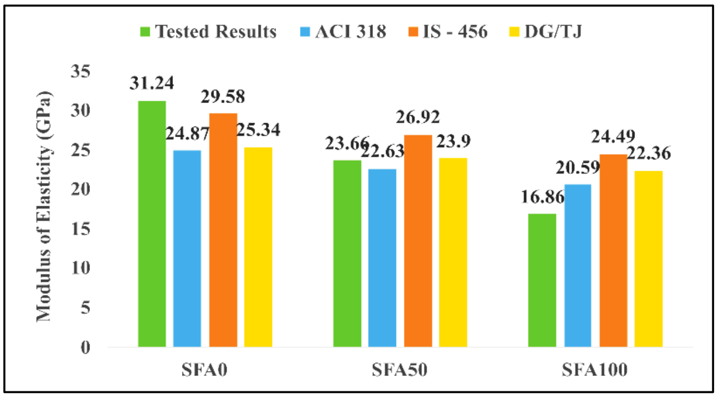

Figure 15. Comparison Between Predicted and Experimental Modulus of Elasticity for The Concrete Mixture Containing Varying Percentages of SFA

concrete mix comprising 50% and 100% SFA exhibits greater values compared to the experimental data. We observed that the IS 456:2000 code yields higher predictions than other codes. Unlike the SFA content, the use of M-sand in concrete shows no signs of degradation.

3.7 Drop Weight Impact Test

A simple drop weight test was used [46] to calculate the impact energy (J) of the concrete mix on nine 150-mm-diameter and 64-mm-high cylindrical specimens. Figure 16 displays the fabricated drop-weight impact tester. The test procedure follows: We released a 4.56 kg cylindrical mass, measuring 7 cm in diameter and 15 cm in height, from a height of 457 mm, and it collided with a 64 mm diameter steel ball that touched the top surface of the concrete specimens. The number of blows until the first crack appears (N1) is recorded. Then the test is continued until the cracks appear from bottom to top and the ultimate failure (N2) of the specimen is recorded.

The impact energy of each specimen was calculated using Equation [1]:

$$Impact\ Energy\ (J) = \left(\frac{mV^2}{2}\right).n = mgh.n \quad [1]$$

The variables under consideration were V, m, g, n, and J. These variables represent the impact velocity, drop weight mass, acceleration due to gravity, number of blows to cause impact, and energy absorbed. Table 6 presents the findings of the 28-day impact energy test. The concrete mix using SFA50 has a comparable energy absorption capacity to that of the concrete mix without SFA (SFA0). The SFA100 mix had a 51.39% reduction in impact energy compared to the SFA0 concrete mix. A regression analysis was conducted on the concrete mix to examine the impact of adjusting the SFA content. The R-square values for the concrete mixes, including SFA0, SFA50, and SFA100, are 0.98, 0.99, and 0.99, respectively. Figure 17 depicts the regression chart for the concrete mix. Figure 18 depicts the failure mechanisms exhibited by the specimens under testing. The SFA50 concrete mix's failure mechanism aligns with the experimental study's observed failure mode [48].

Figure 16. Test Setup for Drop Weight Impact Tester

Table 6. Impact Resistance Results for the Concrete Mix Containing Varying Percentages of SFA

Mix Designation	N1 (mean)	N2 (mean)	N2-N1	N2/N1	J (Nm)	
					First crack	Final crack
SFA0	131	146	15	1.11	2678	2985
SFA50	142	148	6	1.01	2903	3026
SFA100	66	71	5	1.07	1349	1451

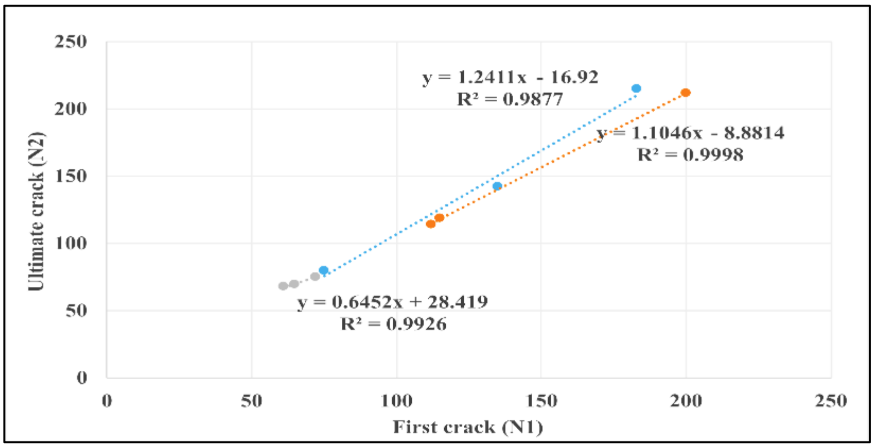

Figure 17. Regression analysis for the concrete mix for varying SFA

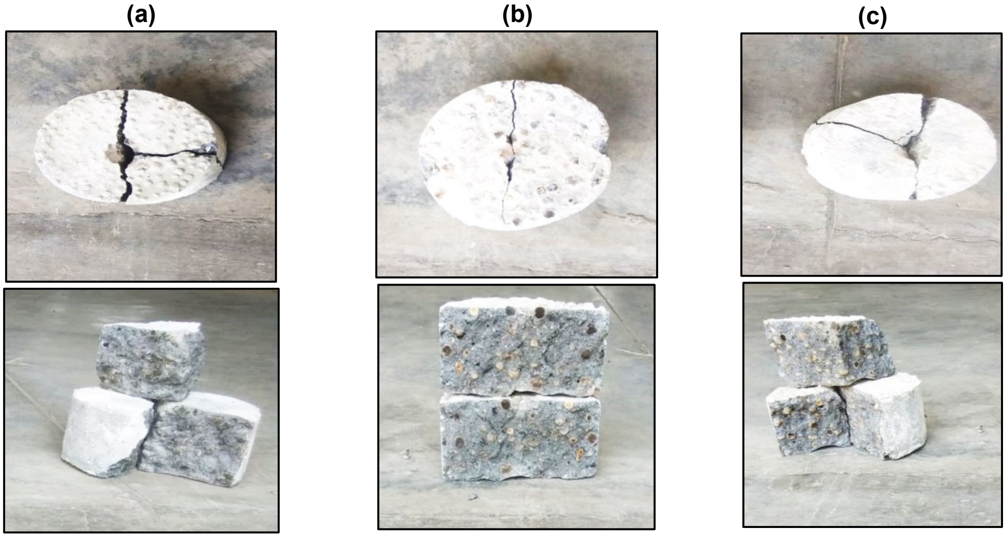

Figure 18. Failure modes of tested concrete mix with varying SFA (a) 0 % (b) 50 % (c) 100 %

3.8 Sorptivity (S)

By measuring the capillary rise absorption rate of the homogenous material, the sorptivity of the concrete mix can be determined. Water in this experiment was used to investigate the phenomenon of capillary action. Figure 19 depicts the test setup for measuring sorptivity on the concrete specimens. To prevent water from moving laterally within the disc, a non-absorbent (epoxy) applied coating was to its side, keeping the water level at no more than 3 mm above the specimen. The following formulas were used to calculate the sorptivity (S), and estimated for 30 minutes [47].

S = $\frac{I}{\sqrt{t}}\ (mm/min^{0.5})$,

whereas

I define rate absorption as $\frac{W_2-W_1}{Ad}$,

t = time in minutes,

w_1 = oven dry weight of specimen in kg,

w_2 = weight of specimen after 30 minutes of capillary suction of water in kg.

A is the surface area in which the water penetrates, and

d is the density of water in kg/mm^3. Table 7 displays the sorptivity results.

Figure 19. Test Setup for Sorptivity of Concrete Cylindrical Specimens

Table 7. Sorptivity (10^{-2} mm/min$^{0.5}$) for Concrete Mix for SFA Content

Mix Designation	W1 (kg)	W2 (kg)	Surface Area (mm^2)	Density of water (kg/mm^3)	Sorptivity value (10^{-2} mm/min$^{0.5}$)	Average sorptivity value (10^{-2} mm/min$^{0.5}$)
SFA0-a	1.069	1.071	9424.77	10^{-6}	0.039	0.068
SFA0-b	1.042	1.047	9424.77	10^{-6}	0.097	
SFA50-a	1.164	1.167	9424.77	10^{-6}	0.058	0.058
SFA50-b	1.128	1.131	9424.77	10^{-6}	0.058	
SFA100-a	0.905	0.908	9424.77	10^{-6}	0.058	0.068
SFA100-b	0.861	0.865	9424.77	10^{-6}	0.077	
a & b indicate the first and second specimens respectively taken for the sorptivity test						

The average findings reveal that incorporating 50% SFA in the concrete mix correlates with a reduction in sorptivity. Furthermore, the sorptivity value of concrete with 0% SFA matches that of concrete with 100% SFA. Partially substituting 50% SFA in concrete leads to a decrease in sorptivity. As per Gomathi et al. 2015 [16], maintaining SFA content within a specified range enhances the durability of the concrete mix. Additionally, M-sand proves to be a superior alternative to river sand in concrete applications.

4 Conclusions

The following conclusions were made based on the results of the previously mentioned experimental examinations:

- The introduction of M-sand into concrete leads to a decreased slump, while the inclusion of SFA results in an increased slump.
- The SFA100 concrete blend demonstrates lightweight properties, as evidenced by its wet density being 20% lower compared to concrete containing natural aggregates (SFA0). Similarly, the SFA100 mix had a 19% lower dry density than the SFA0 mix.
- With higher SFA content, mechanical characteristics such as compressive strength, split tensile strength, flexural strength, and Young's modulus decreased. However, comparing these three mixes was impractical due to variations in their dry and wet densities.
- According to IS 456 code, the minimum compressive strength required for concrete in the field is 20 MPa. Hence, SFA incorporation renders the concrete suitable for field applications while reducing the structure´s self-weight.
- The partial replacement of SFA with natural coarse aggregates (NCA) affected the impact strength of the SFA50 concrete mix. During impact strength testing, both SFA 0 and SFA 100 concrete mixes failed in similar manners.
- The average sorptivity value indicates that replacing 50% of the NCA in concrete with SFA improves the concrete mix's durability.

Declarations:

Fundings: No funds, grants, or other support were received.

Conflicts of interest or competing interests: The authors declare that they have no known competing financial interests or personal relationships that could have appeared to influence the work reported in this paper.

CRediTauthorship contribution statement: Ranjith Babu B: Conceived, planned the experiments and carried out the experiments. **Divyah N:** Analysis of the results and writing of the manuscript.

Acknowledgements: The author extends gratitude to Professor Dr. R. Thenmozhi, Head of the Civil Engineering Department at Government College of Technology in Coimbatore, for invaluable guidance. Acknowledgment is also due to Professor Dr. P. Velumani, Head of the Civil

Engineering Department at PSNA College of Engineering and Technology in Dindigul, for facilitating laboratory testing. We also extend special thanks to Mr. S. Murgesan, a structural engineering lab technician, for his invaluable assistance during laboratory experiments.

References

[1]. Bentur, A., Igarashi, S. I., & Kovler, K. (2001). Prevention of autogenous shrinkage in high-strength concrete by internal curing using wet lightweight aggregates. Cement and concrete research, 31(11), 1587-1591.https://doi.org/10.1016/S00088846(01)00608-1.

[2]. Shelke, A. S., Ninghot, K. R., Kunjekar, P. P., & Gaikwad, S. P. (2014). Coconut shell as partial replacement for coarse aggregate. International Journal of Civil Engineering Research, 5(3), 211-214.https://www.ripublication.com/ijcer_spl/ijcerv5n3spl_02.pdf.

[3]. Noaman, A. T., Jameel, G. S., & Ahmed, S. K. (2020). Producing of workable structural lightweight concrete by partial replacement of aggregate with yellow and/or red crushed clay brick (CCB) aggregate. Journal of King Saud University-Engineering Sciences. https://doi.org/10.1016/j.jksues.2020.04.013.

[4]. https://www.nbmcw.com/equipment-machinery/construction-equipments/concrete-equipment/sintered-fly-ash-light-weight-aggregate-production.html.

[5]. Shen, W., Liu, Y., Wang, Z., Cao, L., Wu, D., Wang, Y., & Ji, X. (2018). Influence of manufactured sand's characteristics on its concrete performance. Construction and Building Materials, 172, 574-583. https://doi.org/10.1016/j.conbuildmat.2018.03.139 .

[6]. Lo, Tommy & Tang, Waiching& Cui, Hongzhi. (2007). The effects of aggregate properties on lightweight concrete. Building and Environment. 42. 3025-3029. https://doi.org/10.1016/j.buildenv.2005.06.031.

[7]. Revilla-Cuesta, V., Faleschini, F., Zanini, M. A., Skaf, M., & Ortega-Lopez, V. (2021). Porosity-based models for estimating the mechanical properties of self-compacting concrete with coarse and fine recycled concrete aggregate. Journal of Building Engineering, 44,103425.https://doi.org/10.1016/j.jobe.2021.103425

[8]. Malysheva, T. & Pavlov, R. (2012). Influence of the mineralogical composition of binders on the strength of sinter. Steel in Translation. 42. https://doi.org/10.3103/S096709121211006X.

[9]. Qifeng Song, Ming-Zhi Guo, Tung-Chai Ling, (2022) A review of elevated-temperature properties of alternative binders: Supplementary cementitious materials and alkali-activated materials, Construction and Building Materials, Volume 341,127894, https://doi.org/10.1016/j.conbuildmat.2022.127894.

[10]. Manikandan, R. & K, Ramamurthy. (2012). Physical characteristics of sintered fly ash aggregate containing clay binders. Journal of Material Cycles and Waste Management. 14. https://doi.org/10.1007/s10163-012-0045-1 .

[11]. Kang Hoon Lee, Jae Hoon Lee, Young Min Wie, Ki Gang Lee, (2019), "Bloating Mechanism of Lightweight Aggregates due to Ramping Rate", Advances in Materials Science and Engineering, vol. 2019, 12 pages. https://doi.org/10.1155/2019/2647391 .

[12]. Tang, Chao-Wei. (2022). The Temperature and Pore Pressure Distribution of Lightweight Aggregate Concrete Slabs Exposed to Elevated Temperatures. Applied Sciences. 12. 10317. https://doi.org/10.3390/app122010317 .

[13]. Yuan Gao, Gao Liu, Xiao Han, Quanqing Gao, Jinghua Ren, (2024), Research on the design method of mix proportion of ceramsite lightweight aggregate concrete, Construction and Building Materials, Volume 433, 136665, https://doi.org/10.1016/j.conbuildmat.2024.136665 .

[14]. Jiwei Cai, Zixian Liu, Gelong Xu, Qing Tian, Weiguo Shen, Bowang Li, Tiao Chen,(2022), Mix design methods for pervious concrete based on the mesostructure: Progress, existing problems and recommendation for future improvement, Case Studies in Construction Materials, Volume 17, https://doi.org/10.1016/j.cscm.2022.e01253 .

[15]. T.Y. Lo, H.Z. Cui, (2004), Effect of porous lightweight aggregate on strength of concrete, Materials Letters, Volume 58, Issue 6, Pages 916-919, https://doi.org/10.1016/j.matlet.2003.07.036 .

[16]. Sivakumar, A., & Gomathi, P. (2012). Pelletized fly ash lightweight aggregate concrete: A promising material. Journal of Civil Engineering and Construction Technology,3(2),42 - 48. https://doi.org/10.5897/JBD11.088 .

[17]. Lo, T. Y., Cui, H., Memon, S. A., & Noguchi, T. (2016). Manufacturing of sintered lightweight aggregate using high-carbon fly ash and its effect on the mechanical properties and microstructure of concrete. Journal of Cleaner Production, 112, 753-762. https://doi.org/10.1016/j.jclepro.2015.07.001 .

[18]. Satpathy, H. P., Patel, S. K., & Nayak, A. N. (2019). Development of sustainable lightweight concrete using fly ash cenosphere and sintered flyash aggregate. Construction and Building Materials, 202, 636-655. https://doi.org/10.1016/j.conbuildmat.2019.01.034.

[19]. Babu, B. R., & Thenmozhi, R. (2018). An investigation of the mechanical properties of sintered fly ash lightweight aggregate concrete (SFLWAC) with steel fibers. Archives of Civil Engineering,64(1). https://journals.pan.pl/Content/115555/PDF/05_073-085_ace-2018-0005.pdf.

[20]. Shen, W., Liu, Y., Cao, L., Huo, X., Yang, Z., Zhou, C., ... & Lu, Z. (2017). Mixing design and microstructure of ultra-high strength concrete with manufactured sand. Construction and building Materials, 143, 312-321. https://doi.org/10.1016/j.conbuildmat.2017.03.092 .

[21]. Akarsh, P. K., Marathe, S., & Bhat, A. K. (2021). Influence of graphene oxide on properties of concrete in the presence of silica fumes and M-sand. Construction and Building Materials, 268, 121093. https://doi.org/10.1016/j.conbuildmat.2020.121093 .

[22]. Pilegis, M., Gardner, D., & Lark, R. (2016). An investigation into the use of manufactured sand as a 100% replacement for fine aggregate in concrete. Materials, 9(6), 440. https://www.mdpi.com/142616 .

[23]. IS: 12269, Indian Standard Specification 53 Grade ordinary Portland cement specification, Bureau of Indian Standards, New Delhi, 1987 [Reaffirmed in 2013].

[24]. IS: 4031, Indian Standard Specification, Methods of Physical Tests for Hydraulic Cement: Part 11, Determination of Density, Bureau of Indian Standards, New Delhi, 1988 [Reaffirmed in 2005].

[25]. IS: 4031, Indian Standard Specification, Methods of Physical Tests for Hydraulic Cement: Part 2, Determination of Fineness by Specific Surface by Blaine Air Permeability Method, Bureau of Indian Standards, New Delhi, 1999[Reaffirmed in 2004].

[26]. IS: 4031, Indian Standard Specification, Methods of Physical Tests for Hydraulic Cement: Part 4, Determination of Consistency of Standard Cement Paste, Bureau of Indian Standards, New Delhi, 1988 [Reaffirmed in 2005].

[27]. IS: 4031, Indian Standard Specification, Methods of Physical Tests for Hydraulic Cement: Part 5, Determination of Initial and Final Setting Times, Bureau of Indian Standards, New Delhi, 1988 [Reaffirmed in 2005].

[28]. IS: 2386, Indian Standard Specification, Methods of Test for Aggregates for Concrete: Part 1, Particle Size and Shape, Bureau of Indian Standards, New Delhi, 1963 [Reaffirmed in 2002].

[29]. IS: 2386, Indian Standard Specification, Methods of Test for Aggregates for Concrete: Part 3, Specific Gravity, Density, Voids, Absorption and Bulking, Bureau of Indian Standards, New Delhi, 1963 [Reaffirmed in 2002].

[30]. IS: 2386, Indian Standard Specification, Methods of Test for Aggregates for Concrete: Part 4, Mechanical Properties Bureau of Indian Standards, New Delhi, 1963 [Reaffirmed in 2002].

[31]. IS: 10500, Indian Standard, Drinking Water – Specification, Bureau of Indian Standards, New Delhi (2012).

[32]. IS: 10262. Indian Standard Concrete Mix Proportioning – Guidelines, Bureau of Indian Standards, New Delhi; 2009.

[33]. IS: 516, Indian Standard Methods of Tests for Strength Concrete, Bureau of Indian Standards, New Delhi, 1959 [Reaffirmed in 1999].

[34]. IS: 5816, Indian Standard Splitting Tensile Strength of Concrete-Method of Test, Bureau of Indian Standards, New Delhi, 1999 [Reaffirmed in 2004].

[35]. ASTM C 642-13, Standard Test Method for Density, Absorption, and Voids in Hardened Concrete, ASTM International, West Conshohocken, 2013.

[36]. ASTM C 1585-04, Standard Test Method for Measurement of Rate of Absorption of Water by Hydraulic Cement Concretes.

[37]. ACI Committee 213, 213R-03, Guide for Structural Lightweight-aggregate Concrete, American Concrete Institute, Farmington Hills, MI, USA, 2003.

[38]. American Concrete Institute, ACI Committee 318: Building Code Requirements for Structural Concrete, Farmington Hills, MI, 2011.

[39]. CEB-FIP, Model Code 1990. Com, Euro-International Du Beton, Paris, 1991.

[40]. EHE, Spanish Code for Structural Concrete EHE, Real Decreto 2661/1998, Madrid, 1998.

[41]. GB: 10010, Code for Design of Concrete Structures, Chinese Standard, Beijing (China), 2002.

[42]. NBR 6118, Design of Concrete Structures, Brazilian association of technical standards, Brazil, 2003.

[43]. A.M. Neville, Properties of Concrete, 5th ed., Person Education Limited, New Delhi, 2013.

[44]. DG/TJ, Technical Code for Application of Recycled Aggregate Concrete, Shangai Construction Standard Society (SCSS), Shangai, 2008.

[45]. IS: 456, Indian Standard Plain and Reinforced Concrete Code of Practice, Bureau of Indian Standards, New Delhi, 2000.

[46]. ACI 544-2R, Measurement of Properties of Fiber Reinforced Concrete, American Concrete Institute, USA (1999).

[47]. Jena, T., & Panda, K. C. (2020). Effect of magnesium sulphate solution on compressive strength and sorptivity of blended concrete. Advances in concrete construction, 9(3), 267-278. https://doi.org/10.12989/acc.2020.9.3.267 .

[48]. 36. Gupta, T., Sharma, R. K., & Chaudhary, S. (2015). Impact resistance of concrete containing waste rubber fiber and silica fume. International Journal of Impact Engineering, 83, 76-87.https://doi.org/10.1016/j.ijimpeng.2015.05.002

Građevinski materijali i konstrukcije
Building Materials and Structures
journal homepage: www.dimk.rs

https://doi.org./10.5937/GRMK2400008M UDK: 666.972:681.625.9
691.322:620.17

Original scientific paper

Experimental investigation of bearing capacity of 3D printed concrete segmental girder

Stefan Ž. Mitrović*[1)], Ivan Ignjatović[2)]

[1)] University of Belgrade, Faculty of Civil Engineering, Bulevar kralja Aleksandra 73, 11000, Belgrade, Serbia. ORCID 0000-0001-7254-6860
[2)] University of Belgrade, Faculty of Civil Engineering, Bulevar kralja Aleksandra 73, 11000, Belgrade, Serbia. ORCID 0000-0002-2679-0982

Article history

Received: 20 August 2024
Received in revised form: 04 September 2024
Accepted: 08 September 2024
Available online: 20 September 2024

Keywords

3D printed concrete,
segmental beam,
connections,
prestressing,
bearing capacity

ABSTRACT

3D concrete printing (3DCP) technology represents a new approach to producing contemporary concrete structures. The application of sophisticated equipment such as a 3D printer has brought numerous advantages, which were noted through significant practical application. Currently, 3DCP technology is being developed in two main directions: on-site production of entire structures and prefabricated construction. However, 3DCP technology has not yet reached its full potential in prefabrication as the connections between individual segments and their capacities under horizontal and vertical loads, have not yet been extensively investigated. This paper focuses on the experimental testing of the bearing capacity of a beam constructed by connecting individual segments of 3D printed concrete. The segments are connected using post-tensioning steel bars. The experimental program included testing a single segment as well as a segmental girder in a 3-point test. In the case of the individual segment, failure occurred due to the loss of tensile capacity of the concrete. For the segmental beam, failure occurred when the shear capacity was reached. Shear fracture was accompanied by diagonal cracks extending from the point of force application towards the beam supports.

1 Introduction

The construction industry has a significant impact on the gross domestic product (GDP) of each country, not only through construction activities but also through related industries such as mechanical engineering, electrical engineering, material production, and others. Over the centuries, the construction industry has undergone constant changes and innovations driven by advancements in science and technology. However, compared to other sectors, construction has experienced a relativelely slow increase in productivity. One potential direction for enhancing productivity development in this sector is the application of 3D concrete printing technology (3DCP). The digitalisation of the building process significantly reduces the time required for construction, material waste, and errors [1]–[3].

3D printing technology is a modern method for creating three-dimensional shapes. It originated as a laboratory technique, with one of the pioneers being Chuck Hull, who successfully printed the first three-dimensional shape in 1986. [4]. The concept of 3D printing can be applied to a variety of materials, such as plastic, composite, concrete or steel. Behroh Hoshnevis from the University of Southern California patented the Contour Crafting (CC) method for 3DCP in the late 20th century [5]–[7] which has since become the most widely used method for concrete printing.

In addition to CC technology, two other methods have been developed and used for 3D concrete printing (3DCP): the Inject Printing method and the Shotcrete 3D Printing (SC3DP) technology [7]–[10].

3DCP using the aforementioned methods has been successfully implemented in various applications, as shown in Figures 1-3:

1. Individual elements, such as columns and walls
2. Decorative elements, including arabesques, ornaments, and facade panels
3. Outdoor furniture, such as benches, tables, and planters
4. Sculptures and monuments
5. Single-story and multi-story buildings, including family houses and residential buildings
6. Pedestrian bridges and similar structures

It is important to note that companies specializing in material production, such as Lafarge and Sika, have recognized 3DCP technology as a new construction method. Ready-made premixes for use in 3D printing are now available on the market. Companies like COBOD BOD2, Apis Cor, Contour Crafting, and XtreeE have developed printers capable of printing large structures, including one-story houses, on-site [11]. Support for these projects has been provided by companies specializing in formwork, such as PERI and DOKA [12].

* Corresponding author:
E-mail address: smitrovic@imk.grf.bg.ac.rs

Figure 1. Two-story Beckum house [13]

Figure 2. Striatus bridge [13]

Figure 3. Horizontally printed panel [1]

The advantages of using 3D printing technology in the production of contemporary concrete structures are numerous [13]. First of all, significant time savings are achieved because the process is automated, reducing the need for labor. A 3D printer requires only a small number of operators. Additionally, 3D printing technology allows for greater freedom in the design of elements and structures. There is no need for complicated formwork, which is often difficult to create for more complex elements and can only be used once [11]. The cost of construction is reduced, as the value of the formwork typically accounts for about 35–60% of the element's price [15]. Furthermore, material waste and construction waste on-site can be minimized. It is also possible to use "green" concrete by incorporating recycled or waste materials [14], [16]. The application of 3D concrete printing enhances workplace safety, reduces human errors and omissions, and is suitable for use in challenging conditions. This technology is particularly well-suited for constructing buildings intended for rapid accommodation following natural disasters such as earthquakes and floods. These structures can also be used to house refugees or patients during pandemics like COVID-19.

There are also some shortcomings and open questions regarding the broader practical application of this technology [17]. A 3D printer is a sophisticated piece of equipment that requires a substantial initial investment, which can hinder the wider adoption of this method, as low cost and simple production are the main reasons for the widespread use of concrete in construction. Additionally, the operator must be adequately qualified. To print an entire structure, a printer larger than the structure itself is required, leading to complex and costly printer construction [18], [19]. Thus, the authors believe that 3DCP technology needs to be adapted for the prefabrication of concrete elements. In such cases, individual segments are produced in a prefabrication plant, transported to the construction site, and then assembled. Challenges include ensuring proper connections between segments, addressing cold joints, and incorporating reinforcement, if needed. A significant obstacle to the wider application of this technology is the inability to achieve consistent quality of printed concrete using the same mixture on different printers. Therefore, the quality of the final product depends on the correlation between the mixture and the printer, as demonstrated in an interlaboratory test conducted by the University of Eindhoven and the University of Delft [20]. The incorporation of reinforcement remains an open question, although various models have been proposed [21]. The development of an adequate and robust static system for safely transmitting loads in 3DCP structures is still unresolved. Additionally, there are currently no material models for the static and dynamic calculation of structures [12], [22].

The scientific community has recognized the open questions and obstacles related to 3DCP technology. The RILEM organization, through its two technical committees, TC 276-DFC and TC 304-ADC, is addressing the issue of standardizing the 3DCP process and laboratory testing of the properties of 3D printed concrete. Namely, there are currently no standardized models or guidelines for the design and calculation of materials and elements, including standards and regulations for the production of fresh concrete mix, testing properties in both fresh and hardened states, the 3D printing process, and the testing of finished elements and structures. Additionally, committees such as ACI Committee 564, ISO/TC 261, and ASTM Committee F42 have been established to focus on these challenges. The preliminary version of the new edition of standard EN 206-4, which pertains to 3DCP technology, is expected to be released in 2027 [12].

The aim of this paper was to analyse the current state-of-the-art in the field of experimental testing of segmental concrete elements produced using 3DCP. Additionally, the paper presents the authors' own experimental results from the initial phase of producing and testing a prototype of precast 3DCP two-segment girder.

2 3D printed concrete segmental elements: state-of-the-art

As mentioned in the previous chapter, prefabrication holds significant potential for the further development of 3D concrete printing technology. Open questions include the manufacturing of connections and the verification of the load-bearing capacity and serviceability of the elements [12], [21]. The first elements that were manufactured and analyzed as segmental components are beams. In addition to being printed as a single piece, beams can also be constructed by connecting smaller individual segments using epoxy adhesives, reinforcement, or post-tensioning. The tests conducted focused on determining the bending or shear capacity of the beams [12]. A summary of the tests from the literature review is presented in Table 1, showing the types of elements and tests performed, the type and content of fibers, and the type of reinforcement or cables used. An example of these tests is shown in Figure 4.

Table 1. Experimental and numerical analysing of 3DCP segmental beams and bridges

Ref.	Type of element	No	Dimension of elements [mm]	Type of test	Type of fibers	Content of fibers [%]	Reinforcement	Type of reinforcement	Cables	Type of cables	FEM Analysis
[23]	Bridge (segmental)	1	1720x460x500	4-point bending	PP	-	Cable (added by printer nozzle)	High-strength steel cable Ø 0.63 mm	Post tensioning	9 Dywidag-system tendons (Ø15.7 mm, Y1860 steel grade), initial load 120 kN	Yes
	Bridge (segmental)	1	3440x920x6500	Live load/reached 100% of SLS Moment in span	PP	-	Cable (added by printer nozzle)	High-strength steel cable Ø 0.63 mm	Post tensioning	16 Dywidag-system tendons (Ø15.7 mm, Y1860 steel grade), initial load 150 kN	Yes
[24]	Beam (segmental)	1	200x450x3000	3-point bending	PP	0.50	Manually placed	Steel rebar Ø 16 mm	/	/	SAP2000
[25]	Beam (segmental)	7	240x240x960	3-point bending	/	/	Manually placed	Standard bar Ø 14 mm Stirrup Ø 8 mm (e= 80 mm)	/	/	No
[26]	Beam (segmental)	1	4000 (span)	Bending under uniformly disturbed load	/	/	Manually placed	Steel rebar Ø 12 mm	Post tensioning	Ø 9.4 mm	Fusion 360
[27]	Beam (segmental)	1	2500 (span)	4-point bending	Glass	-	/	/	Post tensioning	-	Grasshopper Robot Studio
[28]	Beam (segmental)	13	128x216x3300	3-point bending	/	/	Manually placed	Standard bar Ø 12, 16, 25 mm	/	/	Abaqus
[29]	Bridge (segmental)	1	16000 (span)	In situ	/	/	/	/	/	/	compas_3dec Sofistik
[30]	Beam (segmental)	4	150x350x3200	4-point bending	/	/	Manually placed	Standard bar Ø 8,10, 12 mm Steel spirals Ø 8 mm (e= 200 mm)	/	/	No

Figure 4. In situ testing of the bridge with water-filled containers [23]

The tests presented in Table 1 include the measured displacement of bridges or girders under load. Two approaches are usually used to design 3D printed concrete elements: topology optimization and the trial-and-error approach. The main goal of the presented research was to achieve the minimum required amount of material and to demonstrate the potential of 3DCP technology in prefabricated construction. In all cases, the bridges or beam girders had hollow configurations with various types of fillings. Some researchers incorporated fibers into the fresh concrete mixture. It is found that while a great range of element shapes can be created, but tensile strain in concrete cannot be completely eliminated, which is resulted that post-tensioning cables or reinforcement are required. The procedure for incorporation of cables or rebars is the same as that of conventionally made concrete elements, also with the need for filling the joints with injection mortar.

3 Experimental investigation

3.1 Scope of the experimental programme

The experimental phase of this research was divided into two main directions:

1. Determination of the bearing capacity of a single segment made of 3D printed concrete, with dimensions of 435x240x300 mm, using a 3-point test.
2. Determination of the bearing capacity of a two-segment girder created by connecting two individual segments of 3D printed concrete. The total dimensions of the girder were 435x240x600 mm, and it was tested using a 3-point test.

3.2 Preparation of samples

The individual segments were produced using 3D concrete printing technology, as shown in Figures 5 and 6. A 3D printer at the Faculty of Civil Engineering at the University of Belgrade was employed for this purpose [12]. The fresh concrete mixture was made using a ready-to-use, one-component premix with the commercial name Sikacrete®-751 3D, manufactured by Sika [31]. Each segment consisted of 20 layers, with an average layer height of 15 mm. The printing parameters included a printing speed of 1200 mm/min, a nozzle offset of 15 mm, and a pump pressure of 4 bar. The segments, which had a hollow lattice filling and dimensions of 435x240x300 mm, were cured in a dry environment for 28 days.

The beam is manufactured by connecting two individual segments using post-tensioning with two M16 steel bars of quality 8.8, as shown in Figures 7 and 8. The bars are centrally placed through the hollow structure of the segments. Steel plates with dimensions of 500x300x10 mm, along with additional plates, are positioned at the ends of the segments. These steel plates are adhered to the segments using epoxy paste adhesive. The connection of the segments is achieved through post-tensioning. The segments are in dry contact with each other. The steel bars are tightened to the required level using a torque wrench. GEOKON Model 4000 vibrating wire strain gauge sensors (VWSG) were installed on the segments prior to connecting them.

Figure 5. The process of 3DCP of individual segments

Figure 6. Printed individual segments

Figure 7. Individual segments before connection

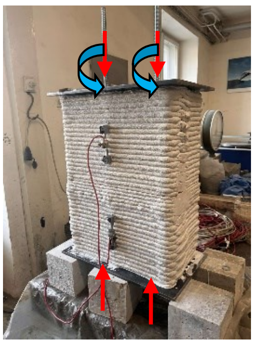

Figure 8. The post-tensioning including the tightening of nuts with a torque wrench

The purpose of the post-tensioning force is to connect the segments into a single element and to ensure the required shear capacity of the beam. The beam, with a span-to-height ratio of less than three, supposed to exhibit shear failure in the 3-point test. The criterion for selecting the prestressing force was based on the contribution of the normal force to the shear capacity of the beam, as outlined in Eurocode 2 [32], through the parameter σ_{cp}. The post-tensioning force was determined by limiting the parameter σ_{cp} to a value of $0.2^{*}f_{cd}$, where f_{cd} represents the design compressive strength of the concrete. The required force was calculated based on a cross-sectional area of 59712 mm² and concrete class C25/30, resulting in a value of 160 kN, or 80 kN per steel bar. The maximum permissible force in a bar of quality 8.8 is 90 kN. To achieve the necessary post-tensioning forces, each bar had to be tightened with a torque of 192 Nm.

The strain of the beam during post-tensioning was measured by means of vibration wire strain gauges (VWSG). The normal force induced in the girder is calculated as the product of the modulus of elasticity, the cross-sectional area, and the mean value of the measured strain. The testing of the modulus of elasticity was performed on two types of samples: mold-cast samples and printed samples. In both cases, the modulus of elasticity exhibited a value of 27 GPa. The nut tightening was performed in several stages. The values of the measured strains are presented in Table 2, along with the difference between the measured force and the expected force based on theoretical calculations. On the first day of post-tensioning, the beam was prestressed and then unloaded to allow for necessary adjustments and fitting of the segments. Final post-tensioning was carried out the following day, after which the beam was subjected to a 3-point test until failure.

3.3 Testing of the individual segment

The first part of the experimental program focused on testing an individual segment without reinforcement or steel fibers using a 3-point test. The experimental setup is illustrated in Figure 9. The segment was supported and subjected to force using steel plates, which were adhered to the segment with epoxy paste adhesive. The segment was positioned on fixed and roller supports, with a span of 240 mm. The test was conducted using an Amsler press with a capacity of 2500 kN.

The load was applied gradually to the sample at a rate of 1 kN/sec until failure occurred. This setup allowed for the evaluation of the segment's bending capacity and the determination of its structural performance under load.

The ultimate load capacity of the segment was 130 kN, and the total test duration was 2.50 minutes. The fracture pattern observed in the individual segment after reaching its bearing capacity is depicted in Figures 10 and 11.

Table 2. Measured strain in the post-tensioning process of segmental beam

First day – 16/07/2024								
Torque [Nm]	Expected Force by bar [kN]	Total expected force [kN]	VWSG 1 [με]	VWSG 2 [με]	VWSG 3 [με]	VWSG 4 [με]	Main value [με]	Measured force [kN]
0	0	0	0	0	0	0	0	0
60	25	50	-12	-28	-33	-8	-20	33
110	46	92	-18	-33	-45	-10	-27	43
160	67	133	-26	-44	-62	-13	-36	59
190	79	158	-31	-50	-72	-15	-42	68
0	0	0	-1	-9	-2	2	-2	4
Second day – 17/07/2024								
Torque [Nm]	Force by bar [kN]	Total force [kN]	VWSG 1 [με]	VWSG 2 [με]	VWSG 3 [με]	VWSG 4 [με]	Main value [με]	Measured force [kN]
0	0	0	0	0	0	0	0	0
60	25	50	-5	-8	-19	-3	-9	15
110	46	92	-10	-16	-35	-7	-17	28
160	67	133	-19	-26	-56	-11	-28	46

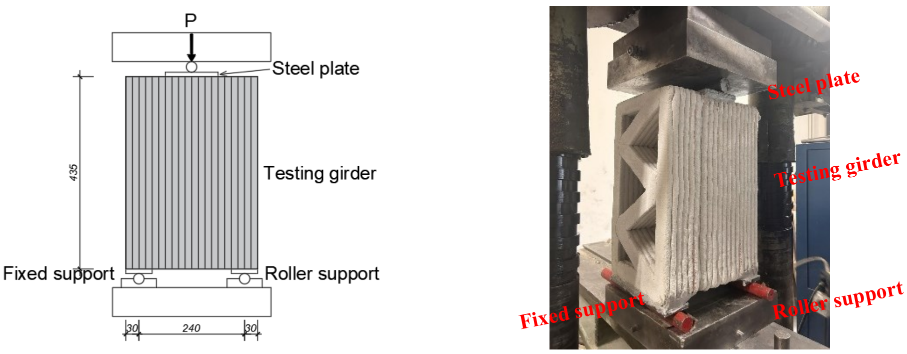

Figure 9. Experimental setup for 3-point test for individual segment

Figure 10. The failure mechanism of the segment in 3-point test - inside

Figure 11. The failure mechanism of the segment in 3-point test - outside

3.4 Testing of the segmental girder

The segmental girder, with dimensions of 435x240x600 mm, was tested using an Amsler press with a capacity of 2500 kN. The beam underwent a 3-point test. Steel plates, adhered with epoxy paste adhesive, were used to provide support and apply force to the beam. The beam was placed on fixed and roller supports with a span of 500 mm. The experimental setup is illustrated in Figure 12.

Before the start of the test, strain values were measured using sensors and axial prestressing force was confirmed. The transversal force (P, Figure 12) was applied incrementally, with initial steps of 5 kN up to 100 kN, followed by 10 kN steps up to 200 kN, and then 20 kN steps. During testing, there were brief pauses, leading to minor force reductions attributed to sample adjustments. The total test duration was 120 minutes with obtained capacity force of 333 kN. Strain measurements were taken at each step until the

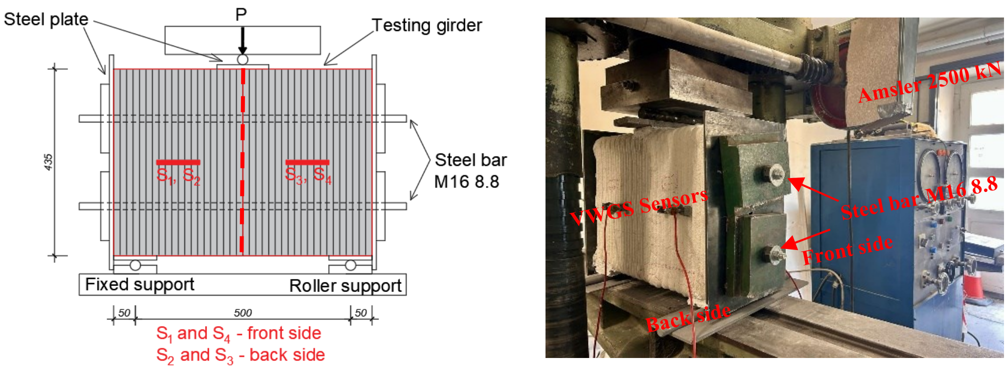

Figure 12. Experimental setup for 3-point test for segmental beam

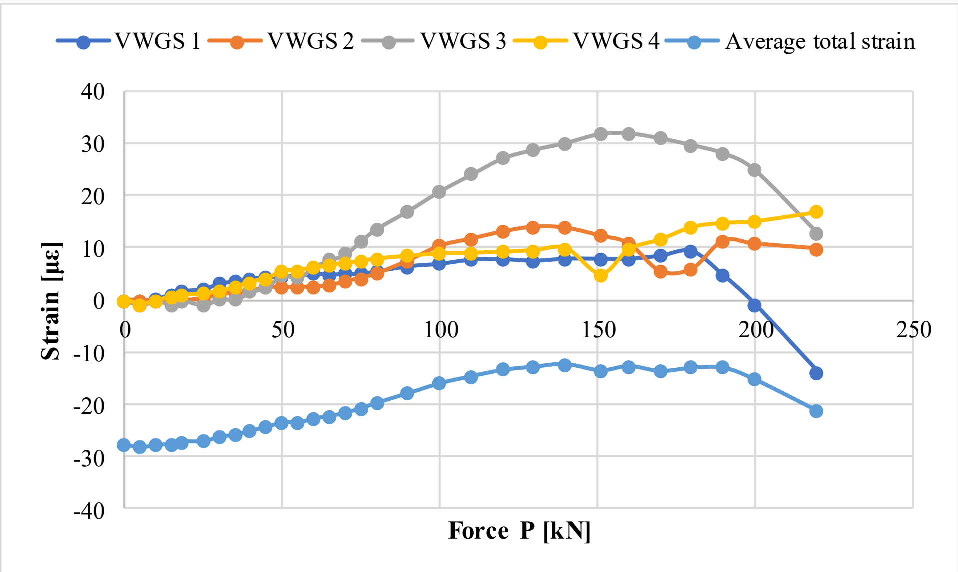

Figure 13. Measured strains in segmental girder

first crack appeared, at which point the sensors were removed to prevent potential damage due to the girder failure. The S1-S4 curves on Figure 13 show the strain value without previous strain from the post-tensioning phase, i.e. only strains resulted from the action of trasversal load P. The blue curves with name "Average total strain" represent the total value of strain of the middle of cross section height with added compressive strain from post-tensioning phase. Figure 14 shows the crack pattern of the segmental beam, including the force values and crack widths. The failure mechanism of the segmental beam in the 3-point bending test is illustrated in Figures 15 and 16.

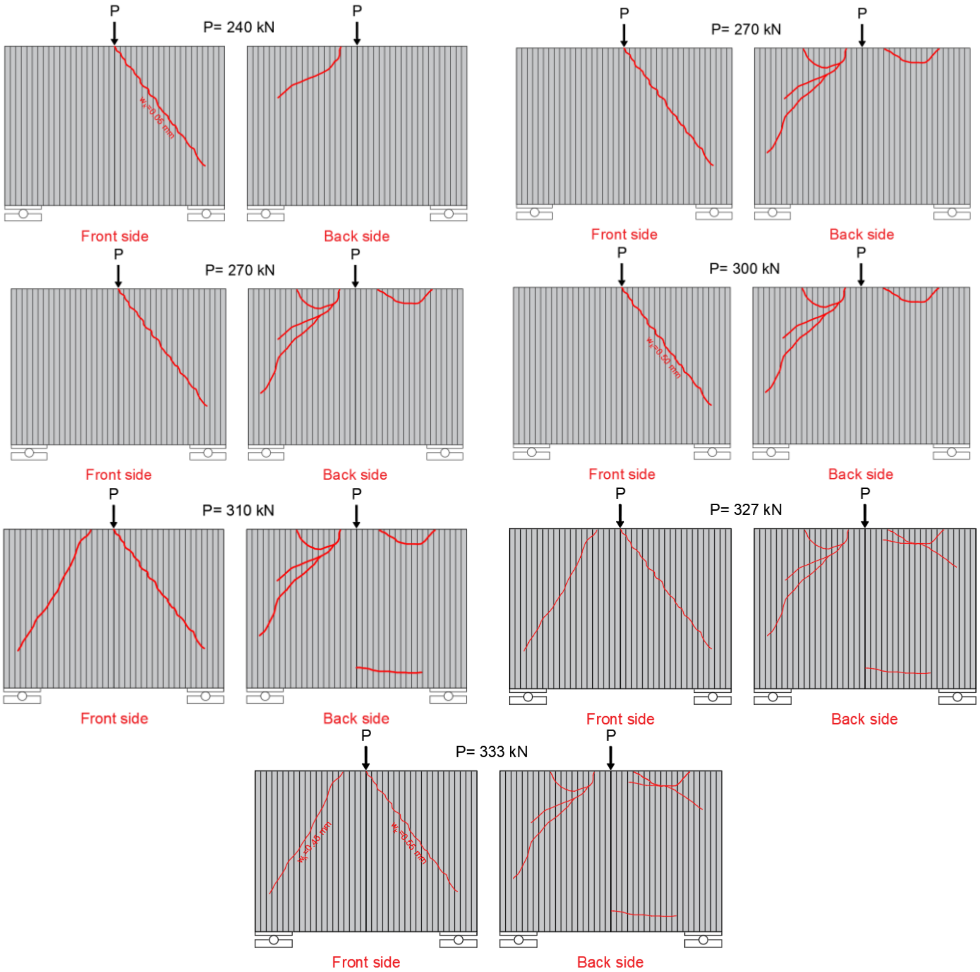

Figures 14. Crack pattern in tested segmental beam

Figure 15. The failure mechanism of the segmental beam in 3-point test – front side

Figure 16. The failure mechanism of the segmental beam in 3-point test – back side

3.5 Discusion of results

The testing of the individual segment revealed bending failure, characterized by the formation of a crack at the mid-span and its subsequent propagation along the height of the segment. This type of failure is anticipated given that the sample was manufactured without reinforcement or steel fibers. Due to the short span and the force application near the segment supports, shear capacity of tested elements was higher.

Previous research [33] determined the splitting strength. For splitting failure, the predicted capacity was 143 kN. For bending failure, the predicted capacity force was 150 kN. The prediction was based on a single calculation of stresses in the cross-section and the tensile stress limitations, which are set to the value of f_{ctm} according to Eurocode 2 [32]. The experimental testing yielded a capacity force of 130 kN. The observed fracture involved a crack opening in the tensile zone, progressing through four layers and continuing between layers to the segment's top. The fracture pattern suggests adequate printing quality and high interlayer bond strength. The behavior of the printed segments is comparable to that of traditionally cast samples. The experimental capacity force is approximately 15% lower than the theoretical prediction, which is based on bending failure.

Measured strains in prestressing phase of two-segment girder testing (Table 2) indicated an eccentric application of the post-tensioning force. The presence of a bending moment around the longitudinal axis of the beam was detected, resulting from the asymmetrical stress distribution across the cross-section, particularly with high values at the edge where sensor S3 was installed. Localized damage at the corners of the segments is evident in Figure 17. The strains did not return to their initial values during the unloading process on the first day, which is likely related to this localized damage.

With a torque of 160 Nm applied to each bar, the theoretical post-tensioning force per bar was 67 kN, totaling entered force of 134 kN for the beam. However, testing revealed that the actual mean post-tensioning force was 46 kN. The difference between the entered and measured post-tensioning force may be due to eccentricity or bending of the supports, including the anchor zone. These factors will be more considered in future research. Given the beam's short span, shear failure with diagonal cracks was anticipated rather than bending failure. According to Eurocode 2 [32], the predicted shear capacity of the beam was 290 kN.

The first diagonal crack appeared at a force of 240 kN (Figure 14) on the beam's front side, detected by an unexpected change in sensor readings. This crack, initially 0.05 mm wide, propagated to 0.55 mm at a force of 333 kN. A significant force drops from 240 kN to 192 kN was observed, with the crack widening further during force application.

A second diagonal crack, symmetrical to the first, developed on the same side at a force of 310 kN, with a width of 0.45 mm at 333 kN, Figure 16. Diagonal cracks also emerged on the back side of the beam, with the first appearing at 300 kN and a second at 327 kN. The experimental testing reached a maximum capacity force of 333 kN, indicating shear failure with diagonal cracks on both sides of the beam from the force application points to the supports (Figures 15 and 16). Theoretical predictions estimated a capacity force of 290 kN, whereas the experimental results yielded 333 kN, showing a 13% difference. The diagonal cracks passed through the layers without delamination between them. Furthermore, there was no failures at the segment joints. Therefore, the connection method proved to be effective.

All sensors without previous strain in girder from post-tensioning, detected tensile strain with increasing force, except for sensor S1, which detected compressive strain after 200 kN. Sensors S1, S2, and S4 recorded similar strain values, while sensor S3 showed the highest strain values, indicating the impact of post-tensioning eccentricity on beam behavior. Sensor S3 recorded the highest strain during the post-tensioning phase. The average value of total strain on the middle of the sample height is negative during the testing, which indicate the compressive strain in that direction. It should also be noted that the experimental testing of individual segments with dry contact resulted in a noticeable gap opening during force application, as shown in Figure 18.

4 Conclussions

Based on the presented findings, the following conclusions can be drawn:

1. 3D concrete printing technology holds significant promise for advancing contemporary concrete structures, particularly as part of the 4.0 industrial revolution. The integration of modern software and 3D printing machines is expected to revolutionize construction practices.

2. While 3D printing facilitates the creation of intricate elements, challenges remain in designing effective connections between segments. There is a need for further research into verifying the bearing capacity of these connections and assessing the long-term performance of 3D printed elements, particularly under lateral loads.

Figure 17. The local destruction of segments

Figure 18. The gap between segments

3. Previous research confirm that post-tensioning has proven to be an effective method for connecting individual segments, enhancing both bending and shear capacities. The hollow structure of printed segments accommodates the installation of cables and reinforcement bars, addressing tensile stresses and improving structural integrity.

4. Own experimental testing of individual printed segments confirmed high print quality and good correlation between the printer and the fresh concrete mixture. The capacity force measured was in line with theoretical predictions for bended elements.

5. Post-tensioning with steel bars introduced compressive forces and provided good connection of the segments; accidental eccentricity of prestressing force caused stress concentrations and relatively small-localized damage.

6. The tested two-segments girder exhibited shear failure, as anticipated based on its span-to-height ratio and relatively high prestressing level. Failure mode and crack pattern suggests that the proposed connection approach is structurally sound. Also, this qualitative test showed the success of this assembling method and confirmed that axial forces in the beam can be achieved with steel rebars tightened with torque wrench only.

CRediT authorship contribution statement

Stefan Mitrović: Data curation, Formal Analysis, Investigation, Project administration, Resources, Validation, Visualization, Writing – original draft prepraration. **Ivan Ignjatović:** Conceptualization, Methodology, Project administration, Resources, Supervision, Validation, Writing— review and editing.

Declaration of competing interest

The authors declare that they have no known competing financial interests or personal relationships that could have appeared to influence the work reported in this paper.

Acknowledgments

The authors gratefully acknowledge the support of Nenad Zorić from SIKA Serbia, Srđan Ilić from ADING Serbia and Elko-var Valjevo which provided materials needed for experimental testing. For assistance in conducting the experimental part, the authors thank their colleagues from the Laboratory for Materials and the Laboratory for Construction Faculty of Civil Engineering University of Belgrade, Associate Professor Zoran Mišković, Siniša Savatović, Sava Stavnjak, Mladen Jović and Dragan Žderić. This research was supported by the Ministry of Science, Technological Development, and Innovation of the Republic of Serbia (grant number 2000093).

References

[1] R. A. Buswell, W. R. Leal de Silva, S. Z. Jones, and J. Dirrenberger, 3D printing using concrete extrusion: A roadmap for research, Cem. Concr. Res., vol. 112, no. June, 2018, 37–49, doi: 10.1016/j.cemconres.2018.05.006.

[2] N. Labonnote, A. Rønnquist, B. Manum, and P. Rüther, Additive construction: State-of-the-art, challenges and opportunities, Autom. Constr., vol. 72, 2016, 347–366, doi: 10.1016/j.autcon.2016.08.026.

[3] S. Marinković, “Concrete structures in the 21 st century and further,” Civ. Eng. 2021 Achiev. Visions, 2021, pp. 2–17.

[4] N. Shahrubudin, T. C. Lee, and R. Ramlan, An overview on 3D printing technology: Technological, materials, and applications, Procedia Manuf., vol. 35, 2019,1286–1296, doi: 10.1016/j.promfg.2019.06.089.

[5] B. Khoshnevis, Automated construction by contour crafting - Related robotics and information technologies, Autom. Constr., vol. 13, no. 1, 2004, 5–19, doi: 10.1016/j.autcon.2003.08.012.

[6] B. Zareiyan and B. Khoshnevis, Effects of interlocking on interlayer adhesion and strength of structures in 3D printing of concrete, Autom. Constr., vol. 83, 2017, 212–221, doi: 10.1016/j.autcon.2017.08.019.

[7] O. Bukvić, V. Radonjanin, M. Malešev, and M. Laban, Basic fresh-state properties of extrusion-based 3D printed concrete, Gradjevinski Mater. i Konstr., vol. 63, no. 4, 2020, 99–117, doi: 10.5937/grmk2004099b.

[8] F. Heidarnezhad and Q. Zhang, Shotcrete based 3D concrete printing: State of art, challenges, and opportunities, Constr. Build. Mater., vol. 323, no. January, 2022, 126545, doi: 10.1016/j.conbuildmat.2022.126545.

[9] D. Lowke, E. Dini, A. Perrot, D. Weger, C. Gehlen, and B. Dillenburger, Particle-bed 3D printing in concrete construction – Possibilities and challenges, Cem. Concr. Res., vol. 112, no. November 2017, 2018, doi: 10.1016/j.cemconres.2018.05.018.

[10] P. Shakor, S. Nejadi, G. Paul, and J. Sanjayan, A Novel Methodology of Powder-based Cementitious Materials in 3D Inkjet Printing for Construction Applications, *6th Int. Conf. Durab. Concr. Struct. ICDCS 2018*, no. July, pp. 685–695, 2018.

[11] I. Ignjatović, S. Mitrović, J. Dragaš, and V. Carević, Structural application of 3D concrete printing technology, in *Proceedings 16th International Congress of Association of Structural Engineers of Serbia 2022*, 2022, no. October, pp. 458–469.

[12] I. Ignjatović, J. Dragaš, S. Mitrović, and M. Vidović, 3D ŠTAMPANI BETONI U SRBIJI – REALNOST ILI DALEKA BUDUĆNOST?, in *Zbornik radova Naučno-stručni skup "'Aktuelni trendovi u oblasti građevinskih materijala i konstrukcija'", Beograd, 10. maj 2024. godine, 2024*, 2024, no. May, pp. 16–30, doi: 10.46793/diimk24.016ii.

[13] F. Bos, R. Wolfs, Z. Ahmed, and T. Salet, Additive manufacturing of concrete in construction: potentials and challenges of 3D concrete printing, Virtual Phys. Prototyp., vol. 11, no. 3, 2016, 209–225, doi: 10.1080/17452759.2016.1209867.

[14] P. Feng, X. Meng, J. F. Chen, and L. Ye, Mechanical properties of structures 3D printed with cementitious powders, Constr. Build. Mater., vol. 93, 2015, 486–497, doi: 10.1016/j.conbuildmat.2015.05.132.

[15] A. Perrot, D. Rangeard, and A. Pierre, Structural built-up of cement-based materials used for 3D-printing extrusion techniques, Mater. Struct. Constr., vol. 49, no. 4, 2016, 1213–1220, doi: 10.1617/s11527-015-0571-0.

[16] K. Kanishka and B. Acherjee, Revolutionizing manufacturing: A comprehensive overview of additive manufacturing processes, materials, developments, and challenges, J. Manuf. Process., vol. 107, no. October, 2023, 574–619, doi: 10.1016/j.jmapro.2023.10.024.

[17] L. Gebhard, L. Esposito, C. Menna, and J. Mata-Falcón, Inter-laboratory study on the influence of 3D concrete printing set-ups on the bond behaviour of various reinforcements, Cem. Concr. Compos., vol.

133, no. March, 2022, doi: 10.1016/j.cemconcomp.2022.104660.
[18] D. Avrutis, A. Nazari, and J. G. Sanjayan, Industrial Adoption of 3D Concrete Printing in the Australian Market, no. Cc. Elsevier Inc., 2019.
[19] S. L. and Z. Q. Lyu Fuyan, Zhao Dongliang , Hou Xiaohui, Applied Sciences Overview of the Development of 3D-Printing Concrete, Applie Sci., 2021.
[20] S. C. F. A. L. van O. K. Nefs, E. Schlangen, T. A. M. Salet, B. Šavija, A. S. J. Suiker, and F. P. Bos, Quality Assessment of Printable Strain Hardening Cementitious Composites Manufactured in Two Different Printing Facilities, in *Second RILEM International Conference on Concrete and Digital Fabrication*, 2020, pp. 824–838, doi: 10.1007/978-3-030-49916-7_81.
[21] V. Mechtcherine et al., A roadmap for quality control of hardening and hardened printed concrete, Cem. Concr. Res., vol. 157, no. March, 2022, 106800, doi: 10.1016/j.cemconres.2022.106800.
[22] P. Narjabadifam, S. Mollaei, F. Noroozinejad, and S. Talebi, Numerical analysis of seismic behavior of an arched-roof 3D-Printed building, Gradjevinski Mater. i Konstr., vol. 67, no. 1, 2024, 1–15, doi: 10.5937/grmk2300014p.
[23] T. A. M. Salet, Z. Y. Ahmed, F. P. Bos, and H. L. M. Laagland, Design of a 3D printed concrete bridge by testing, Virtual Phys. Prototyp., vol. 13, no. 3, 2018, 222–236, doi: 10.1080/17452759.2018.1476064.
[24] D. Asprone, F. Auricchio, C. Menna, and V. Mercuri, 3D printing of reinforced concrete elements: Technology and design approach, Constr. Build. Mater., vol. 165, 2018, 218–231, doi: 10.1016/j.conbuildmat.2018.01.018.
[25] J. J. Assaad, A. A. Yassin, F. Alsakka, and F. Hamzeh, A modular approach for steel reinforcing of 3D printed concrete-preliminary study, Sustain., vol. 12, no. 10, 2020, 1–18, 2020, doi: 10.3390/SU12104062.
[26] G. Vantyghem, W. De Corte, E. Shakour, and O. Amir, 3D printing of a post-tensioned concrete girder designed by topology optimization, Autom. Constr., vol. 112, no. January, 2020, 103084, doi: 10.1016/j.autcon.2020.103084.
[27] Marc-Patrick Pfleger, S. Geyer, C. Hölzl, and M. Vill, Investigations to Improve the Carbon Footprint of Thin Walled Concrete Structures by 3D Printing Prefabricated Elements, in *International RILEM Conference on Synergising Expertise towards Sustainability and Robustness of Cement-based Materials and Concrete Structures, SynerCrete'23 - Volume 2*, 2023, pp. 653–664.
[28] A. Aramburu, I. Calderon-Uriszar-Aldaca, and I. Puente, Parametric modelling of 3D printed concrete segmental beams with rebars under bending moments, Case Stud. Constr. Mater., vol. 18, no. December 2022, 2023, e01910, doi: 10.1016/j.cscm.2023.e01910.
[29] A. Dell'Endice, S. Bouten, T. Van Mele, and P. Block, Structural design and engineering of Striatus, an unreinforced 3D-concrete-printed masonry arch bridge, Eng. Struct., vol. 292, no. July, 2023, 116534, doi: 10.1016/j.engstruct.2023.116534.
[30] S. Maitenaz, R. Mesnil, A. Feraille, and J. F. Caron, Materialising structural optimisation of reinforced concrete beams through digital fabrication, Structures, vol. 59, no. October 2023, 2024, 105644, doi: 10.1016/j.istruc.2023.105644.
[31] Sika, “Sikacrete®-751/-752 3D one-component micro-concrete for 3d printing,” *Prod. Cat.*, 2020.
[32] European committee for standardization, “EN 1992-1-1: Eurocode 2: Design of concrete structures,” *Eur. Stand.*, 2015.
[33] S. Mitrović and I. Ignjatović, Hardened properties of 3D printed concrete – experimental investigation, *20 th Symp. Maced. Assoc. Struct. Eng. Skopje, Repub. North Maced. 28-29 Sept. 2023.*, 1052–1064, 2023.

Građevinski materijali i konstrukcije
Building Materials and Structures
journal homepage: www.dimk.rs

https://doi.org/10.5937/GRMK2400006M UDK: 628.4.038:662.734
666.972.1

Review paper

Mineral carbonation of industrial wastes for application in cement-based materials

Snežana Marinković*[1)]

[1)] *Faculty of Civil Engineering, University of Belgrade, Bulevar kralja Aleksandra 73, Belgrade, Serbia ORCID 0000-0002-1808-392X*

Article history
Received: 02 July 2024
Received in revised form: 10 August 2024
Accepted: 15 August 2024
Available online: 06 September 2024

Keywords
Accelerated carbonation,
alkaline industrial waste,
CO2 sequestration potential,
properties of carbonated wastes,
application in cement-based materials

ABSTRACT

Mineral carbonation is a way to permanently store carbon dioxide (CO_2) in cement-based materials. Demolished concrete waste and other types of alkaline industrial wastes, like iron and steel slags, fly ash, concrete slurry waste and cement kiln dust are prospective candidates for accelerated carbonation application. This paper presents CO2 sequestration potentials, impacts of the accelerated carbonation on the selected properties of wastes and their possible applications in cement-based materials. Based on the analysis of published research in the area it was concluded that porosity, volume stability and heavy metals leaching of different waste types are improved after accelerated carbonation pre-treatment. This increases the effectiveness and broadness their application as substitutes for aggregates and binders in mortar and concrete. The research is however still very limited in the area of the application of the carbonated wastes with highest CO2 sequestration potential, namely recycled concrete powders and iron/steel slags. Besides, for proper conclusions on the environmental benefits, an LCA (Life Cycle Assessment) which includes all the phases of the life cycle must be performed, which is also lacking in the published research.

1 Introduction

The carbon dioxide (CO_2) emissions have increased drastically above the period 1850-1900 and continue to increase [1], Figure 1. This is mainly a result of the unsustainable energy and land use, lifestyles and patterns of consumption and production of humans all over the planet. Due to high concentrations of CO_2 in the atmosphere, global average surface temperature rapidly rises causing climate changes [1], Figure 1. Human-caused climate change has already resulted in rise of the sea level, decrease of Arctic sea ice, ocean acidification, greater frequency and intensity of weather and climate extremes, loss of many spices, etc. [1].

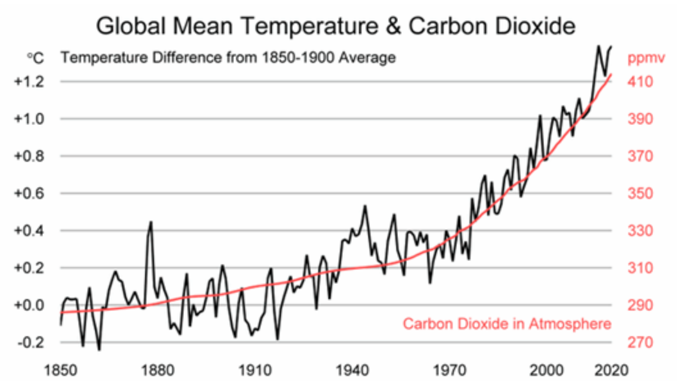

Figure 1. Rise of CO_2 concentration in atmosphere and global mean temperature

* Corresponding author:
E-mail address: sneska@imk.grf.bg.ac.rs

To prevent irreversible consequences, the Intergovernmental Panel on Climate Change (IPCC) in their 2018 Special Report, titled Global Warming of 1.5°C, recommended that global average temperature increase should be limited to 1.5°C above period 1850-1900, by 2100. For that goal to be reached, it is necessary that global CO_2 emissions reach net zero by 2050, while net non-CO_2 radiative forcing (other greenhouse gas) is significantly reduced after 2030 [2].

Reaching carbon net zero in such a short time is global task that requires deep and rapid (in some cases immediate) transition in energy, land use, infrastructure (including transport and buildings), and industrial systems. Humankind faces a huge challenge, probably one of the largest ever.

As for cement and concrete industry, there are multiple pathways toward reaching net zero CO_2 emissions. They can roughly be classified into: (i) savings in clinker production [3], (ii) savings in cement and binder [4, 5], (iii) efficiency in concrete production [6-9], (iv) efficiency in design and construction [10], (v) re-carbonation (CO_2 sink) [11], and (vi) decarbonisation of electricity [3]. However, due to the high degree of process-related CO_2 emissions, cement industry is regarded as one of the rare examples where carbon capture and storage or utilisation (CCUS) technologies must be implemented since conventional mitigations levers will not suffice.

2. Carbon capture and utilization/storage CCUS

Carbon capture and storage includes the separation of CO_2 from industrial and energy-related sources, transformation into a liquid state by compression, transport to a storage location and long-term isolation from the atmosphere [12]. Permanent storage is possible only as geological storage (in geological formations, such as oil and gas fields, coal beds and deep saline formations), ocean storage (direct injection into the ocean water column or onto the deep seafloor) and mineral carbonation [12]. Figure 2 shows the plan of the first industrial-scale carbon capture and storage facility installed at a cement plant in Brewik, Norway. The beginning of the operation is planned by the end of 2024 [13].

Captured CO_2 can be utilised in different carbon containing products, in which case it can be permanently (mineral carbonation) or temporarily stored (production of synthetic fuels, urea, methanol, etc.) [14, 15]. Carbon capture and storage is referred to as CCS and carbon capture and utilisation is referred to as CCU. In general, both pathways are together referred to as CCUS.

Mineral carbonation denotes chemical reactions in which CO_2 is converted to solid inorganic carbonates. It occurs naturally, where it is known as weathering carbonation of natural silicate rocks, such as serpentine, wollastonite and olivine, rich in magnesium oxide (MgO) and calcium oxide (CaO). The process can be accelerated using alkaline solid waste instead of natural rocks, but in both cases, it permanently stores CO_2 in the form of thermodynamically stable carbonate ($CaCO_3$/$MgCO_3$) (Eq. 1):

$$\mathrm{CaO(MgO)} + \mathrm{CO_2} \rightarrow \mathrm{CaCO_3(MgCO_3)} + \mathrm{heat} \quad (1)$$

Since natural mineral carbonation is a very slow process, current research is oriented towards accelerated carbonation of various industrial waste such as iron/steel slags, coal and fuel combustion products (fly ash), mining/mineral processing wastes, incinerator residues, cement and concrete wastes, pulp and paper mill waste, etc. [16, 17].

2.1 CO_2 utilization in the cement and concrete industry

There are multiple ways to utilize the captured CO_2 from cement plant or any other large point source, and to store it permanently in cement and concrete products. They include CO_2 curing of concrete products at early age [18, 19, 20], injection of CO_2 in the fresh concrete mix [21, 22, 23] and mineral carbonation of different wastes. The most investigated one however, is mineral carbonation of alkali industrial waste under accelerated conditions including demolished concrete waste, concrete slurry waste, cement kiln dust, fly ash, and steel slags [24, 25, 26].

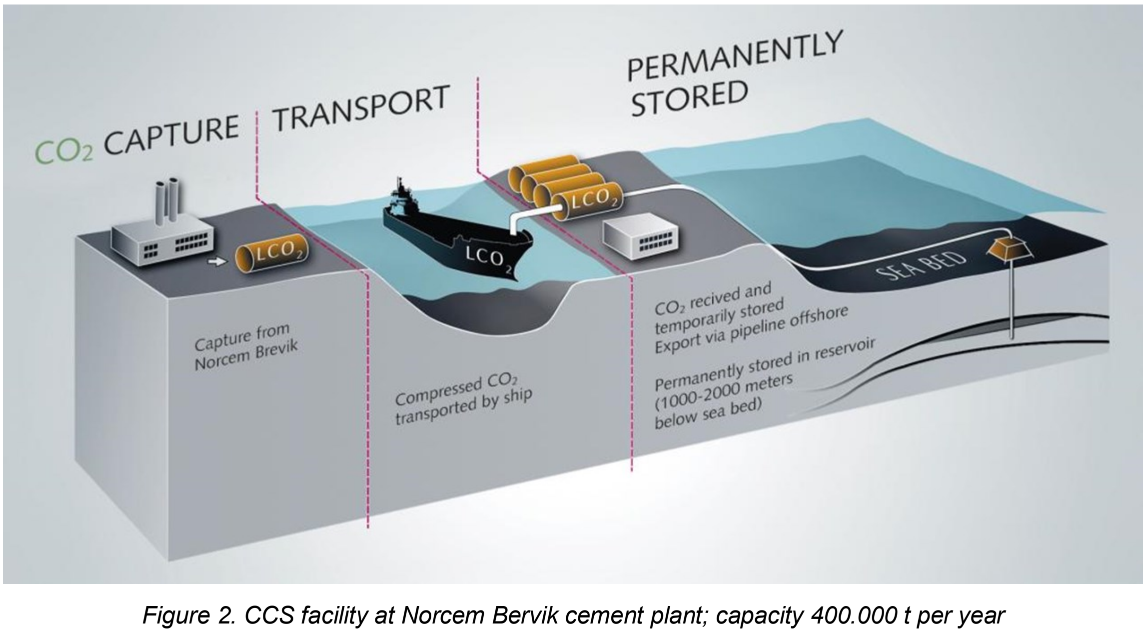

Figure 2. CCS facility at Norcem Bervik cement plant; capacity 400.000 t per year

In this work, a state-of-the-knowledge on the mineral carbonation of alkali industrial wastes is presented. Different technologies, CO_2 sequestration potentials, and possible applications in mortar and concrete production are discussed.

3. Mineral carbonation of demolished concrete waste

On average, industrial recycling of demolished concrete waste results in about 50% coarse recycled concrete aggregates CRCA, up to 40-50% fine recycled concrete aggregates FRCA (particle size <5 mm), and up to 5–10% of recycled concrete powder RCP (particle size <0.15 mm) by weight [27,28,29]. Over the past decade, a lot of research has been performed on the accelerated carbonation of recycled concrete aggregates (RCA). If exposed to accelerated carbonation, these wastes can rapidly absorb CO_2 while their properties are improved. The hydrated cement paste in residual mortar reacts with CO_2 to form $CaCO_3$ that fills the pores and densifies microstructure of RCA.

Due to the inferior quality of RCA compared with natural aggregate (NA), additional cement is usually required in the recycled concrete (RAC) to obtain performance similar to referent natural aggregate concrete (NAC) [30, 31]. If the properties of RCA were improved, lesser amount of added cement would be needed. Even a small reduction in cement content is important for reduction of CO_2 emissions from concrete production. At the same time, a certain amount of CO_2 is permanently stored in concrete.

Generally, accelerated carbonation can be performed in two different environments: dry (gas-solid reaction) and wet (liquid-solid reaction) conditions. In the former case, the aggregates are exposed to constant CO_2 concentration or flow-through of CO_2 under ambient or increased temperature and pressure. In the latter case, aggregates are immersed in aqueous solution with constant flow of CO_2 injected into the solution. In dry conditions, the rate of carbonation depends on the amount of pore water in aggregate, while in wet conditions CO_2 is dissolved in the solution to form carbonate ions and carbonation reaction is not limited by CO_2 diffusion. For that reason, wet carbonation reaction is very fast under ambient pressure and temperature and can be effectively performed with gas that has low CO_2 concentration, like for instance flue gas from cement plants [32-35].

In gas-solid conditions, the efficiency of accelerated carbonation depends on the carbonation conditions and RCA properties. Carbonation conditions include CO_2 concentration and pressure, relative humidity and temperature of the environment, duration, and gas flow rate. As for properties, it depends on the water content, particle size and calcium content in RCA.

Based on extensive published research [33-43], recommendations regarding the most favorable range of mentioned influential factors are summarized in Table 1. Faster carbonation and higher CO_2 sequestration efficiency could be achieved by simultaneous adjustment of several parameters.

3.1 Coarse recycled concrete aggregates CRCA

Carbonation of CRCA leads to their properties improvement and therefore to better properties of the concrete made with CRCA. Carbonated CRCA have lower water absorption and higher density relative to non-carbonated. Figure 3 presents the improvement of water absorption due to carbonation of CRCA with particle size 5-20 mm.

Table 1. Recommended accelerated carbonation conditions and RCA properties

Parameter		Recommendation	Comment
Environmental	Relative humidity (RH)	50%-70%	Lower or higher RH values both have adverse impacts on carbonation efficiency
	CO_2 concentration	20%-50%;	Higher concentration doesn't increase the carbonation degree, but accelerates the process
	Gas pressure	Lower than 0.5 MPa	Higher pressure doesn't significantly impact the carbonation efficiency
	Gas flow rate	Less than 5 L/min	Can achieve satisfactory carbonation efficiency with low CO_2 flue gas (20%)
	Temperature	20-30°C	Positive effect of higher temperature but depends on many parameters; mostly used 20-30°C due to economy and uncertain impact
	Duration	Depends on conditions and particle size	Carbonation degree increases with the carbonation duration but the fastest rate is in the first several hours
RCA properties	Water content	~30% of water absorption	Easily affected by RH; water content and RH should be controlled together
	Particle size	Smaller particle size exhibits significantly higher carbonation degree	Due to much higher specific surface area and much higher residual mortar (cement paste) content
	Calcium content	Adding calcium compounds	Presoaking in $CaOH_2$ solutions, waste water from ready-mixed concrete plant, etc.

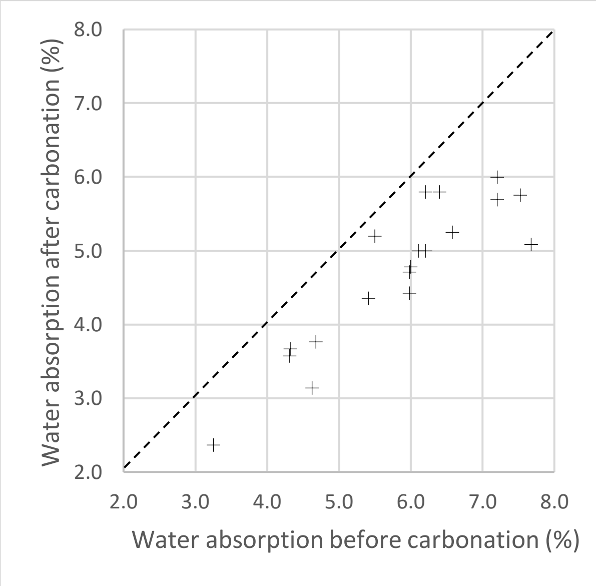

Figure 3. Water absorption of CRCA (5-20 mm) before and after carbonation [43–54]

Concrete made with carbonated CRCA shows lower loss of compressive strength compared to concrete made with non-carbonated CRCA. It can be controlled within 10% of the referent NAC compressive strength even with the complete substitution of coarse natural aggregate by carbonated CRCA. Referent NAC is concrete produced with same cement content and effective w/c ratio as RAC but with natural aggregates CNCA. Figure 4 shows the ratio between compressive strength at 28 days of RAC with carbonated CRCA ($f_{cm,RAC}$) and referent NAC ($f_{cm,NAC}$), based on test results from published research. Relatively large range of published results is due to different conditions applied in accelerated carbonation: 20-100% CO_2 concentration, pressure 0.1-4 bar and duration 30 min to 72 hours.

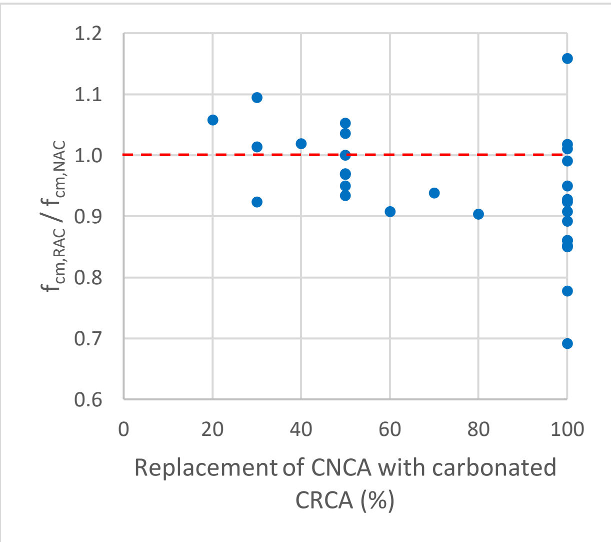

Figure 4. Ratio between compressive strength at 28 days of RAC with carbonated CRCA ($f_{cm,RAC}$) and referent NAC ($f_{cm,NAC}$) [43, 44, 46, 47, 55-62]

As for durability related properties, the results reported on the resistance to carbonation of RAC with carbonated CRCA are contradictory. Some researchers obtained lower [56], while some obtained similar or higher carbonation resistance [37, 50] compared to that of RAC with non-carbonated CRCA. The amount of cement paste in RAC, whether with carbonated or non-carbonated CRCA, is higher than in referent NAC concrete. This has two opposite effects: a higher permeability due to higher porosity and higher amount of $CaOH_2$. The former promotes carbonation; the latter hinders it. Finally, the carbonation resistance depends on which factor of these two prevails. Cement paste in RAC with carbonated CRCA has lower porosity but lesser amount of $CaOH_2$ due to carbonation, compared to RAC with non-carbonated CRCA. Therefore, resulting performance depends on many parameters and it cannot be easily predicted. On the other hand, resistance to chloride penetration of RAC with carbonated CRCA is always improved relative to RAC with non-carbonated CRCA, due to refinement of the pore structure and total porosity reduction [34, 44, 47]. Despite the fact that mechanical and durability related properties of RAC with carbonated CRCA are improved compared to RAC with non-carbonated CRCA, they are still on average inferior to referent NAC except for the low replacement ratios, up to 25%.

3.2 Fine recycled concrete aggregates FRCA

Since the beginning of the RCA application in concrete, the use of FRCA in structural concrete was not recommended [63]. Today, despite the high availability of experimental data, there is still no consensus on its effect on the concrete properties [64-67]. FRCA contains a large amount of weak and porous mortar, consisting of mostly hydrated cement paste and sand. Reported contents of cement paste in FRCA vary widely, from 18 to 70% [63, 68-70]. High water absorption of FRCA (4-16%) causes problems both with workability and strength of concrete. The FRCA's water uptake in concrete mix is uncertain, with reported values 49-89% of its water absorption [71-74], which makes the effective w/c ratio and therefore concrete performance hardly predictable.

When carbonated, FRCA absorbs much more CO_2 than CRCA due to higher specific surface area and higher amount of attached cement paste. The reduction of water absorption of FRCA after carbonation is even more pronounced then in the CRCA case; reported range in published research is 3-60%, Figure 5. Some researchers investigated the possibility of wet instead of dry carbonation [33, 35, 83]. As already mentioned, in wet carbonation FRCA is immersed in water with controlled CO_2 concentration or flow rate. Due to the more rapid dissolution of hydrates and the fact that CO_2 diffusion is not a limiting factor in this case, the carbonation rate can be significantly increased and carbonation efficiency enhanced. Liu et al. [33] reported similar water absorption reduction after 10 minutes of wet carbonation compared to 24 hours of pressurized dry carbonation. When wet and pressurized dry carbonation of the same duration of 10 minutes were compared, Fang et al. [35] reported a 5 times higher CO_2 sequestration in wet carbonation conditions. The reason is that the wet carbonation transformed a gas-solid reaction into a liquid-solid reaction and therefore enhanced the chemical reaction rate [84, 85].

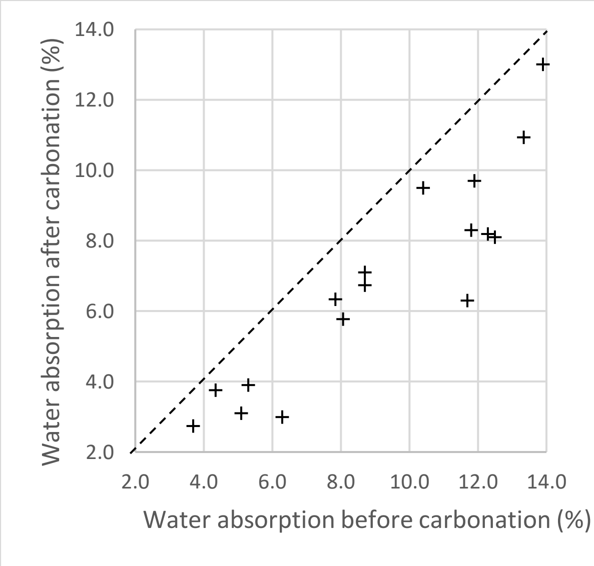

Figure 5. Water absorption of FRCA (< 5 mm) before and after carbonation [35, 41, 53, 75-83]

The negative effect of sand replacement with FRCA on concrete properties can be reduced if FRCA is pre-treated with accelerated carbonation. Moreover, recent research is focused on the full replacement of NA (both coarse and fine) with carbonated RCA.

As shown by Xiao et al. [48], with careful choice of water added to concrete mix to compensate for high water absorption values of FRCA, it was possible to produce concrete with full replacement of NA with carbonated CRCA and FRCA with similar compressive strength compared to referent NAC. In the case of RAC, the two-stage mixing method was followed [86] and the amount of additional water was set as 70% of the aggregate water absorption value minus the aggregate moisture content. Both CRCA and FRCA were obtained from real demolished concrete waste having high water absorption values, i.e. 7.67% and 13.34%, respectively. After carbonation, these values were reduced to 5.09% and 10.94%, which is still high compared to water absorption of natural aggregates (around 1%). Recycled aggregates were carbonated in chamber with a 20% CO_2 concentration and 75% relative humidity for at least 14 days (until full carbonation, which was proved by phenolphthalein test). Results of compressive strength testing showed that concrete mix with full replacement of NA with carbonated coarse and fine recycled aggregates had slightly higher compressive strength at 28 days, and slightly lower compressive strength at 180 days compared to referent NAC.

Liang et al. [76] also tested concrete mixes with full replacement of NA with carbonated and non-carbonated CRCA and FRCA. The objective was to monitor the improvement of RAC properties due to pre-treatment of recycled aggregates by accelerated carbonation. In this experiment, CRCA and FRCA were obtained by crushing and sieving the laboratory prepared mortar specimens with three different water/cement ratios equal to 0.3, 0.4 and 0.5. Recycled aggregates were carbonated in chamber with a 20% CO_2 concentration and 70% relative humidity for 10 days. Upon carbonation, water absorption of both CRCA and FRCA was reduced; for instance, from 12.3% to 8.2% and from 13.9% to 7.6% for FRCA and CRCA, respectively. It can be seen that both FRCA and CRCA had similar water absorption because they were produced from mortar samples and had similar amount of residual mortar. Both non-carbonated and carbonated recycled aggregates were pre-saturated with extra water equal to water absorption value until a saturated surface dry state was obtained and two-stage mixing method was applied. The concrete with carbonated CRCA and FRCA showed the highest compressive strength regardless of the quality of parent mortar. Negative impact of FRCA was therefore annulated by carbonation. Results cannot be compared to referent NAC mix since it was not tested. The resistance of RAC to carbonation was significantly improved by inclusion of the carbonated recycled aggregates. Carbonation depths were measured after accelerated carbonation of concrete samples at 20 ± 3% CO_2 concentration, T= 20 ± 2°C, RH=70 ± 5% for 56 days. Based on these results, authors calculated decrease of carbonation coefficient from 1.054 (RAC with non-carbonated RCA) to 0.63 (RAC with carbonated RCA) indicating higher resistance to carbonation. The pore structure refinement and improvement of ITZ properties prevailed over lower alkalinity of old cement paste in this experiment resulting in lower CO_2 diffusivity. Again, results cannot be compared to referent NAC mix.

Izoret et al. [57] reported results on the properties of concrete incorporating CRCA and FRCA carbonated in pilot installations implemented on a full scale in two industrial cement plants (rotating drum and fluidized bed). Authors tested several mixes with different replacement ratios of NA with carbonated and non-carbonated CRCA and FRCA with highest replacement ratio of 100% and 40% for coarse and fine aggregates, respectively. All mixes with carbonated aggregates, regardless of the replacement ratio, showed compressive strength at 28 days very similar to that of referent concrete, within 5% [57, 87]. Measurements of chloride diffusion coefficient showed no significant negative or positive impacts associated with the use of carbonated RCA compared to non-carbonated RCA; in both cases, this coefficient is higher than that of the referent concrete by 30-70%.

Chinzorigt et al. [88] tested mixes with 100% replacement of coarse NA with CRCA, and 15, 30 and 50% replacement of fine NA with carbonated and non-carbonated FRCA. Both CRCA and FRCA were obtained from commercial producer, while only FRCA was carbonated at 5% CO_2 concentration, RH 60±5%, T=20±2°C and ambient pressure for 72 hours. The loss of compressive strength at 28 days relative to referent concrete was about 10% for all replacement ratios of fine NA with carbonated FRCA. Measured carbonation depths under 56 days accelerated carbonation of all RAC were higher compared to referent concrete. Contrary to [76], in this experiment, concrete mixes with carbonated FRCA showed lower carbonation resistance relative to mixes with non-carbonated FRCA. Carbonation depth of concrete with 50% of carbonated FRCA was about 1.5 times that of referent concrete. The chloride penetration resistance was slightly lower for concrete with carbonated FRCA compared to concrete with non-carbonated FRCA despite lower porosity of the former (and both are lower than that of referent concrete). Possible explanation according to authors lies in the fact that chloride ions, which have been attached to the cement hydrate as Friedel's salt, are released into the pore solution during carbonation causing an increase of chloride ions concentration.

Ha et al. [89] compared mechanical and durability related properties of concrete with 100% replacement of both coarse and fine aggregates with carbonated CRCA and FRCA. Aggregates were carbonated for 4 and 14 days at 20% CO_2, T= 20°C, RH=60% and ambient pressure. Measured compressive strengths at 28 days were practically same for RAC and referent NAC, i.e. full replacement of natural with carbonated recycled aggregates did not decrease the concrete compressive strength. Measured carbonation depths under 28 days accelerated carbonation were only slightly higher in concrete with carbonated RCA (9.2 mm compared to 8.6 mm in referent concrete). The same is valid for chloride diffusion coefficient: 1.47×10^{-11} m^2/s in concrete with carbonated RCA and 1.32×10^{-11} m^2/s in referent concrete.

Liang et al. [53] reported large improvement of resistance to chloride penetration of RAC with carbonated CRCA and FRCA compared to RAC with non-carbonated aggregates. Recycled aggregates were carbonated in chamber with a 20% CO_2 concentration and 70% relative humidity upon full carbonation. Authors tested mixes with full replacement of NA with carbonated and non-carbonated CRCA and FRCA and found decreased chloride permeability and steel corrosion risk in the former case (chloride diffusion coefficient reduced by 68%). Referent NAC was not tested.

Figure 6. Industrial mineral carbonation plant (two reactor containers, CO_2 storage tank and centre for the process control) [90]

Accelerated carbonation of CRCA and FRCA can be implemented at industrial scale. There are already several concrete plants in Switzerland using this approach and selling concrete containing industrially pre-carbonated recycled concrete aggregates [90], Figure 6.

3.3 Recycled concrete powder RCP

The use of recycled concrete powder in its raw form mainly causes the dilution of binder and therefore acts predominantly as filler [91, 92]. Recent research showed however, that recycled concrete powder, if carbonated, might be used as supplementary cementitious material [93, 94, 95]. Its activity as supplementary cementitious material (SCM) depends on the efficiency of separation process during recycling. If it is possible to separate the cement paste from sand and coarse aggregates, clean aggregates are obtained. On the other hand, (mostly) hydrated cement paste readily carbonates and full carbonation can be achieved in few hours under wet carbonation conditions [83-85, 96]. The material obtained in that way has high pozzolanic activity [97] and can be used as clinker replacement by 20% [98, 99] up to 40% [93]. Therefore, there are several benefits from technology – besides producing value-added products such as high quality aggregates and SCM, potentially high CO_2 reductions can be obtained through CO_2 sequestration as well as clinker amount reduction.

Technology is still at the “laboratory proof of concept” level, and no tests on concrete made with such binders were yet performed. However, some research on the level of paste and mortar properties is available [83, 94, 95]. The impact of partial replacement of ordinary Portland cement (OPC) with carbonated RCP on compressive strength of pastes and mortars, based on the published research, is shown in Figure 7. On average, replacement ratios of up to 20% are beneficial, while higher replacement ratios reduces the compressive strength of the blended paste, with the exception of the results reported in [94]. However, if the part of OPC is replaced with carbonated RCP in mortars, strength is always reduced, reduction being higher with higher replacement ratio.

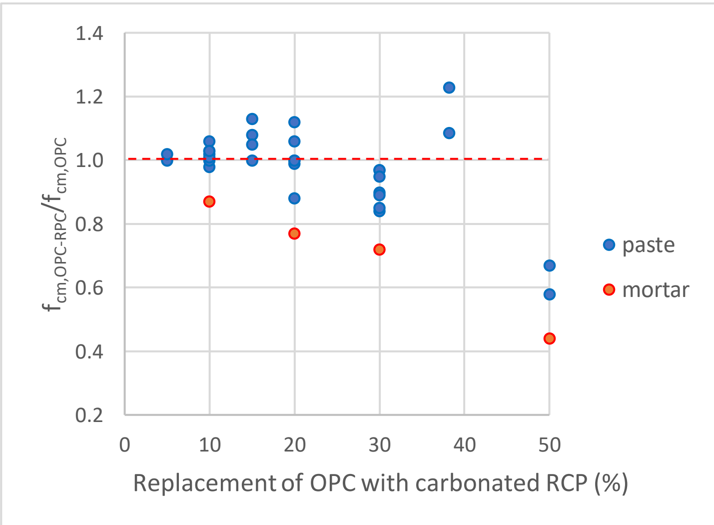

Figure 7. Ratio between compressive strength at 28 days of paste and mortars with carbonated RCP ($f_{cm,OPC-RPC}$) and OPC paste and mortars ($f_{cm,OPC}$) [83, 94, 95, 98-102]

As already mentioned, for efficient separation of recycled cement pastes from aggregates, advanced recycling technologies are necessary. Several are already developed. For instance, mechanical comminution with magnetic separation [103], microwave heating [104], advanced dry recovery ADR [105, 106], Heating-Air classification System HAS [107, 108], or pure mechanical comminution by adjusting the crushing force to an intermediate one between the average compressive strengths of the aggregates and the one of the hardened cement paste - Smart Crusher [109]. Both ADR and HAS are already industrially scaled-up mobile technologies and therefore can be used for on-site recycling of demolished concrete waste. ADR can successfully produce coarse (4-16 mm) and fine (0-4 mm) fractions from wet concrete waste by crushing and using air flow for separation, Figure 8. Fine fraction is further processed with HAS in which the input is heated to a temperature of up to 1410 ˚C while simultaneously separating very fine particles (0-0.25 mm) from the rest using air classification, Figure 9. Finely, the obtained 0.25-4 mm fraction is ground in a ball mill with steel balls to separate send from activated cement paste [106, 107].

Some of presented advanced recycling processes are already applied at industrial scale, like the Smart crusher and ADR technology in the Netherlands.

3.4 CO_2 sequestration potential of demolished concrete waste

The most significant parameter that influences the potential of CO_2 sequestration is particle size of the recycled aggregate. Under same carbonation conditions, FRCA absorbs much more CO_2 than CRCA, while RCP has the highest potential, Table 2.

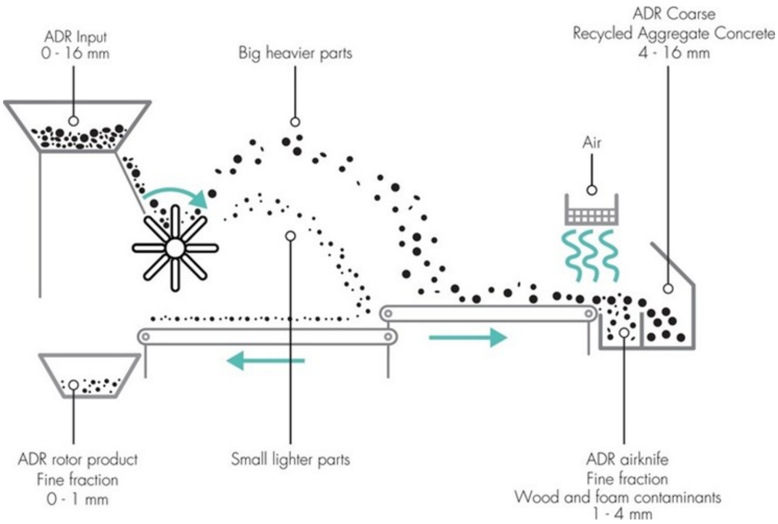

Figure 8. ADR recycling system [110]

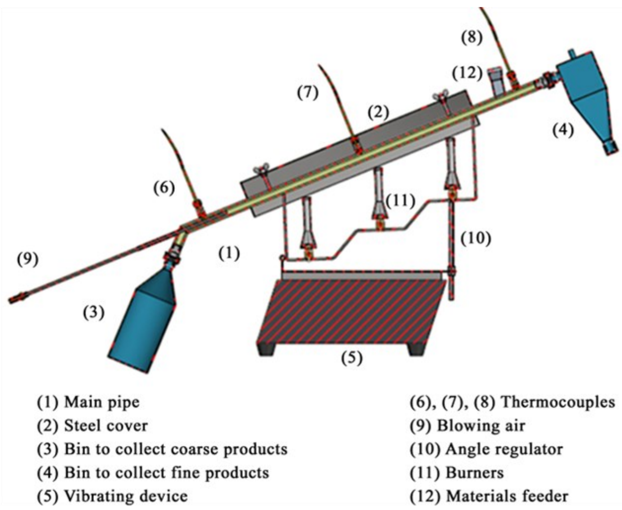

Figure 9. HAC recycling system [107]

Table 2. CO_2 sequestration potential of demolished concrete waste of different particle size [42, 57, 61, 80, 111-114]

Particle size [mm]	Method	Conditions	Duration h (hour)	CO2 uptake [% of aggregate mass]	Ref
5-10	Gas-solid	CO_2 conc.=100% RH=50% T=25°C Pressure =0.1/5 bar	24	2.6/2.8	[111]
10-20	Gas-solid	CO_2 conc.=15% RH=NA T=20°C Pressure =1 bar	24	0.65-0.96	[80]
5-10	Gas-solid	CO_2 conc.=100% RH=40-70% T=NA Pressure =0.1 bar/5bar	24	0.74/0.81	[61]
10-20		CO_2 conc.=100% RH=40-70% T=NA Pressure =0.1/5bar	24	0.65/0.66	
4-16	Gas-solid	CO_2 conc.=20% RH=NA T=20-30°C Pressure =1 bar Fluidized bed, industry	1	1.2	[57]
4-8		CO_2 conc.=100% RH=NA, 100% WA T=NA Pressure =1 bar	1.1	0.15	[42]
1-4	Gas-solid	CO_2 conc.=15% RH=NA T=20°C Pressure =1 bar	24	1.4/2.18/5.0 depending on the origin of the aggregate	[80]
0-4	Gas-solid	CO_2 conc.=20% RH=NA T=20-30°C Pressure =1 bar Fluidized bed, industry	1	3.9	[57]
0-4	Gas-solid	CO_2 conc.=100% RH=NA, 100% WA T=NA Pressure =1 bar	1.1	2.16	[42]
Median diameter 0.0168/0.0962	Liquid-solid	CO_2 conc.=14% Solid/liquid=10g/L T=20°C Pressure =1 bar	1.5	12.0/4.0	[112]
<0.25	Liquid-solid	CO_2 conc.=18.2% Solid/liquid=10g/L T=20°C Pressure =10 bar	0.17	5.0	[113]
<0.5	Liquid-solid	CO_2 conc.=18.2% Solid/liquid=10g/L T=18-25°C Pressure =10 bar	0.25	11	[114]

The results in Table 2 show high variability depending on the carbonation conditions and aggregate origin, whether from laboratory concrete and paste or real demolished concrete waste. Generally, aggregates from industry have lower CO_2 uptake capacity compared to those produced in laboratory conditions, for several reasons: specific operations at recycling plants, already partially carbonated in natural conditions, various impurities, etc. Under gas-solid conditions, results also significantly depend on the water content of recycled concrete aggregates, which mostly was not reported. The average value of CO_2 sequestration, based on this data, is 1.2%, 2.9%, and 8%, for particle size 5-20 mm, 0-4 mm and recycled concrete powder, respectively. If recycled cement paste is separated, much higher CO_2

sequestration can be obtained in liquid-solid carbonation, for instance 13.2% [115], 23% [97], 19.7-28.4% [102] (all at ambient temperature and pressure) and 28% (at elevated temperature of 80°C and pressure of 8 bar) [96]. However, these results were obtained on laboratory prepared samples (from pure cement pastes produced in laboratory), not on the hydrated cement pastes recycled in real industrial conditions.

4. Mineral carbonation of other industrial waste

Various types of industrial waste are rich in calcium and magnesium and therefore suitable for mineral CO_2 sequestration, like fly ash, steel slag, cement kiln dust, concrete slurry waste etc. Their CO_2 sequestration capacity, apart from carbonation conditions, depends mostly on the chemical composition, particle size and microstructure. A lot of research has been devoted to this subject. Carbonation under liquid-solid conditions, and at higher temperatures and pressures, was commonly used to accelerate the process [37].

Fly ash is product of combustion in coal-fired power plants. Globally, the annual production of fly ash is estimated between 0.75–1 billion tons [116]. Its chemical composition varies a lot, depending on the type of coal from which it was obtained. Fly ash produced by combustion of bituminous coal, sub- bituminous coal, and lignite typically contains 1-12%, 5-30%, and 15-40% of CaO, respectively. It is fine material with particles ranging between < 1 – 500 μm in size and having a tri-modal particle size distribution, the bulk of which is below 75 μm [116].

Iron and steel slag is by-product from iron and steel manufacturing. High amounts of this waste is produced each year globally: 330–390 million tons of iron slag and 190–290 million tons of steel slag in 2022 [117]. It is mainly classified into four different types: blast furnace (BF) slag, oxygen furnace (BOF) slag, electric arc furnace (EAF) slag and ladle furnace (LF) slag [118]. Chemical composition of various slags differs a lot depending on the iron/steel manufacturing process [119]. In the case of iron BF slag chemical composition and particle size depend also on whether it is produced with slow cooling (air-cooled slag) or with rapid cooling (granulated slag) [120]. In any case, slag must be further grinded for application in cement or concrete, which helps also in raising the efficiency of accelerated carbonation.

Some of the published results regarding FA and slags CO_2 uptake potential are summarized in Table 3.

Table 3. CO_2 sequestration potential of demolished concrete waste of fly ash and different types of iron and steel slag [121-137]

Type of waste/ CaO content (%)	Particle size mm	Method	Conditions	CO2 uptake [% of aggregate mass]	Reference
FA 4.1	Median diameter d=0.04	Liquid-solid	CO_2 conc.=100% T=30°C Pressure =10 bar Liquid/solid=10 ml/g Duration=NA	2.6	[121]
FA 7.0	Specific surface area 4.73m^2/g	Liquid-solid	CO_2 conc.=100% T=ambient Pressure =ambient Liquid/solid=5 ml/g Duration=24 h	0.8	[122]
FA 3.4	NA	Liquid-solid	CO_2 conc.=100% T=30°C Pressure = NA Liquid/solid=15 ml/g Duration= 15-55 min	3.2	[123]
FA 34.1	NA Petroleum coke ash	Liquid-solid	CO_2 conc.=100% T=60°C Pressure = ambient Liquid/solid=80 ml/g Duration=16.7 h	21.0	[124]
FA 30	0.002-0.01	Liquid-solid	CO_2 conc.=100% T=60°C Pressure = 10 bar Liquid/solid=80 ml/g Duration=1 h	26.4	[125]
FA 31.9	<0.0212	Gas-solid	CO_2 conc.=100% T=45°C Pressure =18 bar Duration=135 min	18.2	[126]
FA 10-15	0.002-0.006	Gas-solid	CO_2 conc.=100% T=160°C Pressure =8 bar Duration=4 h	2.3-5.3	[127]

BF 36.6	<0.075	Liquid-solid	CO_2 conc.=100% T=150°C Pressure =30 bar Liquid/solid=10 Duration=24h	28	[128]
BF 22.5	<0.075	Indirect	CO_2 conc.=98% T=30°C Liquid/solid=10 Duration=60 min (NH_4NO_3, NH_4Cl, CH_3COONH_4)	12.2	[129]
BF 47.2	<0.075	Indirect	T=25°C Pressure =1 bar Liquid/solid=10 Duration=60 min (CH_3COOH + EDTA)	9.0	[130]
BOF 51.1	<0.044	Liquid-solid	CO_2 conc.=100% T=60°C Pressure =1 bar Liquid/solid=10 ml/g Duration=1 h	27.0	[131]
BOF 41.2	<0.044	Liquid-solid	CO_2 conc.=100% T=25°C Pressure =1 bar Liquid/solid=20 ml/g Duration=2 h	28.3	[132]
BOF 46.4	<0.125	Liquid-solid	CO_2 conc.=30% T=30°C Pressure =1 bar Liquid/solid=20 ml/g Duration=20 min	27.7	[133]
BOF 31.1	0.063-0.1	Liquid-solid	CO_2 conc.=40% T=50°C Pressure =5 bar Liquid/solid=5 L/kg Duration=4 h	46.5	[134]
BOF 29.9	<0.15	Liquid-solid	CO_2 conc.=100% T=100°C Pressure =10.0 MPa Liquid/solid=5 L/kg Duration=24 h	32.5	[135]
EAF 33.2	<0.024	Liquid-solid	CO_2 conc.=18.2% T=25°C Pressure =10.68 bar Liquid/solid=10 ml/g Duration=10 min	5.2	[136]
EAF 28.3	<2.0	Liquid-solid	CO_2 conc.=100% T=25°C Pressure =6 bar Liquid/solid=10 ml/g Duration=3 h	8.2	[137]
EAF 49.3	<0.15	Liquid-solid	CO_2 conc.=100% T=100°C Pressure =10.0 MPa Liquid/solid=5 L/kg Duration=24 h	28	[135]

Note: BF – blast furnace slag; BOF – basic oxygen furnace slag; EAF – electric arc furnace slag

CO_2 sequestration potential of fly ash depends on the CaO content: low calcium FA has much lower CO_2 sequestration potential (0.8-3.2%) compared to high-calcium FA (18.2-26.4%). The same is valid for slags, but beside chemical composition, particle size and carbonation conditions, particularly temperature, are important factors. The smaller the particle size, the higher the CO_2 sequestration potential due to larger specific surface area. Temperature range between 50°C and 80°C seems to be optimal providing maximal CO_2 sequestration capacity [37].

Concrete slurry waste (CSW) is result of returned fresh concrete (whether over-ordered or leftovers) which is washed away from truck mixer with water. After washing, aggregates are separated from the slurry waste, which consists of very fine aggregate and cement particles and water. Usually, it is stored in sedimentation tank for a certain period to allow solids to settle and then disposed of in landfills [138]. The waste slurry can be used in wet or hardened state in various applications. If it is in hardened state, it has to be grinded and sieved before any application. The amount of produced slurry wastes is significant, up to 4.0% of freshly mixed concrete annually [25]. It is rich in CaO and can contain between 32% and 53% of CaO by mass [138-140]. Xuan et al. [138] performed a gas-solid carbonation of CSW crushed to a particles <5 mm and pre-treated to reduce the water content from 50% to 10%. Measured CO_2 sequestration after 144 hours in chamber with 100% CO_2 concentration and 0.1 bar pressure was 11%, or 110 g/kg of dry SCW. Kaliyavaradhan et al. [140] tested several carbonation conditions regarding the water-to-solid ratio (0.1, 0.25, 0.4, 0.55, 0.7) and duration time (1, 24, 72, 120, 168 hours) under same conditions: 20% CO_2 concentration, temperature 20°C and 65% RH. Dried CSW was ground and sieved to pass through 0.3 mm. The authors found that maximum CO_2 sequestration was obtained at water-to-solid ratio of 0.25 and duration of 72 h, and it was equal to 20.4 % (204.35g/kg CSW).

Cement kiln dust (CKD) is generated during the clinker production process in rotary kilns. Being a potentially hazardous waste, it is collected by air-pollution control devices. It is a fine-grained solid material, which consists of uncalcined and partially calcined raw feed, and kiln dust. Cement industry produces 30 million tons of CKD annually [141]. Typical content of CaO is between 38% and 50% [141-143] by mass. In liquid-solid carbonation tests (100% CO_2 concentration, 3 bar pressure, T=25°C and liquid-to-solid ratio=5) Medas et al. [141] measured CO_2 sequestration of 11.68% (116.8 g/kg of CKD) after 5h. Huntzinger et al. [144] measured CO_2 sequestration of 7.7% (77.0 g/kg of CKD) under ambient temperature and pressure accelerated carbonation of CKD from landfill without any pre-treatment.

Figure 10 presents the carbonation efficiency of waste materials obtained from referred published research described in previous section. It can be seen that iron and steel slags, CKD and CSW have comparable potential for mineral CO_2 sequestration (10%-30%) and that it depends not only on the CaO content, but also on the accelerated carbonation conditions and particle size. High-calcium FA (over 20% CaO by mass) belongs to that group, while low-calcium FA (below 10% CaO by mass) has small carbonation capacity.

4.1 Application

Generally these wastes, similarly to demolished concrete waste, can be applied as aggregate substitutes, Portland cement substitutes (SCM) or as fillers. If pre-treated with accelerated carbonation, their properties are improved and certain amount of CO_2 is sequestered, which both can result in the reduction of CO_2 emissions in the concrete life cycle.

As aggregates

Carbonated iron and steel slag can be used as a substitute for natural fine and coarse aggregates in mortars and concrete. Beside the significant CO_2 sequestration potential, accelerated carbonation pre-treatment increases the volume stability, reduces the leaching of heavy metals and improves slag mechanical properties [145-147]. Pang et al. [148, 149] tested the impact of partial replacement of fine and coarse natural aggregate with carbonated BOF slag on concrete properties, keeping same w/c and cement content in the concrete mix. The authors reported similar workability despite higher WA, 20% higher compressive strength at 28 days, improved ITZ zone properties, significantly higher freeze-thaw resistance (2-3 times) compared to reference samples with only natural aggregates. However, production of carbonated fine and coarse slag aggregates included grinding, pelletization, carbonation at 70°C and pressure of 3 bar, and crushing again, which all required a significant energy. Bodor et al. [150] tested the properties of cement mortar with 50% of natural sand aggregate replaced by carbonated BOF slag. Carbonation was conducted in liquid-

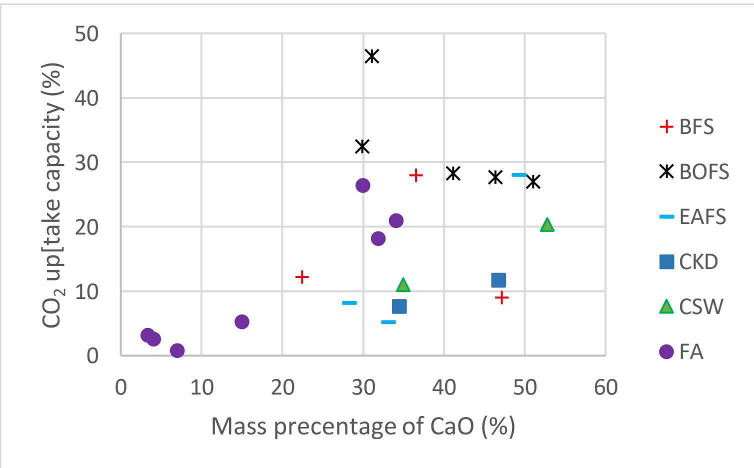

Figure 10. CO_2 sequestration potential of FA, iron and steel slags, CSW and CKD [121-135, 138, 140, 141, 144]

solid conditions at 90 °C and 20 bar CO_2 pressure, for 2 h duration. Mortar mixtures prepared with carbonated BOF slag of <0.5 mm particle size showed similar consistency via flow table test, compressive strength and leaching of toxic elements to referent mortar mixture with only natural sand. In this case, only treatment of slag prior to carbonation was crushing and sieving, while CO_2 sequestration equal to 11-19% was obtained.

Several other works showed the applicability of carbonated steel slags as aggregates for concrete: artificial aggregates obtained by wet granulation process of BOF powder [151] or a combination of slag, fly ash and cement [152]. Shen at al. [153] used original slag as coarse aggregate and ball-milled original slag as powder in production of carbonated steel slag pervious concrete. Although commonly tested concrete property – compressive strength - was obtained similar to referent concrete prepared with natural aggregate, it should be kept in mind that significant pre-treatment operations can annul (cancel) the benefits from sequestered CO_2 and waste reduction [154].

As SCM

Ground granulated BF slag (GGBS) and FA are already used as clinker replacement in commercial cements. Research on utilization of carbonated slag and fly ash as SCM is limited so far. Ebrahimi et al. [123] and Pei et al. [155] reported that up to 10% replacement of clinker with carbonated FA did not impair the compressive strength of blended cement pastes. Sahoo et al. [156] investigated concrete with 25% cement replacement with carbonated fly ash and reported high resistance against salt, sulfate and acid attack. Regarding carbonated slag as SCM, Chen et al. [157] and Pan et al. [158] reported similar results – up to 10% replacement with carbonated slags provided similar compressive strengths to pure OPC pastes and mortars, while maintaining high volume stability. The volume stability of cementitious materials containing slag is usually a problem, but carbonation consumes the expansion phase in slag (CaO) and improves it effectively. For both fly ash and slag, the main result of carbonation reaction is fine calcite ($CaCO_3$) which fills the pores and reduces pastes and mortars porosity, or becomes nucleus for hydration contributing to strength gain (setting time decrease) of cement pastes and mortars [155, 157, 159].

Utilization of ground but non-carbonated concrete slurry waste and cement kiln dust as SCMs was investigated in the previous research. Replacing clinker with CSW and CKD reduces mechanical and durability related properties of mortars and concretes, and general conclusion is that replacement should be limited to 10% to achieve similar strengths and durability of OPC mortars and concretes [28, 160]. Carbonated CSW and CKD should however improve the mortar and concrete performance due to same reasons as in the case of carbonated FA and slag. Kaliyavaradhan et al. [140] for instance, reported higher strength of mortar prepared with carbonated CSW compared to mortar prepared with fresh CSW, at 20% cement replacement ratio. As concluded by the authors, strength improvement was probably result of the reaction of aluminate C3A and calcite to form calcium carboaluminate hydrate. However, it was still slightly lower compared to pure OPC mortar. Sharma et al. [143] investigated carbonation curing of mortars containing CKD, while Xuan et al. [138] studied the carbonation curing of partition wall blocks made of CSW and fine recycled concrete aggregates. In these cases, accelerated carbonation was applied on the final product resulting in the improvement of their performance.

5. Conclusion

Mineral carbonation of alkaline industrial waste is a way to permanently store CO_2 in cement-based materials. On the other hand, pre-treatment with accelerated carbonation improves properties of various wastes enabling in that way their application as substitutes for natural aggregates and OPC.

Accelerated carbonation of coarse and fine aggregates obtained by demolished concrete waste leads to decrease of their porosity due to formation of calcite, which fill in the pores and densify the microstructure. Most of the experimental research showed that full replacement of natural aggregates with carbonated ones didn’t jeopardize the compressive strength of RAC, meaning that there is no need to increase the cement content to obtain strength similar to that of the referent NAC. As for carbonation and chloride penetration resistance of RAC with carbonated aggregates, different results were reported indicating that those concretes, despite lower permeability, may have lower resistances compared to referent NAC. This may be because of lower alkalinity of their pastes in the carbonation resistance case, or due to increased chloride concentration as a consequence of previous carbonation of aggregates in the chloride penetration resistance case. CO_2 sequestration potential depends mostly on the particle size and water content of aggregates under same carbonation conditions: FRCA can absorb up to 5% of their weight depending on the water content, while CO_2 uptake potential of CRCA is modest, 1-2% of their weight. Recycled concrete powder has much higher CO_2 sequestration potential ranging from 5-11% and in the case of pure recycled cement paste reaches 30% of the weight. Carbonated RCP has good pozzolanic activity and can be used as SCM. In the amounts of up to 20% it even increases the strength of paste, while for higher replacement ratios, the strength is decreased.

Similar to demolished concrete waste, the properties of fly ash, slags, cement kiln dust and concrete slurry waste are improved when pre-treated with accelerated carbonation, including higher volume stability and lower leaching of heavy metals. Except for low-calcium FA, these wastes have high CO_2 sequestration potential, between 10% and 30% of their weight, especially iron and steel slags. Carbonated slags can be used as substitute for aggregates, and when ground into powder they can be used as SCM, as well as carbonated FA, CKD and CSW. However, research on the impact of such aggregates and binders on the concrete performance doesn’t exist at the moment. The same is valid for the carbonated RCP utilization as partial replacement of OPC in concrete.

Despite the obvious benefits of the mineral carbonation technology, one should kept in mind that these benefits could easily be cancelled by required energy and CO_2 emissions during process. Beside the accelerated carbonation itself (energy requirement depends on the applied pressure and temperature), some pre-treatment processes are energy intensive, like drying of recycled aggregates for instance. Wet aggregates are common industrial condition and such high water content practically disables carbonation – so, they must be dried. Preparation of slags for application as aggregates or SCM include various pre-treatments beside accelerated carbonation. Therefore, for proper conclusions on environmental benefits of mineral carbonation application in cement-based materials, an LCA (Life Cycle Assessment) which includes all the phases of the life cycle must be performed.

Regarding CO_2 sequestration potential, most promising candidates for mineral carbonation are recycled concrete powders, iron and steel slags, and high-calcium fly ash. The future research should be oriented towards better understanding of the impact of their application as aggregates or SCM in cement based materials, concrete most of all.

CRediT authorship contribution statement

Snežana Marinković: Conceptualization; Methodology; Data curation; Formal analysis; Writing.

Declaration of competing interest

Author declares no conflict of interest.

Acknowledgments

Research was not supported by other persons or institutions.

References

[1] IPCC, 2023: Climate Change 2023: Synthesis Report. Contribution of Working Groups I, II and III to the Sixth Assessment Report of the Intergovernmental Panel on Climate Change [Core Writing Team, H. Lee and J. Romero (eds.)]. IPCC, Geneva, Switzerland,184 pp., doi: 10.59327/IPCC/AR6-9789291691647

[2] IPCC, 2018: Global Warming of 1.5°C. An IPCC Special Report on the impacts of global warming of 1.5°C above pre-industrial levels and related global greenhouse gas emission pathways, in the context of strengthening the global response to the threat of climate change, sustainable development, and efforts to eradicate poverty [Masson-Delmotte, V., P. Zhai, H.-O. Pörtner, D. Roberts, J. Skea, P.R. Shukla, A. Pirani, W. Moufouma-Okia, C. Péan, R. Pidcock, S. Connors, J.B.R. Matthews, Y. Chen, X. Zhou, M.I. Gomis, E. Lonnoy, T. Maycock, M. Tignor, and T. Waterfield (eds.)],

[3] GCCA. Concrete Future – The GCCA 2050 Cement and Concrete Industry Roadmap for Net Zero Concrete, 2021. Available at: https://gccassociation.org/concretefuture/

[4] G. Habert, S.A.Miller, V.M. John et al., Environmental impacts and decarbonization strategies in the cement and concrete industries. Nature Reviews Earth & Environment, 1 (11), 2020, 559-573. https://doi.org/10.1038/s43017-020-0093-3

[5] K. Scrivener, F. Martirena, S. Bishnoi, S. Maity, Calcined clay limestone cements (LC^3), Cement and Concrete Research 114, 2018, 49–56. https://doi.org/10.1016/j.cemconres.2017.08.017

[6] A. Passer, R. Deutsch, M. Scherz, Beton-LCA – Wie grün ist grau?. Baukongress, 63-64, 2018.

[7] W. Shanks, C.F. Dunant, M.P. Drewniok, R.C. Lupton, A. Serrenho, J.M. Allwood, How much cement can we do without? Lessons from cement material flows in the UK, Resources, Conservation & Recycling 141, 2019, 441–454. https://doi.org/10.1016/j.resconrec.2018.11.002

[8] M. Marinković, A. Radović, V. Carević, Carbonation of limestone powder concrete: state-of-the-art overview, Building Materials and Structures 66, 2023, 2300005M. https://doi.org/10.5937/GRMK2300005M

[9] J. Dragaš, S. Marinković, V. Radonjanin, Prediction models for high-volume fly ash concrete practical application: mechanical properties and experimental database, Building Materials and Structures 64, 2021, 19-43. https://doi.org/10.5937/GRMK2101019D

[10] H. Hafez, P. Bajić, S. Aidarov, X. Malija, M. Drewniok, P. Purnell, N. Tošić, Parametric study on the decarbonization potential of structural system and concrete mix design choices for mid-rise concrete buildings, Materials and Structures 57, 2024, 85. https://doi.org/10.1617/s11527-024-02367-1

[11] H. Stripple, C. Ljungkrantz, T. Gustafsson, R. Andersson, CO_2 uptake in cement-containing products, IVL Swedish Environmental Research Institute, Stockholm, Sweden, 2018.

[12] IPCC, 2005: IPCC Special Report on Carbon Dioxide Capture and Storage. Prepared by Working Group III of the Intergovernmental Panel on Climate Change [Metz, B., O. Davidson, H. C. de Coninck, M. Loos, and L. A. Meyer (eds.)]. Cambridge University Press, Cambridge, United Kingdom and New York, NY, USA, 442 pp.

[13] Heidelberg Materials, Annual and Sustainability Report 2023, available at www.heidelbergmaterials.com

[14] J. Patricio, A. Angelis-Dimakis, A. Castillo-Castillo, Y. Kalmykova, L. Rosado, Region prioritization for the development of carbon capture and utilization technologies, Journal of CO_2 Utilization 17 (2017) 50–59, http://dx.doi.org/10.1016/j.jcou.2016.10.002

[15] C. Schmid, A. Hahn, Potential CO_2 utilisation in Germany: An analysis of theoretical CO_2 demand by 2030, Journal of CO2 Utilization 50 (2021) 101580, https://doi.org/10.1016/j.jcou.2021.101580

[16] H. Ostovari, A. Sternberg, A. Bardow, Rock 'n' use of CO_2: carbon footprint of carbon capture and utilization by mineralization, Sustainable Energy Fuels 4 (2020) 4482–4496, DOI: 10.1039/d0se00190b

[17] B. Robertson, M. Mousavian, The Carbon Capture Crux Lessons Learned, Institute for Energy Economics and Financial Analysis (IEEFA) report, 2022, 79 pp.

[18] Y. Shao, A. Z. Morshed, Early carbonation for hollow-core concrete slab curing and carbon dioxide recycling, Materials and Structures (2015) 48:307–319, DOI 10.1617/s11527-013-0185-3

[19] V. Rostami, Y. Shao, A. J. Boyd, Carbonation Curing versus Steam Curing for Precast Concrete Production, J. Mater. Civ. Eng., 2012, 24(9): 1221-1229, DOI:10.1061/(ASCE)MT.1943-5533.0000462

[20] D. Zhang, Y. Shao, Early age carbonation curing for precast reinforced concretes, Construction and Building Materials 113 (2016) 134–143, http://dx.doi.org/10.1016/j.conbuildmat.2016.03.048

[21] S. Monkman, M. MacDonald, On carbon dioxide utilization as a means to improve the sustainability of ready-mixed concrete, Journal of Cleaner Production 167 (2017) 365e375, http://dx.doi.org/10.1016/j.jclepro.2017.08.194

[22] Z. He, Z. Li, Y. Shao, Effect of Carbonation Mixing on CO_2 Uptake and Strength Gain in Concrete, J. Mater. Civ. Eng., 2017, 29(10): 04017176, DOI: 10.1061/(ASCE)MT.1943-5533.0002031.

[23] A. Hosseinpanahi, L. Shen, P. Dera, R. Mirmoghtadaei, Properties and microstructure of concrete and cementitious paste with liquid carbon dioxide additives, Journal of Cleaner Production 414 (2023) 137293, https://doi.org/10.1016/j.jclepro.2023.137293

[24] M. Hanifa, R. Agarwal, U. Sharma, P.C. Thapliyal, L.P. Singh, A review on CO_2 capture and sequestration in the construction industry: Emerging approaches and commercialised technologies, Journal of CO_2 Utilization 67 (2023) 102292, https://doi.org/10.1016/j.jcou.2022.102292

[25] M. Kazemian, B. Shafei, Carbon sequestration and storage in concrete: A state-of-the-art review of compositions, methods, and developments, Journal of CO_2 Utilization 70 (2023) 102443, https://doi.org/10.1016/j.jcou.2023.102443

[26] N. Li, L. Mo, C. Unluer, Emerging CO_2 utilization technologies for construction materials: A review, Journal of CO2 Utilization 65 (2022) 102237, https://doi.org/10.1016/j.jcou.2022.102237

[27] Y.A. Villagrán-Zaccardi, A.T.M. Marsh, M.E. Sosa, C.J. Zega, N. De Belie, S.A. Bernal, Complete re-utilization of waste concretes–Valorisation pathways and research needs, Resources, Conservation & Recycling 177 (2022) 105955, https://doi.org/10.1016/j.resconrec.2021.105955

[28] S.K. Kaliyavaradhan, T.-C. Ling, K.H. Mo, Valorization of waste powders from cement-concrete life cycle: A pathway to circular future, Journal of Cleaner Production 268 (2020) 122358, https://doi.org/10.1016/j.jclepro.2020.122358

[29] J. Schoon, K. De Buysser, I. Van Driessche, N. De Belie, Fines extracted from recycled concrete as alternative raw material for Portland cement clinker production, Cement & Concrete Composites 58 (2015) 70–80, http://dx.doi.org/10.1016/j.cemconcomp.2015.01.003

[30] S. Marinković, V. Carević, Comparative studies of the life cycle analysis between conventional and recycled aggregate concrete, in De Brito J. and Agrela F. (eds.): New Trends in Eco-Efficient and Recycled Concrete, Elsevier Ltd. Woodhead Publishing, 2019, p. 257-291, https://doi.org/10.1016/B978-0-08-102480-5.00010-5

[31] S. Marinković, I. Josa, S. Braymand, N. Tošić, Sustainability assessment of recycled aggregate concrete structures: A critical view on the current state-of-knowledge and practice, Structural Concrete 24(2) (2023) 1956-1979, https://doi.org./10.1002/suco.202201245

[32] D. Meng, C. Unluer, E.-H. Yang, S. Qian, Carbon sequestration and utilization in cement-based materials and potential impacts on durability of structural concrete, Construction and Building Materials 361 (2022) 129610, https://doi.org/10.1016/j.conbuildmat.2022.129610

[33] S. Liu, P. Shen, D. Xuan, L. Li, A. Sojobi, B. Zhan, C.S. Poon, A comparison of liquid-solid and gas-solid accelerated carbonation for enhancement of recycled concrete aggregate, Cement and Concrete Composites 118 (2021) 103988, https://doi.org/10.1016/j.cemconcomp.2021.103988

[34] Y. Pu, L. Li, X. Shi, Q. Wang, A. Abomohra, Recent advances in accelerated carbonation for improving cement-based materials and CO_2 mitigation from a life cycle perspective, Construction and Building Materials 388 (2023) 131695, https://doi.org/10.1016/j.conbuildmat.2023.131695

[35] X. Fang, D. Xuan, P. Shen, C.S. Poon, Fast enhancement of recycled fine aggregates properties by wet carbonation, Journal of Cleaner Production 313 (2021) 127867, https://doi.org/10.1016/j.jclepro.2021.127867

[36] Y. Pu, L. Li, Q. Wang, X. Shi, C. Luan, G. Zhang, L. Fu, A.E.-F. Abomohra, Accelerated carbonation technology for enhanced treatment of recycled concrete aggregates: A state-of-the-art review, Construction and Building Materials 282 (2021) 2671, https://doi.org/10.1016/j.conbuildmat.2021.122671

[37] L. Li , M. Wu, An overview of utilizing CO_2 for accelerated carbonation treatment in the concrete industry, Journal of CO_2 Utilization 60 (2022) 102000, https://doi.org/10.1016/j.jcou.2022.102000

[38] C. Liang, B. Pan, Z. Ma, Z. He, Z. Duan, Utilization of CO_2 curing to enhance the properties of recycled aggregate and prepared concrete: A review, Cement and Concrete Composites 105 (2020) 103446, https://doi.org/10.1016/j.cemconcomp.2019.103446

[39] K. Liu, W. Xu, D. Sun, J. Tang, A. Wang, D. Chen, Carbonation of recycled aggregate and its effect on properties of recycled aggregate concrete: A review, Mater. Express, Vol. 11, No. 9, 2021, doi:10.1166/mex.2021.2045

[40] D. Wang, J. Xiao, Z. Duan, Strategies to accelerate CO_2 sequestration of cement-based materials and their application prospects, Construction and Building Materials 314 (2022) 125646, https://doi.org/10.1016/j.conbuildmat.2021.125646

[41] G.S. dos Reis, B.G. Cazacliu, R. Artoni, J.-m. Torrenti, Effect of the accelerated carbonation treatment on the recycled sand physicochemical characteristics through the rolling carbonation process, Journal of CO_2 Utilization 39 (2020) 101181, https://doi.org/10.1016/j.jcou.2020.101181

[42] A. Leemann, F. Winnefeld, B. Münch, J. Tiefenthaler, Accelerated carbonation of recycled concrete aggregates and its implications for the production of recycling concrete, Journal of Building Engineering 79 (2023) 107779, https://doi.org/10.1016/j.jobe.2023.107779

[43] Y. Pu, L. Li, Q. Wang, X. Shi, L. Fu, G. Zhang, C. Luan, A.El-F. Abomohra, Accelerated carbonation treatment of recycled concrete aggregates using flue gas: A comparative study towards performance improvement, Journal of CO_2 Utilization 43 (2021) 101362, https://doi.org/10.1016/j.jcou.2020.101362

[44] X. Fang, B. Zhan, C.S. Poon, Enhancement of recycled aggregates and concrete by combined treatment of spraying Ca^{2+} rich wastewater and flow-through carbonation, Constr. Build. Mater. 277 (2021), 122202, https://doi.org/10.1016/j.conbuildmat.2020.122202

[45] Y. Li, S. Zhang, R. Wang, Y. Zhao, C. Men, Effects of carbonation treatment on the crushing characteristics of recycled coarse aggregates, Constr. Build. Mater. 201 (2019) 408–420, https://doi.org/10.1016/j.conbuildmat.2018.12.158

[46] B. Lu, C. Shi, Z. Cao, M. Guo, J. Zheng, Effect of carbonated coarse recycled concrete aggregate on the properties and microstructure of recycled concrete, J. Clean. Prod. 233 (2019) 421–428, https://doi.org/10.1016/j.jclepro.2019.05.350

[47] S. Luo, S. Ye, J. Xiao, J. Zheng, Y. Zhu, Carbonated recycled coarse aggregate and uniaxial compressive stress-strain relation of recycled aggregate concrete, Constr. Build. Mater. 188 (2018) 956–965, https://doi.org/10.1016/j.conbuildmat.2018.08.159

[48] J. Xiao, H. Zhang, Y. Tang, Q. Deng, D. Wang, C.-s. Poon, Fully utilizing carbonated recycled aggregates in concrete: strength, drying shrinkage and carbon

emissions analysis, J. Clean. Prod. 377 (2022), 134520, https://doi.org/10.1016/j.jclepro.2022.134520
[49] B. Tang, M. Fan, Z. Yang, Y. Sun, L. Yuan, A comparison study of aggregate carbonation and concrete carbonation for the enhancement of recycled aggregate pervious concrete, Construction and Building Materials 371 (2023) 130797, https://doi.org/10.1016/j.conbuildmat.2023.130797
[50] D. Xuan, B. Zhan, C.S. Poon, Durability of recycled aggregate concrete prepared with carbonated recycled concrete aggregates, Cement and Concrete Composites 84 (2017) 214-221, https://doi.org/10.1016/j.cemconcomp.2017.09.015
[51] A.H. Zadeh, M. Mamirov, S. Kim, J. Hu, CO_2-treatment of recycled concrete aggregates to improve mechanical and environmental properties for unbound applications, Construction and Building Materials 275 (2021) 122180, https://doi.org/10.1016/j.conbuildmat.2020.122180
[52] B. Zhan, D. Xuan, W. Zenga, C.S. Poon, Carbonation treatment of recycled concrete aggregate: Effect on transport properties and steel corrosion of recycled aggregate concrete, Cement and Concrete Composites 104 (2019) 103360, https://doi.org/10.1016/j.cemconcomp.2019.103360
[53] C. Liang, H. Ma, Y. Pan, Z. Ma, Z. Duan, Z. He, Chloride permeability and the caused steel corrosion in the concrete with carbonated recycled aggregate, Constr. Build. Mater. 218 (2019) 506–518, https://doi.org/10.1016/j.conbuildmat.2019.05.136
[54] B. Zhan, C.S. Poon, Q. Liu, S. Kou, C. Shi, Experimental study on CO_2 curing for enhancement of recycled aggregate properties, Construction and Building Materials 67 (2014) 3–7, http://dx.doi.org/10.1016/j.conbuildmat.2013.09.008
[55] S. Kou, B. Zhan, C.S. Poon, Use of a CO_2 curing step to improve the properties of concrete prepared with recycled aggregates, Cement & Concrete Composites 45 (2014) 22–28, http://dx.doi.org/10.1016/j.cemconcomp.2013.09.008
[56] M. Etxeberria, S. Castillo, How the Carbonation Treatment of Different Types of Recycled Aggregates Affects the Properties of Concrete, Sustainability 2023, 15, 3169, https://doi.org/10.3390/su15043169
[57] L. Izoret, T. Pernin, J.-M. Potier, J.-M. Torrenti, Impact of Industrial Application of Fast Carbonation of Recycled Concrete Aggregates, Appl. Sci. 2023, 13, 849, https://doi.org/10.3390/app13020849
[58] S.M.S. Kazmi, M.J. Munir, Y.-F. Wua, I.P.Y. Zhou, F. Xing, Effect of recycled aggregate treatment techniques on the durability of concrete: A comparative evaluation, Construction and Building Materials 264 (2020) 120284, https://doi.org/10.1016/j.conbuildmat.2020.120284
[59] N. Russo, F. Lollini, Effect of carbonated recycled coarse aggregates on the mechanical and durability properties of concrete, Journal of Building Engineering 51 (2022) 104290, https://doi.org/10.1016/j.jobe.2022.104290
[60] H. Sharma, D.K. Ashish, S.K. Sharma, Development of low-carbon recycled aggregate concrete using carbonation treatment and alccofine, Energy, Ecology and Environment 2023, https://doi.org/10.1007/s40974-023-00299-0
[61] D. Xuan, B. Zhan, C.S. Poon, Assessment of mechanical properties of concrete incorporating carbonated recycled concrete aggregates, Cement and Concrete Composites 65 (2016) 67-74, http://dx.doi.org/10.1016/j.cemconcomp.2015.10.018
[62] V.W.Y. Tam, A. Butera, K.N. Le, Carbon-conditioned recycled aggregate in concrete production, Journal of Cleaner Production 133 (2016) 672-680, http://dx.doi.org/10.1016/j.jclepro.2016.06.007
[63] T.C. Hansen, Recycled aggregates and recycled aggregate concrete second state-of-the-art report developments 1945–1985, Materials and Structures 19, 201–246, http://dx.doi.org/10.1007/BF02472036
[64] L. Evangelista, J. de Brito, Durability of crushed fine recycled aggregate concrete assessed by permeability-related properties, Magazine of Concrete Research 71, 1142–1150, https://doi.org/10.1680/jmacr.18.00093
[65] G. Puente de Andrade, G. de Castro Polisseni, M. Pepe, R.D.T. Filho, Design of structural concrete mixtures containing fine recycled concrete aggregate using packing model, Construction and Building Materials 252 (2020) 119091, https://doi.org/10.1016/j.conbuildmat.2020.119091
[66] L. Yu, L. Huang, H. Ding, Rheological and mechanical properties of ultra-high-performance concrete containing fine recycled concrete aggregates, Materials 12, 3717, https://doi.org/10.3390/ma12223717
[67] S.K. Kirthika, S.K. Singh, Durability studies on recycled fine aggregate concrete, Construction and Building Materials 250 (2020) 118850, https://doi.org/10.1016/j.conbuildmat.2020.118850
[68] C.J. Engelsen, H.A. van der Sloot, G. Wibetoe, G. Petkovic, E. Stoltenberg-Hansson, W. Lund, Release of major elements from recycled concrete aggregates and geochemical modelling, Cement and Concrete Research 39 (2009) 446–459, https://doi.org/10.1016/j.cemconres.2009.02.001
[69] M.E. Sosa, L.E. Carrizo, C.J. Zega, Y.A. Villagrán Zaccardi, Water absorption of fine recycled aggregates: effective determination by a method based on electrical conductivity, Materials and Structures (2018) 51:127, https://doi.org/10.1617/s11527-018-1248-2
[70] C.J. Zega, Propiedades físico-mecánicas y durables de hormigones reciclados. Facultad De Ingeniería. Universidad Nacional de La Plata, 2010, p. 166.
[71] M.E. Bouarroudj, S. Remond, F. Michel, Z. Zhao, D. Bulteel, L. Courard, Use of a reference limestone fine aggregate to study the fresh and hard behavior of mortar made with recycled fine aggregate, Materials and Structures (2019) 52:18, https://doi.org/10.1617/s11527-019-1325-1
[72] Z. Li, J. Liu, P. Zhong, Assessment of the absorption of fine recycled aggregates in paste – determination of free water content of paste. In 4th International Conference On Service Life Design For Infrastructure, 2018, Delft.
[73] H. Maimouni, S. Remond, F. Huchet, P. Richard, V. Thiery, Y. Descantes, Quantitative assessment of the saturation degree of model fine recycled concrete aggregates immersed in a filler or cement paste, Construction and Building Materials 175 (2018) 496–507, https://doi.org/10.1016/j.conbuildmat.2018.04.211
[74] M. Velay-Lizancos, I. Martínez-Lage, C. Vázquez-Herrero, P. Vázquez-Burgo, Empirical definition of effective water/cement ratio in mortars with recycled aggregate depending on the absorption, Proceedings of the II International and IV National Congress on Sustainable Construction and Eco-Efficient

SolutionsConstruction and Eco-efficient Solutions, Sevilla, 2015.
[75] Y. Leng, Y. Rui, S. Zhonghe, F. Dingqiang, W. Jinnan, Y. Yonghuan, L. Qiqing, H. Xiang, Development of an environmental Ultra-High Performance Concrete (UHPC) incorporating carbonated recycled coarse aggregate, Construction and Building Materials 362 (2023) 129657, https://doi.org/10.1016/j.conbuildmat.2022.129657
[76] C. Liang, N. Lua, H. Ma, Z. Ma, Z. Duan, Carbonation behavior of recycled concrete with CO_2-curing recycled aggregate under various environments, Journal of CO_2 Utilization 39 (2020) 101185, https://doi.org/10.1016/j.jcou.2020.101185
[77] J. Zhang, C. Shi, Y. Li, X. Pan, C.S. Poon, Z. Xie, Influence of carbonated recycled concrete aggregate on properties of cement mortar, Construction and Building Materials 98 (2015) 1–7, http://dx.doi.org/10.1016/j.conbuildmat.2015.08.087
[78] Y. Jiang, L. Li, J. Lu, P. Shen, T.-C. Ling, C.S. Poon, Enhancing the microstructure and surface texture of recycled concrete fine aggregate via magnesium-modified carbonation, Cement and Concrete Research 162 (2022) 106967, https://doi.org/10.1016/j.cemconres.2022.106967
[79] M.T. Le, C. Tribout, G. Escadeillas, Durability of mortars with leftover recycled sand, Construction and Building Materials 215 (2019) 391–400, https://doi.org/10.1016/j.conbuildmat.2019.04.179
[80] M. Sereng, A. Djerbi, O.O. Metalssi, P. Dangla, J.-M. Torrenti, Improvement of Recycled Aggregates Properties by Means of CO_2 Uptake, Appl. Sci. 2021, 11, 6571, https://doi.org/10.3390/app11146571
[81] C. Shi, Z. Wu, Z. Cao, T.C. Ling, J. Zheng, Performance of mortar prepared with recycled concrete aggregate enhanced by CO_2 and pozzolan slurry, Cement and Concrete Composites 86 (2018) 130-138, https://doi.org/10.1016/j.cemconcomp.2017.10.013
[82] G. Pan, M. Zhan, M. Fu, Y. Wanga, X. Lu, Effect of CO_2 curing on demolition recycled fine aggregates enhanced by calcium hydroxide pre-soaking, Construction and Building Materials 154 (2017) 810–818, http://dx.doi.org/10.1016/j.conbuildmat.2017.07.079
[83] Y. Jiang, L. Li, J.-x. Lu, P. Shen, T.-C. Ling, C.S. Poon, Mechanism of carbonating recycled concrete fines in aqueous environment: the particle size effect, Cem. Concr. Compos. 133 (2022), 104655, https://doi.org/10.1016/j.cemconcomp.2022.104655
[84] M. Zajac, J. Skibsted, J. Skocek, P. Durdzinski, F. Bullerjahn, M. Ben, Phase assemblage and microstructure of cement paste subjected to enforced, wet carbonation, Cement Concr. Res. 130, 105990, https://doi.org/10.1016/j.cemconres.2020.105990
[85] M. Zajac, J. Skibsted, P. Durdzinski, F. Bullerjahn, J. Skocek, M. Ben Haha, Kinetics of enforced carbonation of cement paste. Cement Concr. Res. 131 (2020), 106013. https://doi.org/10.1016/j.cemconres.2020.106013
[86] V.W.Y. Tam, X.F. Gao, C.M. Tam, Microstructural analysis of recycled aggregate concrete produced from two-stage mixing approach, Cement and Concrete Research 35 (2005) 1195– 1203 https://doi.org/10.1016/j.cemconres.2004.10.025
[87] J.-M. Torrenti et al., The FastCarb project: Taking advantage of the accelerated carbonation of recycled concrete aggregates, Case Studies in Construction Materials 17 (2022) e01349, https://doi.org/10.1016/j.cscm.2022.e01349
[88] G. Chinzorigt, M.K. Lim, M. Yu, H. Lee, O. Enkbold, D. Choi, Strength, shrinkage and creep and durability aspects of concrete including CO2 treated recycled fine aggregate, Cement and Concrete Research 136 (2020) 106062, https://doi.org/10.1016/j.cemconres.2020.106062
[89] J.-S. Ha, J.-H. Shin, L. Chung, H.-S. Kim, Performance Evaluation of Recycled Aggregate Concrete Made of Recycled Aggregate Modified by Carbonation, Journal of the Korea Concrete Institute Vol. 28, No. 4, pp. 445~454, 2016, http://dx.doi.org/10.4334/JKCI.2016.28.4.445
[90] J. Tiefenthaler, L. Braune, C. Bauer, R. Sacchi, M. Mazzotti, Technological Demonstration and Life Cycle Assessment of a Negative Emission Value Chain in the Swiss Concrete Sector, Frontiers in Climate 3:729259 (2021), http://doi.org/10.3389/fclim.2021.729259
[91] S. Li, J. Gao, Q. Li, X. Zhao, Investigation of using recycled powder from the preparation of recycled aggregate as a supplementary cementitious material, Constr. Build. Mater. 267 (2021), 120976, https://doi.org/10.1016/j.conbuildmat.2020.120976
[92] H. Zhang, C. Zhang, B. He, S. Yi, L. Tang, Recycling fine powder collected from construction and demolition wastes as partial alternatives to cement: A comprehensive analysis on effects, mechanism, cost and CO_2 emission, Journal of Building Engineering 71 (2023) 106507, https://doi.org/10.1016/j.jobe.2023.106507
[93] M. Zajac, J. Skocek, J. Skibsted, M. Ben Haha, CO_2 mineralization of demolished concrete wastes into a supplementary cementitious material – a new CCU approach for the cement industry, RILEM Technical Letters (2021) 6: 53-60, https://doi.org/10.21809/rilemtechlett.2021.141
[94] M. Zajac, J. Skocek, Ł. Gołek, J. Deja, Supplementary cementitious materials based on recycled concrete paste, J. Clean. Prod. 387 (2023) 135743, https://doi.org/10.1016/j.jclepro.2022.135743
[95] S.K. Kaliyavaradhan, L. Li, T.-C. Ling, Response surface methodology for the optimization of CO_2 uptake using waste concrete powder, Construction and Building Materials 340 (2022) 127758, https://doi.org/10.1016/j.conbuildmat.2022.127758
[96] J. Skocek, M. Zajac, M. Ben Haha, Carbon Capture and Utilization by mineralization of cement pastes derived from recycled concrete, Scientific Reports (2020) 10:5614, https://doi.org/10.1038/s41598-020-62503-z
[97] P. Shen, Y. Zhang, Y. Jiang, B. Zhan, J. Lu, S. Zhang, D. Xuan, C.S. Poon, Phase assemblance evolution during wet carbonation of recycled concrete fines, Cem. Concr. Res. 154 (2022), 106733, https://doi.org/10.1016/j. cemconres.2022.106733
[98] B. Lu, C. Shi, J. Zhang, J. Wang, Effects of carbonated hardened cement paste powder on hydration and microstructure of Portland cement, Construct. Build. Mater. 186 (2018) 699–708, https://doi.org/10.1016/j.conbuildmat.2018.07.159
[99] H. Mehdizadeh, T.C. Ling, X. Cheng, K.H. Mo, Effect of particle size and CO_2 treatment of waste cement powder on properties of cement paste, Can. J. Civ.

Eng. 48 (2021) 522–531, https://doi.org/10.1139/cjce-2019-0574
[100] L. Qin, X. Gao, Recycling of waste autoclaved aerated concrete powder in Portland cement by accelerated carbonation, Waste Management 89 (2019) 254–264, https://doi.org/10.1016/j.wasman.2019.04.018
[101] H. Wu, C. Liang, J. Xiao, Z. Ma, Properties and CO_2-curing enhancement of cement-based materials containing various sources of waste hardened cement paste powder, J. Build. Eng. 44 (2021), 102677, https://doi.org/10.1016/j.jobe.2021.102677.
[102] H. Mehdizadeh, X. Cheng, K.H. Mo, T.C. Ling, Upcycling of waste hydrated cement paste containing high-volume supplementary cementitious materials via CO_2 pre-treatment, J. Build. Eng. 52 (2022), 104396, https://doi.org/10.1016/j.jobe.2022.104396
[103] A. Carriço, J.A. Bogas, S. Hu, S. Real, M.F.C. Pereira, Novel separation process for obtaining recycled cement and high-quality recycled sand from waste hardened concrete, Journal of Cleaner Production 309 (2021) 127375, https://doi.org/10.1016/j.jclepro.2021.127375
[104] A. Akbarnezhad, K.C.G. Ong, M.H. Zhang, C.T. Tam, T.W.J. Foo, Microwave-assisted beneficiation of recycled concrete aggregates, Construction and Building Materials 25 (2011) 3469–3479, https://doi.org/10.1016/j.conbuildmat.2011.03.038
[105] W. de Vries, ADR The use of Advanced Dry Recovery in recycling fine moist granular materials, TU Delft, 2017, 10.4233/uuid:c3c8578d-fd2c-493f-b4c5-79e63bc6d70c
[106] S. Lotfi, J. Deja, P. Rem, R. Mróz, E. van Roekel, H. van der Stelt, Mechanical recycling of EOL concrete into high-grade aggregates, Resources, Conservation and Recycling 87 (2014) 117–125, http://dx.doi.org/10.1016/j.resconrec.2014.03.010
[107] S. Lotfi, P. Rem, Recycling of End of Life Concrete Fines into Hardened Cement and Clean Sand, Journal of Environmental Protection (2016), 7, 934-950, http://dx.doi.org/10.4236/jep.2016.76083
[108] J. Moreno-Juez , I.J. Vegas, A.T. Gebremariam, V. García-Cortés, F. Di Maio, Treatment of end-of-life concrete in an innovative heating-air classification system for circular cement-based products, Journal of Cleaner Production 263 (2020) 121515, https://doi.org/10.1016/j.jclepro.2020.121515
[109] M.V.A. Florea, H.J.H. Brouwers, Properties of various size fractions of crushed concrete related to process conditions and re-use, Cement and Concrete Research 52 (2013) 11–21, http://dx.doi.org/10.1016/j.cemconres.2013.05.005
[110] http://www.c2ca.eu/activities/the-recyclingprocess/
[111] X. Fang, D. Xuan, C.S. Poon, Empirical modelling of CO_2 uptake by recycled concrete aggregates under accelerated carbonation conditions, Materials and Structures (2017) 50:200, https://doi.org/10.1617/s11527-017-1066-y
[112] H.-J. Ho, A. Iizuka, E. Shibata, H. Tomita, K. Takano, T. Endo, Utilization of CO_2 in direct aqueous carbonation of concrete fines generated from aggregate recycling: Influences of the solid–liquid ratio and CO2 concentration, J. Clean Prod. 312 (2021), 127832, https://doi.org/10.1016/j.jclepro.2021.127832
[113] A.B. Ghacham, L.-C. Pasquier, E. Cecchi, J.-F. Blais, G. Mercier, Valorization of waste concrete through CO_2 mineral carbonation: Optimizing parameters and improving reactivity using concrete separation, Journal of Cleaner Production 166 (2017) 869-878, http://dx.doi.org/10.1016/j.jclepro.2017.08.015
[114] L.-C. Pasquier, N. Kemache, J. Mocellin, J.-F. Blais, G. Mercier, Waste Concrete Valorization; Aggregates and Mineral Carbonation Feedstock Production, Geosciences 2018, 8, 342, https://doi.org/10.3390/geosciences8090342
[115] Y. Zhang, H. Chen, Q. Wang, Accelerated carbonation of regenerated cementitious materials from waste concrete for CO_2 sequestration, Journal of Building Engineering 55 (2022) 104701, https://doi.org/10.1016/j.jobe.2022.104701
[116] A. Dindi, D.V. Quang, L.F. Vega, E. Nashef, M.R.M. Abu-Zahra, Applications of fly ash for CO_2 capture, utilization, and storage, Journal of CO_2 Utilization 29 (2019) 82–102, https://doi.org/10.1016/j.jcou.2018.11.011
[117] Mineral Commodity Summaries 2022 By: U.S. Geological Survey, https://doi.org/10.3133/mcs2022
[118] S.-Y. Pan, R. Adhikari, Y.-H. Chen, P. Li, P.-C. Chiang, Integrated and innovative steel slag utilization for iron reclamation, green material production and CO_2 fixation via accelerated carbonation, J. Clean. Prod. 137 (2016) 617–631, https://doi.org/10.1016/j.jclepro.2016.07.112
[119] Z. Chen, Z. Cang, F. Yang, J. Zhang, L. Zhang, Carbonation of steelmaking slag presents an opportunity for carbon neutral: A review, Journal of CO2 Utilization 54 (2021) 101738, https://doi.org/10.1016/j.jcou.2021.101738
[120] S. Wang, J. Kim, T. Qin, Mineral carbonation of iron and steel by-products: State-of-the-art techniques and economic, environmental, and health implications, Journal of CO2 Utilization 81 (2024) 102707, https://doi.org/10.1016/j.jcou.2024.102707
[121] G. Montes-Hernandez, R. Pérez-López, F. Renard, J.M. Nieto, L. Charlet, Mineral sequestration of CO_2 by aqueous carbonation of coal combustion fly-ash, J. Hazard. Mater. 161 (2009) 1347–1354, https://doi.org/10.1016/j. jhazmat.2008.04.104
[122] H.Y. Jo, J.H. Kim, Y.J. Lee, M. Lee, S.J. Choh, Evaluation of factors affecting mineral carbonation of CO_2 using coal fly ash in aqueous solutions under ambient conditions, Chem. Eng. J. 183 (2012) 77–87, https://doi.org/10.1016/j. cej.2011.12.023
[123] A. Ebrahimi, M. Saffari, D. Milani, A. Montoya, M. Valix, A. Abbas, Sustainable transformation of fly ash industrial waste into a construction cement blend via CO_2 carbonation, J. Clean. Prod. 156 (2017) 660–669, https://doi.org/10.1016/j. jclepro.2017.04.037
[124] A. González, N. Moreno, R. Navia, CO_2 carbonation under aqueous conditions using petroleum coke combustion fly ash, Chemosphere 117 (2014) 139–143, https://doi.org/10.1016/j.chemosphere.2014.06.034
[125] Y. Sun, V. Parikh, L. Zhang, Sequestration of carbon dioxide by indirect mineralization using Victorian brown coal fly ash, J. Hazard. Mater. 209–210 (2012) 458–466, https://doi.org/10.1016/j.jhazmat.2012.01.053
[126] A. Mazzella, M. Errico, D. Spiga, CO_2 uptake capacity of coal fly ash: influence of pressure and temperature on direct gas-solid carbonation, J. Environ. Chem. Eng. 4 (2016) 4120–4128, https://doi.org/10.1016/j.jece.2016.09.020

[127] A. Ćwik, I. Casanova, K. Rausis, K. Zarebska, Utilization of high-calcium fly ashes through mineral carbonation: the cases for Greece, Poland and Spain, J. CO_2 Util. 32 (2019) 155–162, https://doi.org/10.1016/j.jcou.2019.03.020

[128] E. Ren, S. Tang, C. Liu, H. Yue, C. Li, B. Liang, Carbon dioxide mineralization for the disposition of blast-furnace slag: reaction intensification using NaCl solutions, Greenh. Gases: Sci. Technol. 10 (2020) 436–448. 10.1002/ghg.1837

[129] S. Lee, J.-W. Kim, S. Chae, J.-H. Bang, S.-W. Lee, CO_2 sequestration technology through mineral carbonation: an extraction and carbonation of blast slag, J. CO_2 Util. 16 (2016) 336–345, https://doi.org/10.1016/j.jcou.2016.09.003

[130] M. Mun, H. Cho, Mineral carbonation for carbon sequestration with industrial waste, Energy Procedia 37 (2013) 6999–7005, https://doi.org/10.1016/j.egypro.2013.06.633

[131] E.E. Chang, C.-H. Chen, Y.-H. Chen, S.-Y. Pan, P.-C. Chiang, Performance evaluation for carbonation of steel-making slags in a slurry reactor, J. Hazard. Mater. 186 (1) (2011) 558–564, https://doi.org/10.1016/j.jhazmat.2010.11.038

[132] E.E. Chang, A.-C. Chiu, S.-Y. Pan, Y.-H. Chen, C.-S. Tan, P.-C. Chiang, Carbonation of basic oxygen furnace slag with metalworking wastewater in a slurry reactor, Int. J. Greenh. Gas Control. 12 (2013) 382–389, https://doi.org/10.1016/j. ijggc.2012.11.026.

[133] E.E. Chang, T.-L. Chen, S.-Y. Pan, Y.-H. Chen, P.-C. Chiang, Kinetic modeling on CO_2 capture using basic oxygen furnace slag coupled with cold-rolling wastewater in a rotating packed bed, J. Hazard. Mater. 260 (2013) 937–946, https://doi.org/10.1016/j.jhazmat.2013.06.052

[134] A. Polettini, R. Pomi, A. Stramazzo, Carbon sequestration through accelerated carbonation of BOF slag: influence of particle size characteristics, Chem. Eng. J. 298 (2016) 26–35, https://doi.org/10.1016/j.cej.2016.04.015

[135] R. Baciocchi, G. Costa, M. Di Gianfilippo, A. Polettini, R. Pomi, A. Stramazzo, Thin-film versus slurry-phase carbonation of steel slag: CO_2 uptake and effects on mineralogy, J. Hazard. Mater. 283 (2015) 302–313, https://doi.org/10.1016/j. jhazmat.2014.09.016

[136] A.B. Ghacham, L.-C. Pasquier, E. Cecchi, J.-F. Blais, G. Mercier, CO_2 sequestration by mineral carbonation of steel slags under ambient temperature: parameters influence, and optimization, Environ. Sci. Pollut. Res. - Int. 23 (17) (2016) 17635–17646, https://doi.org/10.1007/s11356-016-6926-4

[137] T.D. Rushendra Revathy, K. Palanivelu, A. Ramachandran, Direct mineral carbonation of steelmaking slag for CO_2 sequestration at room temperature, Environ. Sci. Pollut. Res. - Int. 23 (8) (2016) 7349–7359, https://doi.org/ 10.1007/s11356-015-5893-5

[138] D. Xuan, B. Zhan, C.S. Poon, W. Zheng, Carbon dioxide sequestration of concrete slurry waste and its valorisation in construction products, Constr. Build. Mater. 113 (2016) 664–672, https://doi.org/10.1016/j.conbuildmat.2016.03.109

[139] P. Tang, D. Xuan, H.W. Cheng, C.S. Poon, D.C.W. Tsang, Use of CO_2 curing to enhance the properties of cold bonded lightweight aggregates (CBLAs) produced with concrete slurry waste (CSW) and fine incineration bottom ash (IBA), J. Hazard. Mater. 381 (2020), 120951, https://doi.org/10.1016/j.jhazmat.2019.120951

[140] S.K. Kaliyavaradhan, T.C. Ling, K.H. Mo, CO_2 sequestration of fresh concrete slurry waste: optimization of CO2 uptake and feasible use as a potential cement binder, J. CO_2 Util. 42 (2020), 101330, https://doi.org/10.1016/j. jcou.2020.101330

[141] D. Medas, G. Cappai, G. De Giudici, M. Piredda, S. Podda, Accelerated carbonation by cement kiln dust in aqueous slurries: chemical and mineralogical investigation, Greenh. Gases Sci. Technol. 7 (2017) 692–705, https://doi.org/10.1002/ghg.1681

[142] D.N. Huntzinger, J.S. Gierke, S.K. Kawatra, T.C. Eisele, L.L. Sutter, Carbon dioxide sequestration in cement kiln dust through mineral carbonation, Environ. Sci. Technol. 43 (2009) 1986–1992, https://doi.org/10.1021/es802910z.

[143] D. Sharma, S. Goyal, Accelerated carbonation curing of cement mortars containing cement kiln dust: an effective way of CO_2 sequestration and carbon footprint reduction, J. Clean. Prod. 192 (2018) 844–854, https://doi.org/10.1016/j.jclepro.2018.05.027

[144] D.N. Huntzinger, J.S. Gierke, L.L. Sutter, S.K. Kawatra, T.C. Eisele, Mineral carbonation for carbon sequestration in cement kiln dust from waste piles, J. Hazard. Mater. 168 (2009) 31–37, https://doi.org/10.1016/j. jhazmat.2009.01.122

[145] R.M. Santos, J. Van Bouwel, E. Vandevelde, G. Mertens, J. Elsen, T. Van Gerven, Accelerated mineral carbonation of stainless steel slags for CO_2 storage and waste valorization: effect of process parameters on geochemical properties, Int. J. Greenh. Gas Control 17 (2013) 32–45, https://doi.org/10.1016/j. ijggc.2013.04.004

[146] Q. Song, M.Z. Guo, L. Wang, T.C. Ling, Use of steel slag as sustainable construction materials: a review of accelerated carbonation treatment, Resour. Conserv. Recycl. 173 (2021), 105740, https://doi.org/10.1016/j.

[147] M.S. Ko, Y.L. Chen, J.H. Jiang, Accelerated carbonation of basic oxygen furnace slag and the effects on its mechanical properties, Constr. Build. Mater. 98 (2015) 286–293, https://doi.org/10.1016/j.conbuildmat.2015.08.051

[148] B. Pang, Z. Zhou, H. Xu, Utilization of carbonated and granulated steel slag aggregate in concrete, Constr. Build. Mater. 84 (2015) 454–467, https://doi.org/10.1016/j.conbuildmat.2015.03.008

[149] B. Pang, Z. Zhou, X. Cheng, P. Du, H. Xu, ITZ properties of concrete with carbonated steel slag aggregate in salty freeze-thaw environment, Constr. Build. Mater. 114 (2016) 162–171, https://doi.org/10.1016/j. conbuildmat.2016.03.168

[150] M. Bodor, R.M. Santos, G. Cristea, M. Salman, Ő. Cizer, R.I. Iacobescu, Y. W. Chiang, K. Van Balen, M. Vlad, T. Van Gerven, Laboratory investigation of carbonated BOF slag used as partial replacement of natural aggregate in cement mortars, Cem. Concr. Compos. 65 (2016) 55–66, https://doi.org/10.1016/j.cemconcomp.2015.10.002

[151] Y. Jiang, T. Ling, Production of artificial aggregates from steel-making slag: influences of accelerated carbonation during granulation and/or post-curing. J. CO_2 Util. 36, (2020) 135–144, https://doi.org/10.1016/j.jcou.2019.11.009

[152] L. Mo, S. Yang, B. Huang, L. Xu, S. Feng, M. Deng, Preparation, microstructure and property of carbonated artificial steel slag aggregate used in concrete, Cement and Concrete Composites 113 (2020) 103715, https://doi.org/10.1016/j.cemconcomp.2020.103715

[153] W. Shen, Y. Liu, M. Wu, D. Zhang, X. Du, D. Zhao, G. Xu, B. Zhang, X. Xiong, Ecological carbonated steel slag pervious concrete prepared as a key material of sponge city, Journal of Cleaner Production 256 (2020) 120244, https://doi.org/10.1016/j.jclepro.2020.120244

[154] L. Li, Y. Jiang, S.-Y. Pan, T.-C. Ling, Comparative life cycle assessment to maximize CO_2 sequestration of steel slag products, Construction and Building Materials 298 (2021) 123876, https://doi.org/10.1016/j.conbuildmat.2021.123876

[155] S.L. Pei, S.Y. Pan, X. Gao, Y.K. Fang, P.C. Chiang, Efficacy of carbonated petroleum coke fly ash as supplementary cementitious materials in cement mortars, J. Clean. Prod. 180 (2018) 689–697, https://doi.org/10.1016/j. jclepro.2018.01.055

[156] S. Sahoo, B.B. Das, S. Mustakim, Acid, alkali, and chloride resistance of concrete composed of low-carbonated fly ash, J. Mater. Civ. Eng. 29 (2017), 04016242, https://doi.org/10.1061/(asce)mt.1943-5533.0001759

[157] Z. Chen, R. Li, J. Liu, Preparation and properties of carbonated steel slag used in cement cementitious materials, Constr. Build. Mater. 283 (2021), 122667, https://doi.org/10.1016/j.conbuildmat.2021.122667.

[158] S.Y. Pan, T.C. Chung, C.C. Ho, C.J. Hou, Y.H. Chen, P.C. Chiang, CO_2 mineralization and utilization using steel slag for establishing a waste-to-resource supply chain, Sci. Rep. 7 (2017) 1–11, https://doi.org/10.1038/s41598-017- 17648-9

[159] X. Wang, W. Ni, J. Li, S. Zhang, M. Hitch, R. Pascual, Carbonation of steel slag and gypsum for building materials and associated reaction mechanisms, Cem. Concr. Res. 125 (2019), 105893, https://doi.org/10.1016/j.cemconres.2019.105893

[160] Kunal, R. Siddique, A. Rajor, Use of cement kiln dust in cement concrete and its leachate characteristics, Resour. Conserv. Recycl. 61 (2012) 59–68, https://doi.org/10.1016/j.resconrec.2012.01.006

Building Materials and Structures

GUIDE FOR AUTHORS

In the journal *Building Materials and Structures*, the submission and review processes take place electronically. Manuscripts are submitted electronically (online) on the website **https: //** www.dimk.rs. The author should register first, then log in and finally submit the manuscript which should be in the form of editable files (e.g. Word) to enable the typesetting process in journal format. All correspondence, including Editor´s decision regarding required reviews and acceptance of manuscripts, take place via e-mail.

TYPES OF ARTICLES

The following types of articles are published in *Building Materials and Structures:*

Original scientific article. It is the primary source of scientific information, new ideas and insights as a result of original research using appropriate scientific methods. The results are presented briefly, but in a way to enable readers to assess the results of experimental or theoretical/numerical analyses, so that the research can be repeated and yield with the same or results within the limits of tolerable deviations.

Review article. It presents the state of science in particular area as a result of methodically systematized, analyzed and discussed reference data. Only critical review manuscripts will be considered as providing novel perspective and critical evaluation of the topics of interest to broader BMS readership.

Preliminary report. Contains the first short notifications of research results without detailed analysis, i.e. it is shorter than original research paper.

Technical article. Reports on the application of recognized scientific achievements of relevance to the field of building materials and structures. Contain critical analysis and recommendations for adaption of the research results to practical needs.

Projects Notes. Project Notes provide a presentation of a relevant project that has been built or is in the process of construction. The original or novel aspects in design or construction should be clearly indicated.

Discussions. Comment on or discussion of a manuscript previously published in *Building Materials and Structures*. It should be received by the Editor-in-Chief within six months of the online publication of the manuscript under discussion. Discussion Papers will be subject to peer review and should also be submitted online. If Discussion Paper is selected for publication the author of the original paper will be invited to respond, and Discussion Paper will be published alongside any response that the author.

Other contributions

Conference Reports. Reports on major international and national conferences of particular interest to *Building Materials and Structures*. Selected and/or awarded papers from the ASES Conferences are published in Special issues.

Book Reviews. Reviews on new books relevant to the scope of *Building Materials and Structures*.

PREPRINTS

These are the author's own write-up of research results and analysis that has not been peer reviewed, nor had any other value added to it by a publisher (such as formatting, copy-editing, technical enhancements and the like). Authors can share their preprint anywhere at any time. If accepted for publication, we encourage authors to link from the preprint to their formal publication via its Digital Object Identifier (DOI). Preprints should not be added to or enhanced in any way in order to appear more like, or to substitute for, the final versions of articles.

MANUSCRIPT STRUCTURE

The manuscript should be typed one-sided on A4 sheets. Page numbers should be included in the manuscript and the text should be single spaced with **consecutive line numbering** - these are essential peer review requirements. The figures and tables included in the single file should be placed next to the relevant text in the manuscript. The corresponding captions should be placed directly below the figure or table. If the manuscript contains Supplementary material, it should also be submitted at the first submission of the manuscript for review purposes.

There are no strict rules regarding the structure of the manuscript, but the basic elements that it should contain are: Title page with the title of the manuscript, information about the authors, abstract and keywords, Introduction, Materials / Methods, Results and Conclusions.

The front page

The front page contains the title of the manuscript which should be informative and concise; abbreviations and formulas should be avoided.

Information about the authors are below the title; after the author's name, a superscript number is placed indicating his/her affiliation, which is printed below the author's name, and before the abstract. It is obligatory to mark the corresponding author with superscript *) and provide his/her e-mail address. The affiliation should contain the full name of the institution where the author performed the research and its address.

Abstract

Abstract should contain 150-200 words. Motivation and objective of the conducted research should be presented; main results and conclusions should be briefly stated as well. References and abbreviations should be avoided.

Keywords

Keywords (up to 10) should be listed immediately after the abstract; abbreviations should be used only if they are generally accepted and well-known in the field of research.

Division into chapters

The manuscript should be divided into chapters and sub-chapters, which are hierarchically numbered with Arabic numbers. The headings of chapters and sub-chapters should appear on their own separate lines.

At the end of the manuscript, and before the references, it is obligatory to list the following statements:

CRediT authorship contribution statement

For transparency, we require corresponding authors to provide co-author contributions to the manuscript using the relevant CRediT roles. The CRediT taxonomy includes 14 different roles describing each contributor’s specific contribution to the research output. The roles are: Conceptualization; Data curation; Formal analysis; Funding acquisition; Investigation; Methodology; Project administration; Resources; Software; Supervision; Validation; Visualization; Roles/Writing - original draft; and Writing - review & editing. Note that not all roles may apply to every manuscript, and authors may have contributed through multiple roles.

Declaration of competing interest

Corresponding authors, on behalf of all the authors of a submission, must disclose any financial and personal relationships with other people or organizations that could inappropriately influence their work. Examples of potential conflicts of interest include employment, consultancies, stock ownership, honoraria, paid expert testimony, patent applications/registrations, and grants or other funding. All authors, including those *without* competing interests to declare, should provide the relevant information to the corresponding author (which, where relevant, may specify they have nothing to declare).

Declaration of generative AI in scientific writing

This guidance only refers to the writing process, and not to the use of AI tools to analyze and draw insights from data as part of the research process. Where authors use generative artificial intelligence (AI) and AI- assisted technologies in the writing process, authors should only use these technologies to improve readability and language. Applying the technology should be done with human oversight and control, and authors should carefully review and edit the result, as AI can generate authoritative-sounding output that can be incorrect, incomplete or biased. AI and AI-assisted technologies should not be listed as an author or co-author, or be cited as an author. Authorship implies responsibilities and tasks that can only be attributed to and performed by humans. Authors should disclose in their manuscript the use of AI and AI- assisted technologies in the writing process by following the instructions below. A statement will appear in the published work. Please note that authors are ultimately responsible and accountable for the contents of the work.

Disclosure instructions

Authors must disclose the use of generative AI and AI-assisted technologies in the writing process by adding a statement at the end of their manuscript in the core manuscript file, before the References list. The statement should be placed in a new section entitled ‘Declaration of Generative AI and AI-assisted technologies in the writing process’.

Statement: During the preparation of this work the author(s) used [NAME TOOL / SERVICE] in order to [REASON]. After using this tool/service, the author(s) reviewed and edited the content as needed and take(s) full responsibility for the content of the publication.
This declaration does not apply to the use of basic tools for checking grammar, spelling, references etc. If there is nothing to disclose, there is no need to add a statement.

Acknowledgments

State the institutions and persons who financially or in some other way helped the presented research. If the research was not supported by others, it should also be stated in this part of the manuscript.

Appendices

The manuscript may have appendices. If there is more than one appendix, they are denoted by A, B, etc. Labels of figures, tables and formulas in appendices should contain the label of the appendix, for example Table A.1, Figure A.1, etc.

ABBREVIATIONS

All abbreviations should be defined where they first appear. Consistency of abbreviations used throughout the text should be ensured.

MATH FORMULAE

Formulae should be in the form of editable text (not in the format of figures) and marked with numbers, in the order in which they appear in the text. The formulae and equations should be written carefully takinginto account the indices and exponents. Symbols in formulae should be defined in the order they appear, right below the formulae.

FIGURES

- figures should be made so that they are as uniform in size as possible and of appropriate quality for reproduction;
- the dimensions of the figures should correspond to the format of the journal: figures with a width approximately equal to the width of 1 column (± 80 mm width), width of 2 columns (± 170 mm width) or width of 1.5 columns (± 130 mm width);
- figures should be designed so that their size is not disproportionately large in relation to the content;
- the text on the figures should be minimal and the font used should be the same on all figures (Arial, Times New Roman, Symbol);
- figures should be placed next to the appropriate text in the manuscript and marked with numbers in the order in which they appear in the text;
- each figure should have a caption that is placed below the figure - the caption should not be on the figure itself.

In cases of inadequate quality of reproduction, the author should be required to submit figures as separate files. In this case, the figure should be saved in TIFF (or JPG) format with a minimum resolution of 500 dpi.

TABLES

- tables should be in the form of editable text (not in the format of figures);
- tables should be placed next to the appropriate text in the manuscript and marked with numbers in the order in which they appear in the text;
- each table should have a caption that is placed below the table;
- the tables should not show the results that are already presented elsewhere in the manuscript - duplicating the presentation of results should be avoided;
- tables are without vertical lines as boundaries between cells and shading cells.

REFERENCES

Citation in the text

Each reference cited in the text should be in the reference list (and vice versa). It is not recommended to list unpublished results or personal communications in the reference list, but they can be listed in the text. If they are still listed in the reference list, the journal style references are used, with 'Unpublished results' or 'Personal communication' instead of the date of publication. Citing a reference as ‘in press’ means that it is accepted for publication.

Web references

Web references are minimally listed with the full URL and the date when the site was last accessed. These references can be included in the reference list, but can also be given in a separate list after the reference list.

Reference style

In text: References are given in the text by a number in square brackets in the order in which they appear in the text. Authors may also be referred to directly, but the reference number should always be given.

In reference list: References marked with a number in square brackets are sorted by numbers in the list.

Examples

Reference to a journal publication:

[1] V.W.Y. Tam, M. Soomro, A.C.J. Evangelista, A review of recycled aggregate in concrete applications (2000-2017), Constr. Build. Mater. 172 (2018) 272-292. https://doi.org/10.1016/j.conbuildmat.2018.03.240.

Reference to a book:

[3] A.H. Nilson, D. Darwin, C.W. Dolan, Design of Concrete Structures, thirteenth ed., Mc Graw Hill, New York, 2004.

Reference to a chapter in an edited book:

[4] J.R. Jimenez, Recycled aggregates (RAs) for roads, in: F Pacheco-Torgal, V.W.Y. Tam, J.A. Labrincha, Y. Ding, J. de Brito (Eds.), Handbook of recycled concrete and demolition waste, Woodhead Publishing Limited, Cambridge, UK, 2013, pp. 351–377.

Reference to a website:

[5] WBCSD, The Cement Sustainability Initiative, World. Bus. Counc. Sustain. Dev. http://www.wbcsdcement.org.pdf/CSIRecyclingConcrete-FullReport.pdf, 2017 (accessed 7 July 2016).

SUPPLEMENTARY MATERIAL

Supplementary material such as databases, detailed calculations and the like can be published separately to reduce the workload. This material is published ‘as received’ (Excel or PowerPoint files will appear as such online) and submitted together with the manuscript. Each supplementary file should be given a short descriptive title.

ETHICS IN PUBLISHING

Authors are expected to respect intellectual and scientific integrity in presentation of their work. The journal publishes manuscripts that have not been previously published and are not in the process of being considered for publication elsewhere. All co-authors as well as the institution in which the research was performed should agree to the publication in the journal.
Authors are expected to submit completely original research; if the research of other researchers is used, it should be adequately cited. Authors who wish to include in their manuscript images, tables or parts of text that have already been published somewhere, should obtain permission from the Copyright owner and provide a proof in the process of submitting the manuscript. All material for which there is no such evidence will be considered the original work of the author. To determine the originality of the manuscript, it can be checked using the Crossref Similarity Check service. For more information, please see our Ethics and Malpractice Statement.

The Journal and Publishers imply that all authors, as well as responsible persons of the institute where the research was performed, agreed with the content of the submitted manuscript before submitting it. The Publishers will not be held legally responsible should there be any claims for compensation.

PEER REVIEW

This journal uses a single blind review process, which means that the authors do not know the names of the reviewers, but the reviewers know who the authors are. In the review process, the Editor-in-Chief first assesses whether the contents of the manuscript comply with the scope of the journal. If this is the case, the paper is sent to at least two independent experts in the field, with the aim of assessing its scientific quality and making recommendation regarding publication. If the manuscript needs to be revised, the authors are provided with the reviewers' remarks. The authors are obliged to correct the manuscript in accordance with the remarks, submit the revised manuscript and a special file with the answers to the reviewers within the given deadline. The final decision, whether the paper will be published in journal or not, is made by the Editor-in-Chief.

AFTER ACCEPTANCE

Once accepted for publication, the manuscript is set in the journal format. Complex manuscript is sent to the authors in the form of proof, for proof reading. Then, authors should check for typesetting errors, and whether the text, images, and tables are complete and accurate. Authors are asked to do this carefully, as subsequent corrections will not be considered. In addition, significant changes to the text and authorship at this stage are not allowed without the consent of the Editor-in-Chief. After online publication, changes are only possible in the form of Erratum which will be hyperlinked to manuscript.

COPYRIGHT

Authors retain copyright of the published papers and grant to the publisher the non-exclusive right to publish the article, to be cited as its original publisher in case of reuse, and to distribute it in all forms and media.

The published articles will be distributed under the Creative Commons Attribution ShareAlike 4.0 International license (CC BY-SA). It is allowed to copy and redistribute the material in any medium or format, and remix, transform, and build upon it for any purpose, even commercially, as long as appropriate credit is given to the original author(s), a link to the license is provided, it is indicated if changes were made and the new work is distributed under the same license as the original.

Users are required to provide full bibliographic description of the original publication (authors, article title, journal title, volume, issue, pages), as well as its DOI code. In electronic publishing, users are also required to link the content with both the original article published in *Building Materials and Structures* and the license used.

Authors are able to enter into separate, additional contractual arrangements for the non-exclusive distribution of the journal's published version of the work (e.g., post it to an institutional repository or publish it in a book), with an acknowledgement of its initial publication in this journal.

OPEN ACCESS POLICY

Journal *Building Materials and Structures* is published under an Open Access license. All its content is available free of charge. Users can read, download, copy, distribute, print, search the full text of articles, as well as to establish HTML links to them, without having to seek the consent of the author or publisher.
The right to use content without consent does not release the users from the obligation to give the credit to the journal and its content in a manner described under *Copyright*.

Archiving digital version

In accordance with law, digital copies of all published volumes are archived in the legal deposit library of the National Library of Serbia in the Repository of SCIndeks - The Serbian Citation Index as the primary full text database.

Cost collection to authors

Journal Building Materials and Structures does not charge authors or any third party for publication. Both manuscript submission and processing services, and article publishing services are free of charge. There are no hidden costs whatsoever.

DISCLAIMER

The views expressed in the published works do not express the views of the Editors and the Editorial Staff. The authors take legal and moral responsibility for the ideas expressed in the articles. Publisher shall have no liability in the event of issuance of any claims for damages. The Publisher will not be held legally responsible should there be any claims for compensation.

Financial support

MINISTRY OF EDUCATION, SCIENCE AND TECHNOLOGICAL DEVELOPMENT OF REPUBLIC OF SERBIA

INSTITUTE FOR TESTING OF MATERIALS-IMS INSTITUTE, BELGRADE

SERBIAN CHAMBER OF ENGINEERS

INŽENJERSKA KOMORA SRBIJE

PROVIDING
ATTPAC
COMPLETE SCAFFOLDING SOLUTIONS

ИМС IMS INSTITUT IMS AD BEOGRAD

CENTAR ZA PUTEVE I GEOTEHNIKU

U okviru centra posluju odeljenja za geotehniku, nadzor i terenska ispitivanja, projektovanje saobraćajnica, laboratorija za puteve i geotehniku. Značajna aktivnost centra usmerena je ka terenskim i laboratorijskim geološko - geotehničkim istraživanjima i ispitivanjima terena za potrebe izrade projekno - tehničke dokumentacije, za različite faze i nivoe projektovanja objekata visokogradnje, niskogradnje, saobraćaja i hidrogradnje, kao i za potrebe prostornog planiranja i zaštite životne sredine. Stručni nadzor, kontrola kvaliteta tokom građenja, rekonstrukcije i sanacije objekata različite namene, izrada studija, ekspertiza, konsultantske usluge, kompletan konsalting u oblasti geotehničkog inženjeringa, neke su od delatnosti centra.

<u>Ispitivanje šipova</u>

- **SLT metoda (Static load test)**
- **DLT metoda (Dynamic load test)**
- **PDA metoda (Pile driving analysis)**
- **PIT (SIT) metoda (Pile (Sonic) integrity testing)**
- **CSL - Crosshole Sonic Logging**

ИМС IMS INSTITUT IMS AD BEOGRAD

- **<u>Ispitivanje šipova</u>**
    - **<u>Geotehnička istraživanja i ispitivanja – in situ</u>**
        - **<u>Laboratorija za puteve i geotehniku</u>**
            - **<u>Projektovanje puteva i sanacija klizišta</u>**
                - **<u>Nadzor</u>**

Институт ИМС а.д – Булевар војводе Мишића 43, Београд
Центар за путеве и геотехнику – одељење за геотехнику
www.institutims.rs

PUT INŽENJERING

Put inženjering d.o.o punih 25 godina radi kao specijalizovano preduzeće za izgradnju infrastrukture u niskogradnji i visokogradnji, kao i proizvodnjom kamenog agregata i betona. Preduzeće se bavi i transportom, uslugama građevinske mehanizacije i specijalne opreme.

Za spravljanje betona koristimo drobljeni krečnjački agregat sa našeg kamenoloma, deklarisanih frakcija, kontrolisane vlažnosti. Kompletan proces proizvodnje i kontrole kvaliteta vršimo prema važećim standardima.

Kao generalni izvođač radova, vršimo koordinaciju svih učesnika na projektu, planiranje, praćenje i nabavku materijala, kontrolu kvaliteta izvedenih radova, poštujući zadate vremenske rokove i finansijski okvir investitora.

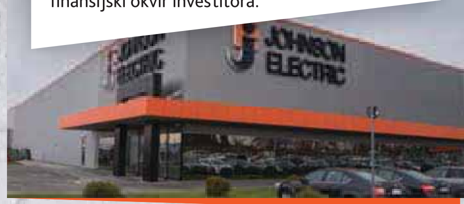

Obradu armature vršimo brzo, stručno i kvalitetno, sa kompjuterskom preciznošću i dimenzijama po projektu.

Osnovi princip našeg poslovanja zasniva se na individualnom pristupu svakom klijentu i pronalaženje najoptimalnijeg rešenja za njegove transportne i logističke potrebe.

Koristeći inovativne tehnike i kvalitetan građevinski materijal iz sopstvenih resursa, spremni smo da odgovorimo na mnoge zahteve naših klijenata iz oblasti niskogradnje.

Naša kompanija u oblasti visokogradnje primenjuje sistem prefabrikovnih betonskih elemenata koji u odnosu na klasičnu gradnju ima brojne prednosti.

Usluge građevinskom mehanizacijom vršimo tehnički ispravnim mašinama, sa potrebnim sertifikatima kako za rukovaoce građevinskim mašinama tako i za same mašine.

Osnovna prednost prefabrikovane konstrukcije jeste brzina kojom konstrukcija može biti projektovana, proizvedena, transportovana i namontirana.

Prednapregnute šuplje ploče su konstruktivni elementi visokog kvaliteta, proizvedeni u fabrički kontrolisanim uslovima.

Raspolažemo opremom i mašinama za sve zemljane radove, kipere i dampere za rad u teškim terenskim uslovima, automiksere i pumpe za beton, autodizalice, podizne platforme.

Izvodimo hidrograđevinske radove u izgradnji kanalizacionih mreža za odvođenje atmosferskih, otpadnih i upotrebljenih voda, izvođenjem hidrograđevinskih radova u okviru regulacije rečnih tokova, kao i izvođenjem hidrotehničkih objekata.

Izrađujemo betonske "New Jersey profile" koji se u svetu koriste za preusmeravanje saobraćaja i zaštitu pešaka u toku izgradnje puta, kao i Betonblock sistem betonskih blokova.

Sakupljanje i privremeno skladištenje otpada vršimo našim specijalizovanim vozilima i deponujemo na našu lokaciju sa odgovarajućom dozvolom. Kapacitet mašine je 250 t/h građevinskog neopasnog otpada.

Površinski kop udaljen je 35 km od Niša. Savremene drobilice, postrojenje za separaciju i sejalica efikasno usitnjavaju i razdvajaju kamene agregate po veličinama. Tehnički kapacitet trenutne primarne drobilice je 300 t/h.

Uslugu transporta vršimo automikserima, kapaciteta bubnja od 7 m^3 do 10 m^3 betonske mase. Za ugradnju betona posedujemo auto-pumpu za beton, radnog učinka 150 m^3/h, sa dužinom strele od 36 m.

NIŠ
Knjaževačka bb, 18000 Niš - Srbija
+381 18 215 355
office@putinzenjering.com

BEOGRAD
Jugoslovenska 2a, 11250 Beograd – Železnik
+381 11 25 81 111
beograd@putinzenjering.com

MOBECO

www.putinzenjering.com

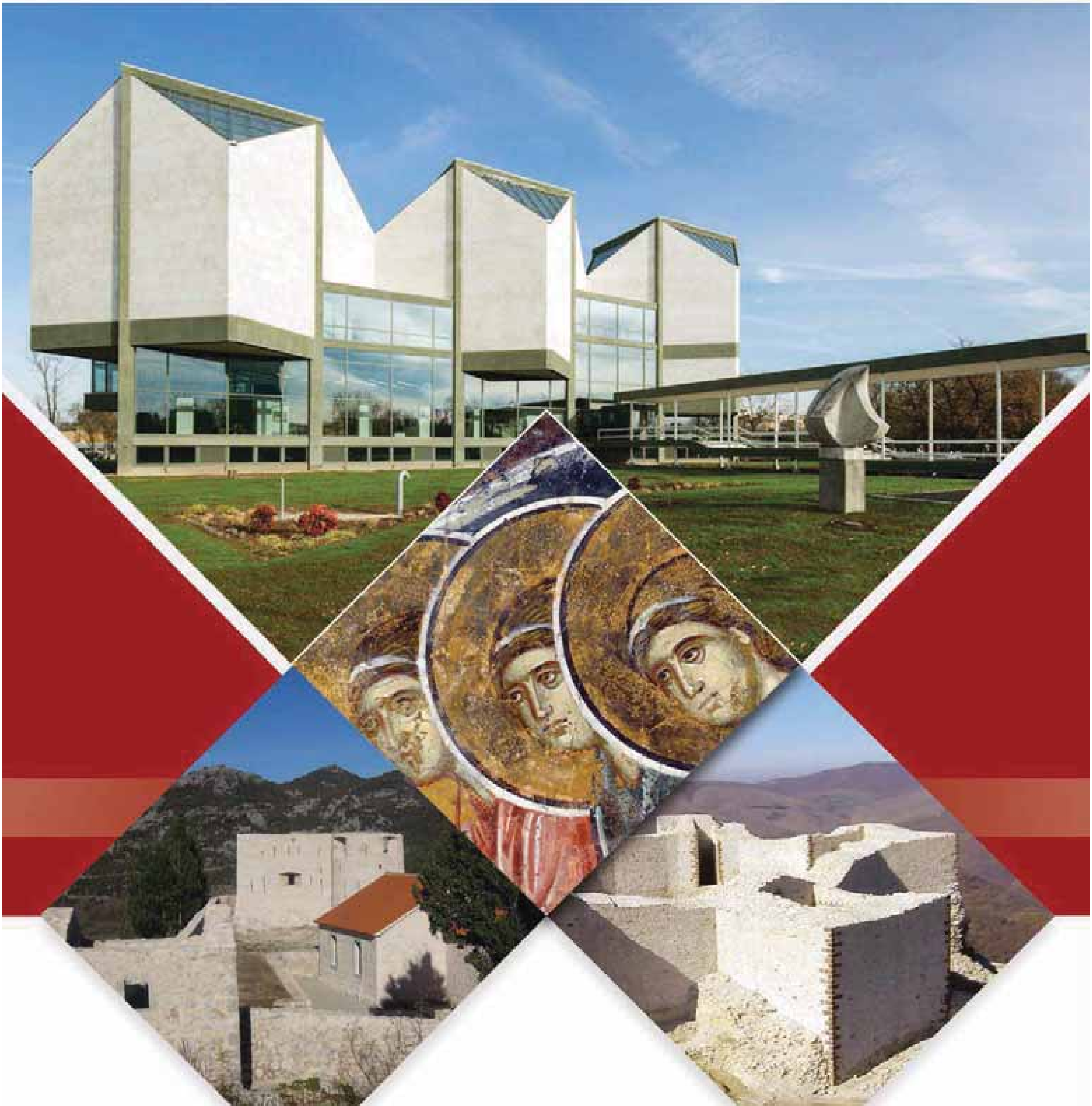

INNOVATIVE CONSTRUCTION TECHNOLOGIES

NOVKOL

Samarska 6
(bivši Surčinski put 1k),
11077, Novi Beograd, Srbija

+381117129180
+381117129194
+381117129324
+381112607979
+381112607981

Fax:
+381117129183

office@novkol.co.rs
priprema@novkol.co.rs